DESIGN OF THERMOCHEMICAL PLANTS FOR

BIOBUTANOL PRODUCTION

DESIGN AND ASSESSMENT OF NOVEL

THERMOCHEMICAL PLANTS FOR PRODUCING

SECOND AND THIRD GENERATION BIOBUTANOL

By

CHINEDU OKOLI, B.Eng., M.Sc.

Submitted to the School of Graduate Studies
in partial fulfillment of the requirements for the degree of
Doctor of Philosophy

McMaster University

DOCTOR OF PHILOSOPHY (2016), Department of Chemical Engineering

McMaster University, Hamilton, Ontario

TITLE: Design and assessment of novel thermochemical plants for

producing second and third generation biobutanol

AUTHOR: Chinedu Okoli

B.Eng. (University of Port-Harcourt)

M.Sc. (University of Manchester)

SUPERVISOR: Dr. Thomas A. Adams II

NUMBER OF PAGES: xvii, 212

Abstract

The use of biofuels as an alternative to gasoline in the transportation sector is seen by policy makers as an important strategy to reduce global greenhouse gas emissions. Biobutanol is one such biofuel that is gathering increasing attention in the biofuel community, because of its preferable fuel qualities over bioethanol. However, despite increasing research into biobutanol production, the thermochemical route for biobutanol production has not been adequately studied in the peer-reviewed literature. In light of this motivation, this thesis considers the design, and economic and environmental assessment of thermochemical plants for producing second and third generation biobutanol. In addition, the potential for using process intensification technology such as dividing wall columns (DWC) in place of conventional distillation columns is also investigated as a way to improve thermochemical biobutanol plants. As a first step, a novel thermochemical plant for producing second generation biobutanol is developed. Detailed economic analysis of this plant show that it is competitive with gasoline under certain process, and market conditions. The designed plant is then extended, with some modifications, to evaluate the economic and environmental potential of a thermochemical plant for producing third generation biobutanol from macroalgae. It was concluded from the results that the thermochemical route is preferable for producing second generation biobutanol over third generation biobutanol. The novel thermochemical plant design is then updated by using a kinetic model of a pilot-scale demonstrated catalyst to represent the critical mixed alcohol synthesis reaction step. This change allows optimal unreacted syngas recycle configurations for maximizing butanol yield to be established. Furthermore, integrating a DWC, designed using a methodology developed in the thesis, into the updated thermochemical plant leads to additional plant improvements. Overall, the work carried out in this thesis demonstrates that the thermochemical route is a viable option for producing second generation biobutanol.

Acknowledgements

This thesis is a culmination of my four years of research work, and an incredible journey of personal and career development. As in any successful endeavour there are individuals who have played important roles, and I want to use this opportunity to express my gratitude to them.

First, my deepest gratitude is extended to my supervisor Dr. Thomas A. Adams II. I am thankful for the opportunity he granted me to work under his supervision, as well as the trust and freedom he gave me to explore my research interests. Furthermore, his ever present optimism, and drive for research excellence have pushed me to never settle for mediocrity but to keep improving to be an excellent researcher. I cannot imagine ever having a better supervisor and mentor for my PhD studies.

Besides my supervisor, I would like to thank the rest of my supervisory committee; Dr Christopher Swartz and Dr Jim Cotton for their excellent research feedback over the years which have contributed immensely to improving the quality of this thesis. I would also like to thank Dr. Jay Liu of the Pukyong National University in South Korea for his wonderful insights into the macroalgae supply chain, leading to a productive research collaboration between our research groups.

One of the best things during my four years of PhD school has been the opportunity to be a part of the great and inspirational student community of the McMaster Advanced Control Consortium (MACC). Over the years I have formed strong friendships with my fellow MACC students, which I believe will last a lifetime, and will miss all the amazing discussions in the penthouse. However, particular past and present students deserve mention for their contributions to this thesis. I would like to mention Jaffer Ghouse, Yaser Khojasteh, Vida Meidanshahi, Jake Nease, Brandon Corbett, Mudassir Rashid, Chris Ewaschuk, Dominic Seepersad, Alicia Pascall, Pedro Castillo, Kushlani Wijesekera, Giancarlo Dalle Ave, James Scott, Zhiwen Chong, Phil Tominac, Tokiso Thato, Ian

Table of Contents

List of Figures

List of Tables

List of Abbreviations and Symbols

Abbreviations

ABE	Acetone-butanol-ethanol
ASTM	American society for testing and materials
BEQ	Butanol equivalent
CCA	Cost of CO_2 equivalent emissions avoided
CIB	Carbon intensity of biobutanol
CIG	Carbon intensity of gasoline
CO_2e	CO_2 equivalent emissions
DCFROR	Discounted cash flow rate of return
DWC	Dividing wall columns
ECN	Energy research center of the Netherlands
EIA	Energy information administration
EPA	Environmental protection agency
GA	Genetic algorithm
GHG	Greenhouse gas
GHSV	Gas hourly space velocity
GPSA	Gas Processors and Suppliers Association
HEN	Heat exchanger network
HHV	Higher heating value
HK	Heavy key
HP	High pressure
INL	Idaho national laboratory
IRR	Internal rate of return
LCA	Life cycle assessment
LK	Light key
LP	Low pressure
MAS	Mixed alcohol synthesis

MBSP	Minimum butanol selling price
MESH	Material equilibrium summation and heat
MINLP	Mixed integer nonlinear programming
NG	Natural gas
NPV	Net present value
NREL	National renewable energy laboratory
NRTL	Non-random two-liquid
PSO	Particle swarm optimization
RFS	Renewable fuel standard
RIN	Renewable identification number
TAC	Total annualized cost
TCI	Total capital investment
TOC	Total operating costs
VBA	Visual Basic for Applications
VLE	Vapor liquid equilibrium
V_{min}	Minimum energy mountain
VOC	Variable operating cost
WTI	West Texas intermediate

Symbols

ΔT_{min}	Minimum approach temperature (℃)
B	Bottoms flow rate (kmol/hr)
BR	Boilup ratios
D	Distillate (kmol/hr)
Dia	Column diameter (m)
f	Annualization factor
F	Feed flowrate (kmol/hr)
H	Column height (m)
i	Fractional interest rate per year
n	Annualization period in years (yr)

N_{feed}	Tray number of feed location
N_j	Number of trays in the jth section of the product column
N_{min}	Minimum number of trays
NT	Number of trays
q	Feed quality, liquid fraction
Q_{cond}	Condenser duty (MW)
Q_{reb}	Reboiler duty (MW)
r_L	Liquid split ratio
RR	Reflux ratios
r_V	Vapour split ratio
s	Tray spacing (m)
T_{reb}	Reboiler temperature (°C)
T_{cond}	Condenser temperature (°C)
L_B	Liquid flow at the bottom of the column (kmol/hr)
L_T	Liquid flow at the top of the column (kmol/hr)
V_B	Vapour flow at the bottom of the column (kmol/hr)
V_T	Vapour flow in the top section of the column (kmol/hr)
z	Composition

Research Contributions

- Developed and assessed first-of-its kind designs of thermochemical plants for producing second and third generation biobutanol. These designs mainly used technology that have been either demonstrated at the pilot-scale or are commercially available thus making these plants potentially ready for near-term implementation.

- Used quantitative metrics such as the minimum butanol selling price, and cost of carbon dioxide equivalent emissions avoided to perform first-of-its kind economic and environmental assessments of thermochemical plants for producing second and third generation biobutanol. The results demonstrated that second generation biobutanol from a thermochemical route is economically and environmentally competitive with the biochemical route over a wide range of economic conditions.

- Demonstrated the benefits of using a kinetic reactor model of a pilot-scale tested mixed alcohol synthesis (MAS) catalyst in the design of a thermochemical plant for producing second generation biobutanol. Using a kinetic model for the MAS reactor allowed optimal unreacted recycle configurations to be established for various novel thermochemical plant designs.

- Developed a methodology for the optimal design of three-product and four-product dividing wall columns (DWCs) for the separation of zeotropic multicomponent mixtures.

- Applied the DWC design methodology to develop a four-product DWC to separate a multicomponent biobutanol rich stream from a thermochemical plant into four products. The designed four-product DWC saves 31% operating costs and 28% total annualized costs in comparison to a standard three conventional distillation column sequence.

- Demonstrated the plant-wide benefits of integrating DWCs into a thermochemical plant for biobutanol production.

CHAPTER 1   Introduction

1.1   Research background and motivation

The transportation sector is a major contributor to the increase of greenhouse gas (GHG) emissions globally. In North America for example, GHG emissions in the transportation sector made up 26% of total GHG emissions in the United States (U.S.) [1], and 23% in Canada [2] in 2014. These contributions illustrate why biofuel utilization is increasingly championed by policy makers as a key strategy for GHG emission reduction in the transportation sector, with analysts expecting the contribution of biofuels to global road-transport fuel use to rise from 3% in 2013 to 8% by 2035 [3].

A critical consideration in the production of biofuels is the source of biomass. Biofuels can be grouped into "generations" depending on the type of biomass from which they are derived. First generation biofuels are biofuels derived from food crops such as corn, sugarcane, grain, and other crops with proportionally high sugar content. These were the early sources considered for biofuel production because of the ease of extracting their sugars, and oils for conversion to fuels. However their disadvantages, such as competition with food production for arable land use, mean that they are no longer considered as a sustainable option for biofuel production. In this regard, second generation biofuels aim to address the limitations of first generation biofuels through fuel production from non-food crops, particularly cellulosic/lignocellulosic terrestrial biomass such as wood chips and grasses, as well as organic and food crop wastes. Feedstocks for second generation biofuels can potentially be made more widely available than first generation biofuel feedstocks because they can be produced on "marginal land" that cannot be effectively used for food production. Third generation biofuels are the next category of biofuels that have been considered by researchers, and are produced from lower level plant forms such as micro and macro algae. Biomass sourced from micro and macro algae offer advantages such as fast growth rates, high

productivity, and the ability to be grown aquatically. However, despite the inherent advantages arising from their feedstock source, third generation biofuels might require significant technological improvement throughout their supply chain, including harvesting, transportation, pre-treatment, and fuel conversion technologies, before they can become economically competitive with first and second generation biofuels [4–6].

Collectively, second and third generation biofuels are important for achieving the GHG emission reduction potential of biofuels. This fact is highlighted by the U.S. Congress Renewable Fuel Standard (RFS) mandate for a minimum production of 36 billion gallons/year of second and third generation biofuels by 2022 [7]. Technological improvements of the biomass-to-biofuel conversion processes, as well as improved production and supply of biomass are required to achieve this target. As a positive step towards achieving the U.S. RFS mandate, the U.S. Department of Energy and the U.S. Department of Agriculture collectively champion a goal of developing a biomass supply chain which by 2030 is able to produce 1 billion tons per year of biomass, solely to be used for second and third generation biofuels production [8].

One such biofuel gaining increasing interest in the biofuel research community is biobutanol. The interest around biobutanol lies in the fact that it has superior fuel qualities to the more commonly studied bioethanol, including a higher energy content, lower affinity for water, and better compatibility with current automobile engines and gasoline pipeline networks [9,10]. It is thus seen as being preferable to bioethanol as a potential replacement for gasoline in automobiles. Table 1-1 gives a comparison of some of the properties of n-butanol, i-butanol, ethanol and gasoline.

Table 1-1. Properties of some biofuels and gasoline

Property	n-Butanol	i-Butanol	Ethanol	Gasoline
Density at 20 $^{\circ}$C (g/cm^3)	0.810	0.802	0.794	0.791
Research Octane Number	94-96	102-105	112-122	85-87
Energy content (% of gasoline)	82.3	82	65	100
Water solubility (wt %)	7.7	8.5	100	-
Oxygen content (wt %)	22	22	35	-

Second and third generation butanol production processes from biomass sources can be grouped into either biochemical or thermochemical routes. The major biochemical route is the Acetone-Butanol-Ethanol (ABE) fermentation process, which converts biomass to butanol via bacterial fermentation using mainly species of *Clostridia*. The ABE process has a long history of application. It was originally developed in the United Kingdom in 1912 and was a commercial route for acetone and butanol production from first generation biofuel feedstock (such as corn and potatoes) up until the 1950s before the advent of petrochemical derived butanol [11,12]. Its key challenges, however, are the low productivity of the fermentation process, difficulty in handling second generation biofuel feedstock such as lignocellulosic biomass (lignin is difficult to break down in biochemical processes) [9], and the difficulty of product removal from the dilute fermentation broth.

As an alternative to biochemical processing routes, which are inefficient in the conversion of second generation biofuel feedstocks, a thermochemical processing route may be more viable. The thermochemical route is based on gasification of biomass feedstock into a syngas composed of carbon monoxide and hydrogen gases. Thereafter, a clean up step is used to remove impurities from the syngas, after which it is converted over an inorganic mixed alcohol synthesis (MAS) catalyst to butanol and other alcohols. The thermochemical route offers advantages such as an ability to handle a wide range of feedstock including lignin-rich biomass because of the ease of gasifying the carbon-rich

lignin into syngas, and an easier separation step in comparison to the biochemical route, as the butanol is present in the mixed alcohols at a high concentration [13]. However, the chief disadvantage of the thermochemical route is the low CO conversion of current MAS catalysts [14]. Furthermore, this route requires capital-intensive equipment and thus may not be economically competitive with the biochemical route at small processing scales.

Even though the qualitative advantages and disadvantages of both conversion routes for butanol production have been demonstrated in the literature, quantitative assessments are still required for more robust evaluations and concrete decision-making by biofuel stakeholders. Such quantitative frameworks should include metrics for evaluating the economic and environmental potential of biobutanol production technologies. In this regard, only very few studies exist in the peer reviewed literature for second and third generation biobutanol, with all of them pertaining to second generation biobutanol production through the biochemical route [15–17]. Despite the discussed viability of the thermochemical route as an alternative to the biochemical route for biobutanol production, neither economic nor environmental studies on biobutanol production from a thermochemical route exist in the peer-reviewed literature, to the best of the researcher's knowledge. In fact, a detailed process design for the production of biobutanol via the thermochemical route does not appear to have been presented in the literature at all.

Besides establishing thermochemical plant designs for second and third generation biobutanol production, it is also imperative that any such designs should consider the use of advanced technology such as process intensification technologies to drive further process improvements. Process intensification is a term used to define chemical process technologies in which novel equipment and techniques are used to meet production

objectives, offering reduced equipment sizes, higher efficiencies and lower energy consumption, thereby leading to cheaper and more sustainable processes. As separation processes, such as distillation, can account for between 40-70% of separation costs in a typical process plant [18], there is a motivation to evaluate the potential savings that can be obtained by using process intensification technologies for product separation in thermochemical biobutanol production processes. One such process intensification technology is called a dividing wall column (DWC). DWCs intensify the distillation process by avoiding the internal re-mixing of streams which occur in conventional distillation columns. This intensification reduces the entropy of mixing and thus the energy required for component separation of mixtures. In past research it has been shown that DWCs can reduce the investment and energy consumption of a multicomponent distillation process by up to 30% in comparison to conventional distillation sequences [19–21]. However, it can be challenging to evaluate the benefits of using DWCs in process plants because of the absence of clear heuristics in the literature for modeling and designing DWCs. Despite this challenge, it is imperative that the potential savings gained through the use of DWCs in thermochemical biobutanol plants are investigated on a plant-wide level, as any economic and environmental benefits might be critical for the uptake of thermochemical biobutanol technologies.

1.2 Thesis objectives and outline

Motivated by the discussion above, this thesis aims to address the research gap surrounding the understanding of the thermochemical route for biobutanol production. The overall objective of this thesis is to develop novel thermochemical plant designs for second and third generation biobutanol production that are economically competitive and environmentally sustainable. This entails using process systems engineering tools to develop the thermochemical plant designs, and using appropriate quantitative metrics to

assess their economic and environmental potential. The benefits of integrating relevant process intensification technologies such as DWCs into the thermochemical plant designs will also be evaluated. The rest of the thesis is organized as follows:

Chapter 2: considers the design of a novel process for producing second generation biobutanol through a thermochemical route and MAS reaction process. The design considers the use of lignocellulosic biomass (wood chips) as feedstock and is "self-sufficient", meaning that it makes use of no external hot utilities nor power i.e. it is 100% driven by renewable energy. The MAS reactor used here incorporates a low-pressure modified methanol synthesis catalyst, with the reactor modelled using simple conversion models based on U.S. National Renewable Energy Laboratory (NREL) future conversion targets for MAS catalysts [22]. A techno-economic analysis was then carried out to determine the minimum butanol selling price (MBSP) of the process. The MBSP serves as a metric for quantifying the economic potential of the process with respect to second generation biobutanol from the biochemical route. Finally, different plant and cost parameter scenarios were rigorously explored using a sensitivity analysis. This work has led to peer-reviewed publications in the *Chemical Aided Computer Engineering* [23] and *Industrial Engineering & Chemistry Research* [24] journals.

Chapter 3: the thermochemical plant design developed in chapter 2 for second generation biobutanol production is extended with modifications to the production of third generation biobutanol. The choice of third generation biofuel feedstock in this process is macroalgae, which is preferable to microalgae for biofuel production because its plant-like characteristics make it easier to harvest, and its high concentration of carbohydrates in comparison to microalgae make it a potentially better biofuel feedstock [5,25,26]. Alongside the self-sufficient configuration considered in Chapter 2, two new configurations based on the use of external fossil-based hot utilities and power are

considered. These new configurations lead to important trade-offs in terms of economics and the environment, which are then assessed. The MBSP is used as the metric to quantify the economic potential of the configurations, while the cost of CO_2 equivalent emissions avoided (CCA) is used as the metric to quantify their environmental potential. Furthermore, all the configurations are assessed in the U.S. and South Korean markets to demonstrate that plant location can be a key factor in the choice of a plant configuration. This work has led to a peer-reviewed publication in the *Energy Conversion and Management* [27] journal.

Chapter 4: develops a methodology for designing optimal 3-product and 4-product DWCs for separation of multicomponent zeotropic mixtures. The developed methodology uses a short-cut method to provide initial estimates of the DWCs operating and structural design variables. Thereafter an acyclic simulation structure, which avoids the problems encountered when trying to converge recycle streams in sequential modular commercial process simulators, is then used to represent the column in a commercial process simulator. Finally, a black-box optimization technique based on the particle swarm optimization (PSO) algorithm is used to optimize the DWCs through a two-tier simulation-optimization approach. The methodology is then applied to design DWCs to separate a multicomponent butanol-rich feed stream from the reactor product of the thermochemical plant developed in chapter 2 into four major products, with a key final product being a biobutanol rich stream that meets American Society for Testing and Materials (ASTM) fuel standard [28]. The resulting DWC designs are then compared, based on similar feed inputs, to an optimized conventional distillation sequence for thermochemical biobutanol production. This work has led to a peer-reviewed publication in the *Chemical Engineering Processing: Process Intensification* [29] journal.

Chapter 5: considers improved designs of thermochemical plants for second generation biobutanol production. It improves on the thermochemical plant design from Chapter 3 by replacing the simplistic MAS reactor model with a detailed kinetic model using a pilot-scale demonstrated catalyst leading to a more realistic representation of the process, and enabling the impact of design parameters to be investigated for various novel process designs. Furthermore, economic and environmental metrics such as the MBSP, and CCA were used to assess the potential of the process designs. In addition, the plant-wide benefit of using DWCs instead of conventional columns in the separation section of a thermochemical biobutanol plant is evaluated for a self-sufficient thermochemical plant design. This was accomplished by integrating a DWC, designed using the methodology developed in chapter 4, into the self-sufficient thermochemical biobutanol plant. A completed manuscript of this work has been prepared for submission to the *Industrial Engineering & Chemistry Research* journal.

Chapter 6: summarizes the major conclusions of the thesis and discusses future research directions.

1.3   References

[1]   EPA. Sources of Greenhouse Gas emissions. U.S. Environ Prot Agency 2016. https://www3.epa.gov/climatechange/ghgemissions/sources/transportation.html (accessed June 7, 2016).

[2]   ECCC. Canadian Environmental Sustainability Indicators: Greenhouse Gas emissions. Gatineau, Canada: 2016.

[3]   EIA UEIA. Annual Energy Outlook 2014 with Projections to 2040. Washington DC: 2014.

[4]   Wei N, Quarterman J, Jin Y-S. Marine macroalgae: an untapped resource for producing fuels and chemicals. Trends Biotechnol 2013;31:70–7. doi:10.1016/j.tibtech.2012.10.009.

[5]   Chen H, Zhou D, Luo G, Zhang S, Chen J. Macroalgae for biofuels production: Progress and perspectives. Renew Sustain Energy Rev 2015;47:427–37. doi:10.1016/j.rser.2015.03.086.

[6]   van Hal JW, Huijgen WJJ, López-Contreras AM. Opportunities and challenges for seaweed in the biobased economy. Trends Biotechnol 2014;32:231–3. doi:10.1016/j.tibtech.2014.02.007.

[7]   EPA. Renewable Fuel Standard Program. U.S. Environ Prot Agency 2016. https://www.epa.gov/renewable-fuel-standard-program/program-overview-renewable-fuel-standard-program (accessed July 6, 2016).

[8]   Perlack RD, Wright LL, Turhollow AF, Graham RL, Stokes BJ, Erbach DC. Biomass as feedstock for a bioenergy and bioproducts industry: the technical feasibility of a billion-ton annual supply. Oak Ridge, Tennessee: DTIC Document; 2005.

[9]   Kumar M, Gayen K. Developments in biobutanol production: New insights. Appl Energy 2011;88:1999–2012. doi:10.1016/j.apenergy.2010.12.055.

[10]   Ranjan A, Moholkar VS. Biobutanol: science, engineering, and economics. Int J Energy Resour 2012;36:277–323. doi:10.1002/er.

[11]   Green EM. Fermentative production of butanol—the industrial perspective. Curr Opin Biotechnol 2011;22:337–43. doi:10.1016/j.copbio.2011.02.004.

[12]   García V, Päkkilä J, Ojamo H, Muurinen E, Keiski RL. Challenges in biobutanol production: How to improve the efficiency? Renew Sustain Energy Rev 2011;15:964–80. doi:10.1016/j.rser.2010.11.008.

[13]   Nexant. Equipment Design and Cost Estimation for Small Modular Biomass Systems, Synthesis Gas Cleanup, and Oxygen Separation Equipment Task 9 : Mixed Alcohols From Syngas — State of Technology. San Francisco, California: 2006.

[14]   Herman R. Advances in catalytic synthesis and utilization of higher alcohols. Catal Today 2000;55:233–45. doi:10.1016/S0920-5861(99)00246-1.

[15]   Qureshi N, Saha BC, Cotta MA, Singh V. An economic evaluation of biological conversion of wheat straw to butanol: A biofuel. Energy Convers Manag 2013;65:456–62. doi:http://dx.doi.org/10.1016/j.enconman.2012.09.015.

[16]   Tao L, Tan ECD, McCormick R, Zhang M, Aden A, He X, et al. Techno-economic analysis and life-cycle assessment of cellulosic isobutanol and comparison with cellulosic ethanol and n-butanol. Biofuels, Bioprod Biorefining 2014;8:30–48. doi:10.1002/bbb.1431.

[17]   Kumar M, Goyal Y, Sarkar A, Gayen K. Comparative economic assessment of ABE fermentation based on cellulosic and non-cellulosic feedstocks. Appl Energy 2012;93:193–204. doi:10.1016/j.apenergy.2011.12.079.

[18]   Giridhar A, Agrawal R. Synthesis of distillation configurations: I. Characteristics of a good search space. Comput Chem Eng 2010;34:73–83. doi:10.1016/j.compchemeng.2009.05.003.

[19]   Agrawal R, Fidkowski ZT. Are Thermally Coupled Distillation Columns Always Thermodynamically More Efficient for Ternary Distillations ? 1998;5885:3444–54.

[20] Rewagad RR, Kiss A a. Dynamic optimization of a dividing-wall column using model predictive control. Chem Eng Sci 2012;68:132–42. doi:10.1016/j.ces.2011.09.022.

[21] Asprion N, Kaibel G. Dividing wall columns: Fundamentals and recent advances. Chem Eng Process Process Intensif 2010;49:139–46. doi:10.1016/j.cep.2010.01.013.

[22] Phillips S, Aden A, Jechura J, Dayton D. Thermochemical Ethanol via Indirect Gasification and Mixed Alcohol Synthesis of Lignocellulosic Biomass Thermochemical Ethanol via Indirect Gasification and Mixed Alcohol Synthesis of Lignocellulosic Biomass 2007.

[23] Okoli C, Adams T. Techno-economic Analysis of a Thermochemical Lignocellulosic Biomass-to-Butanol Process. Comput Aided Chem Eng 2014;33:1681–6.

[24] Okoli C, Adams TA. Design and economic analysis of a thermochemical lignocellulosic biomass-to-butanol process. Ind Eng Chem Res 2014;53:11427–41.

[25] Jung KA, Lim S-R, Kim Y, Park JM. Potentials of macroalgae as feedstocks for biorefinery. Bioresour Technol 2013;135:182–90. doi:10.1016/j.biortech.2012.10.025.

[26] Ben Yahmed N, Jmel MA, Ben Alaya M, Bouallagui H, Marzouki MN, Smaali I. A biorefinery concept using the green macroalgae Chaetomorpha linum for the coproduction of bioethanol and biogas. Energy Convers Manag 2016;119:257–65. doi:10.1016/j.enconman.2016.04.046.

[27] Okoli CO, Adams II TA, Brigljević B, Liu JJ. Design and economic analysis of a macroalgae-to-butanol process via a thermochemical route. Energy Convers Manag 2016;123:410–22. doi:http://dx.doi.org/10.1016/j.enconman.2016.06.054.

[28] ASTM Standard D7862-15. Standard Specification for Butanol for Blending with Gasoline for Use as Automotive Spark-Ignition Engine Fuel 2015. doi:10.1520/D7862-15.

[29] Okoli CO, Adams TA. Design of dividing wall columns for butanol recovery in a thermochemical biomass to butanol process. Chem Eng Process Process Intensif 2015;95:302–16. doi:10.1016/j.cep.2015.07.002.

CHAPTER 2 Design and economic analysis of a lignocellulosic biomass-to-butanol process

The contents of this chapter have been published in the following peer reviewed literature journals:

Okoli, C. and Adams, T.A., 2014. Design and economic analysis of a thermochemical lignocellulosic biomass-to-butanol process. Industrial & Engineering Chemistry Research, 53(28), pp.11427-11441.

Okoli, C. Adams, T.A., 2014. Techno-economic Analysis of a Thermochemical Lignocellulosic Biomass-to-Butanol Process. Computer Aided Chemical Engineering, 33, pp.1681–1686.

2.1   Introduction

Second generation biofuels show great promise for addressing some of the major challenges of achieving a sustainable society, such as global climate change, energy security, and land use (food vs. fuel). Though definitions vary, the term "second generation" usually refers to biofuels which are derived from cellulosic or lignocellulosic biomass (such as wood and grass). Although both first generation (typically derived from corn, sugar, and other food crops) and second generation biofuels processes both can theoretically approach carbon-neutral life cycles, second generation biofuels are better-suited to address these challenges because they are significantly less competitive with food production for land, and their feedstocks are or can be made widely available.

For example, the 2002 annual biomass harvest from Canada's forestry and agricultural sectors had an energy content of 5.1 EJ/year (One Exajoule (EJ) = 10^{18} Joules) which is equivalent to 62 % of the country's by fossil fuels energy consumption [1]. In the U.S., the 2009 estimates of the total annual agricultural residue and forestry produce was 136 million dry tons/year or 2.3 EJ/year, equivalent to 2.8 % of the country's fossil fuel energy consumption [2,3].

In terms of global biofuels production, the world's non-petroleum liquids production (consisting of biofuels, coal-to-liquids, and gas-to-liquids) totalled 74 billion L/year in 2012 with biofuels contributing 82 % of this total [3]. In 2013 biofuels contributed 3 % to total road-transport fuel demand with this value expected to reach 8 % by 2035 [4]. This vast potential for cellulose/lignocellulose to biofuels technologies is highlighted by the U.S. Renewable Fuel Standard (RFS) target of a minimum of 21 billion gallons/year (79.5 billion L/year) of cellulosic biofuels production by 2022, a vast increase from 2011 estimates of 5 billion gallons/year [5].

Biobutanol is a biofuel which is receiving increased attention as a potential replacement for ethanol as a gasoline substitute because of its advantages over bioethanol such as a higher energy content, lower affinity for water, and better compatibility with existing internal combustion engines and fuel pipeline networks [6,7].

The production of biobutanol can be grouped into biochemical and thermochemical routes. The major biochemical route is the acetone-butanol-ethanol (ABE) fermentation process, which converts biomass to butanol via fermentation with *Clostridia* bacteria such as *Clostridium beijerinckii* and *Clostridium acetobutylicum* [6,8]. The ABE process has a long history of application and is currently the most established biobutanol production process [6]. However its key challenges are the low productivity of the fermentation process, difficulty in handling second generation biofuel feedstock such as lignocellulosic biomass because of their high lignin content which is difficult to break down in biochemical processes [9], and the difficulty in removal of the product from the dilute fermentation broth. These challenges are being addressed through research into the use of continuous fermentation processes with recycle membrane reactors, improved bacteria strains, novel feed pre-treatment methods, and hybrid separation processes [6,10,11].

Thermochemical routes on the other hand, proceed through the gasification of biomass feedstock into a syngas consisting of carbon monoxide (CO) and Hydrogen (H_2). The syngas is subsequently cleaned to remove impurities, and converted to butanol and other alcohols over an inorganic mixed alcohol synthesis (MAS) catalyst. These MAS catalysts can be classified into four groups; modified high pressure methanol synthesis catalysts, modified low pressure methanol synthesis catalysts, modified Fischer-Tropsch catalysts, and alkali-doped molybdenum catalysts [12,13]. Of particular interest for butanol production are the modified methanol catalysts as they have better selectivity to

butanol. The formation of butanol and other higher alcohols over modified methanol catalysts follow the aldol condensation reaction step in which branched chain higher alcohols formation is favoured [14,15]. Advantages of the thermochemical route include an ability to handle a wide range of feedstock including lignocellulosic biomass as the gasification process efficiently converts lignin into syngas, and an easier separation step in comparison to the biochemical route, as the butanol is present in the mixed alcohols at a high concentration. However, its disadvantages include a low catalyst CO conversion, and high temperature and pressure requirements with difficult temperature control for the highly exothermic reaction. To counter these problems, researchers have proposed novel reactor concepts such as double reactor configurations to improve CO conversion, and slurry reactors for good temperature control [14-16]. There is also ongoing research being carried out for improved MAS catalysts for butanol production [13,16,17]. However despite the potential of the MAS process, the MAS reactor and catalyst technologies are still at development stages, and have not been commercially demonstrated.

Even though the qualitative merits and demerits of both routes for butanol production have been demonstrated, it is important to develop quantitative frameworks for more robust evaluations. One such quantitative framework is a techno-economic analysis, which can be defined as a methodology for the joint assessment of technology and economic models to ascertain the market potential of a venture, process or product. A well-designed and thought out techno-economic analysis can be an invaluable tool in determining performance and cost boundaries of a technological venture, helping to appropriately direct investments and research efforts. The American Association of Cost Engineering guidelines provides definitions for capital cost estimates for process industries, with the estimating methodology and level of effort carried out in this work

corresponding to a class 4 estimate with an accuracy of -15 % to -30 % on the low side and +20 % to +50 % on the high side [18]. Reviews of techno-economic analyses have been carried out for a wide range of first and second generation biofuels utilizing both biochemical and thermochemical platforms [7,19,20]. In particular, techno-economic studies based on n^{th}-plant assumptions (meaning the process is commercially mature and the learning curve has been overcome) have found minimum selling prices of thermochemical bioethanol to range from \$0.38/L to \$0.90/L [21-24], and minimum selling prices of biochemical butanol ranging from \$0.59 - \$2.71/L [8,25-27], adjusted for 2012 U.S. dollars.

However, despite the importance of techno-economic analyses for assessing emerging technologies and the viability of thermochemical butanol as an alternative to biochemical butanol especially for second generation biofuel feedstocks, no techno-economic platforms for assessing thermochemical butanol exist in the peer-reviewed literature to the best of the authors' knowledge. In fact, a detailed process design for the production of biobutanol via the thermochemical route does not appear to have been presented in the literature as well. Therefore this work address these questions by developing a novel base case thermochemical biobutanol process using lignocellulosic feedstock and the MAS process, and assessing its economic feasibility. Detailed sensitivity analyses are used to investigate the impact of economic parameters on the minimum butanol selling price (MBSP), and to quantify how much research into and improvement of the considered MAS catalyst is required to make the technology economically competitive.

Some of the critical questions that will be addressed by this techno-economic study on a thermochemical biomass to butanol process are: (i) What is the overall efficiency of the process and what butanol yields can be expected? (ii) How does the valuation of co-

products affect the butanol selling price? (iii) How does the MBSP compare to that of biochemical butanol, and butanol equivalent (BEQ) gasoline prices? (iv) What research targets need to be achieved in the near-term for an economically competitive process to be established?

This article provides a detailed analysis of this subject, a summarized version of this work has been published in the proceedings of the 24th European Symposium on Computer Aided Process Engineering [28].

2.2 Methods

2.2.1 Process simulation overview

A detailed design of this process was simulated using Aspen Plus V.8 software. No single physical property package was sufficient to model the whole process, as three phases of matter (solid, liquid, and gas) as well as non-conventional components (biomass, ash and char) are present in the system. The ASME 1967 steam table correlations were used for the steam cycle and cooling water sections calculations. The non-random, two-liquid (NRTL) activity coefficient model with Redlich-Kwong model for the gas phase was used to model the alcohol separation and quench water system calculations. The Redlich-Kwong-Soave equation of state with Boston-Mathias modifications was used for the remainder of the process simulation. The heat integration analysis was carried out using Aspen Energy Analyzer® software.

2.2.2 Process description and design criteria

The design used for this process was inspired by designs proposed by the National Renewable Energy Laboratory (NREL) for a thermochemical biomass-to-ethanol process, with major modifications made to the gas cleanup, mixed alcohols synthesis and alcohol separation sections for the production of butanol [9,21]. The proposed

design with modifications from the NREL designs are detailed in sections 2.2.2.1 –
2.2.2.7. As with these NREL designs, this process was designed to be energy sufficient
(avoid the use of external hot utilities) and minimize water use.

Fig. 2-1 displays a simplified process flow diagram of the process showing the key
processing steps for the conversion of woody biomass via gasification, syngas
production, and mixed alcohol synthesis to butanol. The different areas of the process
are further discussed in sections 2.2.2.1 – 2.2.2.7. Table 2-1 also shows the major design
parameters for these process areas.
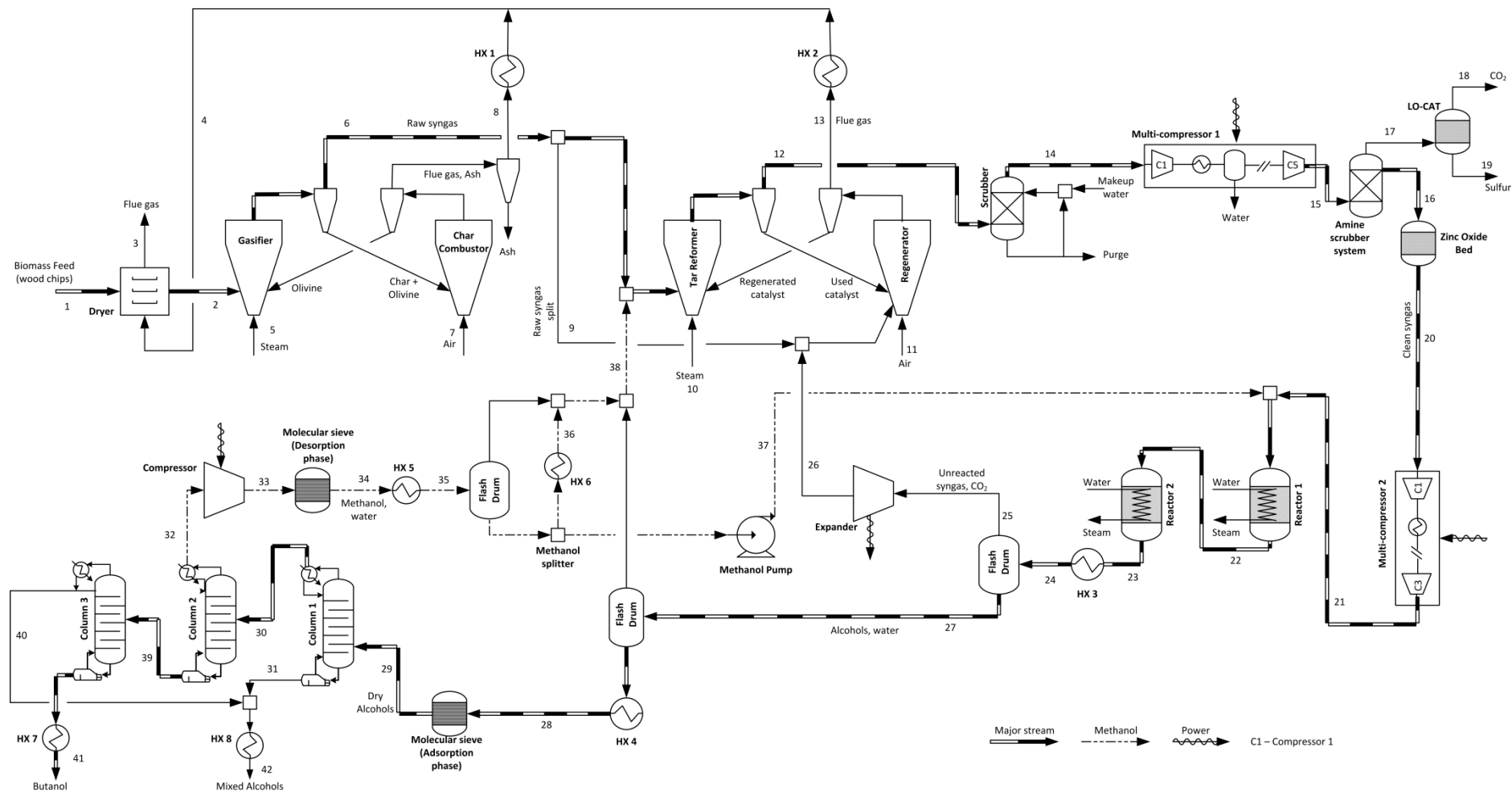
Figure 2-1. Process flow diagram of the proposed thermochemical biomass-to-butanol process. Full stream conditions are shown in the supplementary material on www. macsphere.mcmaster.ca.

Table 2-1. Major design parameters of process areas

Gasification		Gas cleanup (acid gas removal)	
Feed rate per train (gasifier inlet)	1,000 dry tonnes/ day	Amine used	Monoethanolamine
Parallel trains required	Two (2)	Amine concentration, wt %	35
Gasifier operating pressure	2.28 bar	Amine circulation rate (L/s)	97.64
Gasifier operating temp.	868 °C	Amine temperature in absorber (°C)	43.33
Char combustor pressure	2 bar	Absorber pressure (bar)	31
Char combustor temp.	995 °C	Stripper pressure (bar)	4.12
Syngas composition (simulation results)		Stripper reboiler duty (MW)	33
Components	Mole %	Stripper condenser duty (MW)	21.8
H_2	13.46	Amine cooler duty (MW)	10.9
CO	23.45	Heat duty to remove CO_2 (kJ/kg)	5337
CO_2	7.27		
Water	43.84	Alcohol synthesis reactors	
CH_4	8.72	H_2/CO ratio (reactor 1 inlet)	1.23
C_2H_2	0.23	Gas hourly space velocity (h^{-1})	5000
C_2H_4	2.47	Reactor 1 temperature (°C)	325
C_2H_6	1689 ppmv	Reactor 1 volume (m^3)	32.89
Benzene	719 ppmv	Reactor 2 temperature (°C)	340
Tar	1314 ppmv	Reactor 2 volume (m^3)	22.24
H_2S	144 ppmv	Pressure (bar)	76
NH_3	1831 ppmv	CO_2 concentration (mol %)	5
		Sulphur concentration (ppmv)	0.1
Gas cleanup (tar reforming)		CO conversion per-pass (CO_2 free basis)	40 mol%
Reformer operating pressure (bar)	1.86	Total alcohol selectivity	87.27 mol%
Reformer operating temp. (°C)	910	Catalyst alcohols prod. (g/kg-catalyst/hr)	455.26
Reformer space velocity (h^{-1})	2,476	Product distribution of alcohols and hydrocarbons (mole %)	
Reformer volume (m^3)	59.7	Methanol	41.92
Outlet H_2/CO molar ratio	1.269	Ethanol	1.08
Tar reformer conversions (%)		Propanol	6.79
Methane (CH_4)	80%	Isobutanol	15.91
Ethane (C_2H_6)	99%	Pentanol	1.28
Ethylene (C_2H_4)	90%	Hexanol	1.22
Tars (C_{10+})	99%	CH_4	2.92
Benzene (C_6H_6)	99%	C_2H_6	0.71
Ammonia (NH_3)	90%	C_3H_8	9.78
		C_4H_{10}	11.24
Alcohol separation (distillation columns)		Water	7.15
Column 1			100.00
Butanol recovery in overhead	99.2 mol%		
Pentanol recovery in bottoms	99 mol%		
Murphree Tray efficiency	60%	Steam system and power generation	
Total number of trays	28	Turbine design	Three stage turbine
		High pressure inlet conditions	58 bar, 482 °C
		Medium pressure inlet conditions	12 bar, 303 °C
Column 2		Low pressure inlet conditions	4.5 bar, 210 °C
Methanol recovery in overhead	99 mol%	Condenser outlet conditions	0.304 bar, saturated
Ethanol recovery in bottoms	99 mol%		
Tray efficiency	60%	Cooling water	
Total number of trays	48	Supply temperature (°C)	32
		Return temperature (°C)	43
Column 3		Supply rate (m^3/h)	759.55
Propanol recovery in overhead	99.3 mol%		
Butanol purity in bottoms	99.5 wt%	Alcohol separation (Molecular sieve)	
Tray efficiency	60%	Inlet water content (wt %)	7.93
Total number of trays	56	Outlet water content (wt %)	0.5

2.2.2.1   Feed handling and drying

2,000 tonnes per day (dry basis) of pine woody biomass feedstock with properties shown in Table 2-2 is delivered to the plant's gate were it is dried from 30 wt% moisture to 10 wt% moisture by contact with hot flue gas from the steam generation section. The feedstock supply and cost model of the Idaho National Laboratory (INL) as interpreted in Dutta et al. [9] is used for this analysis. The INL model accounts for the logistical, capital and operating costs associated with feed delivery, handling and drying to the required 10 wt% moisture content, and the simulated dryer model is consistent with this requirement. It should be noted that the choice of biomass drying to 10% moisture content is not an arbitrary decision. Phillips et al. [21] mention in their sensitivity analysis discussion that very low moisture contents do not give a corresponding increase in alcohol yields. In fact, from their graphical sensitivity analysis on moisture content, the impact of drying below 15% is negligible on the alcohol yield and minimum selling price. Therefore drying to 10% is a good conservative value. The details of the dryer and feedstock costs are further discussed in section 2.2.3.

The temperature specification for the flue gas exhaust leaving the steam generation section (stream 4 in Fig. 2-1) is adjusted to about 316 °C to ensure that the biomass is dried to 10 wt% and that the humidified flue gas exits the system above its dew point temperature (113 °C in this case). The temperature of 316 °C was determined by using a simple custom model in Aspen Plus which computes the heat duty necessary to dry the biomass and the corresponding temperature and humidity change of the flue gas stream.

Table 2-2. Analysis of woody biomass feedstock [9]

Component	Weight % (dry basis)
Carbon	50.94
Hydrogen	6.04
Nitrogen	0.17
Sulphur	0.03
Oxygen	41.9
Ash	0.92
Higher Heating Value (MJ/kg)	19.99
Lower Heating Value (MJ/kg)	18.59

2.2.2.2　　　Gasification

The dried biomass is fed to the gasifier were it is indirectly gasified using low pressure steam supplied at 0.4 kg per kg bone-dry wood as the fluidization medium and reactant [9]. The gasifier used is a low pressure allothermal indirect circulating fluidized bed gasifier whose output is modeled with temperature correlations from the Batelle Columbus Laboratory's test facility obtained from Dutta et al. [9]. Overall, the gasification reactions are endothermic, and the heat required is supplied by circulating heated olivine from the char combustor through the gasifier, in direct contact with the syngas. The gasification product consists mainly of syngas (CO and H_2), CH_4, tars, and char (solid). The olivine and char are separated from the gaseous products using a cyclone and sent to the char combustor. There, the char is combusted with air thus heating the olivine, with the olivine and ash formed subsequently being separated from the hot combustion gases via a series of cyclones. The loop is completed when the hot olivine flows back to the gasifier. The hot combustion gases are used for biomass drying, with the excess heat used to generate steam in the steam system.

2.2.2.3　　　Gas cleanup

Gas cleanup is required to remove impurities such as tars, sulphur and CO_2 which foul process equipment and are detrimental to the MAS catalyst performance. The cleanup steps consist initially of the reforming of tars, methane and other hydrocarbons in a

circulating, fluidized, heterogeneous catalyst system which utilizes separate beds for reforming and catalyst regeneration. This reformer bed is assumed to be isothermal with the temperature being maintained by the transfer of heat from the exothermic catalyst regenerator. A fluidizable Ni/Mg/K catalyst with Al_2O_3 as support [9] catalyzes the reforming reaction between the syngas and steam, with the catalyst separated from the syngas via a cyclone at the reformer exit and passed to the catalyst regenerator. The catalyst is regenerated via the combustion of coke (from the reforming reaction) entrained on the catalyst, with the hot catalyst flowing back to the tar reformer after separation from the flue gas in a cyclone. Additional unreacted syngas and off-gases from the MAS reactors and alcohol separation sections are combusted in the regenerator to provide additional heat for the endothermic reforming reactions. The heat from the flue gas is recovered for steam generation and process heating, with the remaining low quality heat used for drying the feedstock. In Aspen Plus, the tar reformer is modeled with an RGibbs reactor block with conversion specifications set for individual tar and hydrocarbon reactions. These conversion specifications are set at 2012 target design performance values discussed by Dutta et al. [9], and are shown alongside the operating conditions of the tar reformer system in Table 2-1. These targets have been demonstrated by the NREL at bench scale, with current research efforts focused on pilot scale demonstrations [9].

The hot syngas from the tar reformer is cooled to 60 $^{\circ}$C, quenched and scrubbed with water to remove remnant particulates, tars, ammonia and other impurities. The scrubber water is circulated through the quench system at a rate of 0.001 m^3 liquid per m^3 of syngas [9]. Makeup water is added at 0.0038 m^3 per min with a purge water stream continuously sent to a waste water treatment facility for treatment.

Prior to entering the amine system for acid gas removal, the cool syngas is compressed to 30 bar in a five-stage compressor with forced-air inter-stage cooling. The compressor is designed to have a stage pressure ratio close to two, polytropic efficiency of 78% and inter cooling to 60 $^\circ$C. These values are consistent with those used by Phillips et al. [21] and are reasonable parameters to choose.

The H_2S concentration of the syngas is reduced to 10 ppm by the amine scrubber with further reduction to 0.1 ppm by a ZnO bed [12,29]. The modified methanol catalyst used for the MAS reactor has a very low tolerance to sulphur, thus the very stringent H_2S cleanup requirement [12]. The acid gas from the amine system is sent to a LO-CAT process where elemental sulphur is regenerated from H_2S with a CO_2 effluent stream also produced. The LO-CAT process was chosen over the Claus process for sulphur regeneration because it is cheaper when sulphur removed is less than 20 tonnes per day [12].

The amine system was modeled in Aspen Plus with a SEP block representing the acid gas scrubber, with the acid gas (CO_2 and H_2) removal rate adjusted to meet the design conditions of 0.1 ppmv H_2S and 5 mole% CO_2 at the inlet to the first MAS reactor. The acid gas removal rate is then used in a calculator block to determine the amine circulation rate using guidelines from section 21 of Gas Processors and Suppliers Association (GPSA) [30]. The amine circulation rate is subsequently used in another calculator block as a basis for determining the heating and cooling duties of the amine system using guidelines from section 21 of GPSA [30]. The operating conditions are shown in Table 2-1.

2.2.2.4   Alcohol Synthesis

The cleaned, cool, intermediate pressure syngas is compressed to the MAS reactor inlet pressure of 76 bar using a three-stage multi compressor with forced air inter-cooling and heated to the first reactor inlet temperature of 325 $^{\circ}$C. The reactor system consists of two fixed-bed reactors in series with equal portions of a modified low pressure methanol synthesis catalyst (Cs/Cu/ZnO/Cr$_2$O$_3$ based) [15,31]. Both reactors are at 76 bar, with the second reactor at 340 $^{\circ}$C. The first reactor produces mainly $C_1 - C_3$ oxygenates as the lower temperature favours higher equilibrium amounts of methanol, while the conversion to higher alcohols in the second reactor is favoured by the higher temperatures [31]. The experimental results of Burcham et al. [31] confirm that the double bed reactor configuration is better than a single reactor configuration as there is a significantly higher butanol yield for the double bed reactor configuration. Although there might be a capital cost versus yield trade-off between the different reactor configurations, it is not considered in this analysis.

The syngas is mixed with recycled methanol and water from the alcohol separation section and passed through the reactors were it is catalytically converted to methanol, ethanol, propanol, isobutanol, water, methane, other higher alcohols and small amounts of some other hydrocarbon products. The recycled methanol helps to improve the higher alcohol yield [15,31]. The reactors have a shell and tube configuration with the reactions taking place within the tubes while the exothermic heat generated is removed via steam generation on the shell side. The shell side steam generation also serves to maintain isothermal reactor conditions. The reactor products are cooled via heat exchange with process streams and cooling water to 60 $^{\circ}$C. The gaseous unconverted syngas is separated from the liquid alcohols, expanded through a turbo expander to recover power and sent to the catalyst regenerator in the gas cleanup section where it is

combusted to help meet the system's heat requirements. The liquid alcohols are sent downstream to the alcohols separation section.

The CO conversion (CO_2 - free basis) of the low pressure modified methanol catalyst used for this process was reported as 8.5% by Herman [15]. This particular catalyst was chosen as a sample type for our analysis because it was the only one in the peer-reviewed literature which has both high selectivity to isobutanol and sufficient yield data to model the MAS reactors. Note that the 8.5 % CO conversion is only for this particular catalyst and in fact is not indicative of the general trend for high butanol selective MAS catalysts. A review paper by Verkerk et al. [14] shows that high CO-conversions (CO_2 free basis) of up to 18.5 % have been demonstrated for some high pressure modified methanol catalysts albeit at very high pressures. For this work a futuristic CO conversion of 40 % is assumed and is in line with a NREL target for greater than 50% single-pass CO conversion for MAS catalysts discussed in appendix B of Phillips et al. [21]. The impact of the catalyst conversion on the economic results is explored in further detail in section 2.3.3.2.

The reactors are modelled in Aspen Plus as RStoic reactors with the conversion of each reaction set to achieve a particular product distribution of alcohols [15], target conversions and selectivity as shown in Table 2-1. In the Aspen Plus model the heat generated from the exothermic reaction was accounted for by using it to create steam in the steam system.

2.2.2.5 Alcohol separation

The raw mixed alcohols are flashed to 4 bar to remove absorbed gases which are recycled to the tar reformer in the gas cleanup section. The liquid alcohols are then superheated and sent to a molecular sieve for dehydration. The dehydrated alcohols are

then separated with the goal of obtaining a 99.5 wt% isobutanol product with mixed alcohol co-products. Three distillation columns in series were used to achieve this objective using a design based on a heuristic indirect sequencing approach in which the easiest separation (according to the relative volatilities of the feed components) is done first. The indirect sequence was chosen over a direct sequence approach (final products are removed one at a time as distillates) because a preliminary analysis showed a higher reboiler steam requirement and thus higher operating cost was required for the direct sequence. The designs for the individual columns are shown in Table 2-1.

The molecular sieve operates in an adsorption-desorption cycle, in which water is adsorbed from the superheated alcohols product during the adsorption phase, and then water is removed in the desorption (regeneration) phase using the methanol vapour product stream recovered in the distillate of the second column as a sweep gas. Because the molecular sieve is cyclic, two molecular sieves will be used in parallel such that one is always adsorbing and one is always regenerating. The sweep gas effluent (methanol vapour with the recovered water) is then recycled to the MAS reactor inlet and tar reformer at a split ratio of 80 to 20. The methanol rich sweep gas recycled to the MAS reactor improves the overall alcohols yield while the recycle to the tar reformer is reformed back to syngas. The 80 to 20 split ratio was chosen as it resulted in the maximum butanol yield for the process simulation. The bottoms product of column 1 and the distillate product of column 3 are subsequently mixed to obtain a raw mixed alcohol co-product which can be further processed to meet the U.S. Environmental Protection Agency (EPA) octamix regulation for sale [32]. The distillation columns are modelled in Aspen Plus as Radfrac blocks in equilibrium mode with a Murphree efficiency of 60% specified for all the stages.

2.2.2.6   Utilities (Steam system, power generation and cooling)

A steam cycle is integrated into the design to produce high pressure (HP) steam for power generation and low pressure (LP) steam for direct injection into the biomass gasifier and tar reformer. LP steam is also used indirectly to provide the reboiler heat duty requirements of the amine system and distillation columns, with the condensate returned to the steam cycle in a loop. HP steam in the steam cycle is generated via heat exchange with hot process streams like the flue gases from the char combustor and catalyst regenerator, and the exothermic heat from the MAS reactors. The steam system design conditions [21] are shown in Table 2-1.

Process power requirements are met by power generated by the expansion of high pressure steam to condensate through a series of steam turbines. Additional power is generated by the expansion of unconverted syngas through the turboexpander in the alcohol synthesis section.

The cooling requirements of the system are met by the use of forced-air heat exchangers and cooling water with the aim of reducing the water demand of the process. Forced-air heat exchangers are used to provide cooling for the multistage compressors, distillation and amine system condensers, and for condensing the steam turbine exhaust.

The fan power requirements of the forced-air heat exchangers are determined in Aspen Plus calculator blocks using correlations from chapter 11 of Hicks [33] between the fan power per area of a bare tube and the overall heat transfer coefficient, U. The value of U (for air cooled heat exchangers) is obtained from Perry [34] for different process fluids (i.e. water, light hydrocarbons etc.), while the heat exchanger area is determined from the heat exchanger heat duty and temperature conditions of the relevant processes.

The process design also includes a cooling water system to meet the cooling requirements of streams not provided for by heat exchange with other process streams or by forced-air heat exchangers.

2.2.2.7 Heat Integration

Heat integration was carried out alongside the utility system design to maximize the heat recovery from the process and improve energy efficiency. Maximum heat recovery targets were set using pinch analysis with the results used to design a heat exchanger network (HEN). The pinch analysis and HEN design were carried out with Aspen Energy Analyzer software. Stream data and heating and cooling duties from all sections were extracted from the Aspen Plus design, except dedicated steam, air and cooling water use systems, and air and water cooling utilities. These hot and cold process stream data and a minimum approach temperature (ΔT_{min}) of 5 °C, were used to construct composite and grand composite curves (graphical presentations of stream temperature vs. enthalpy data) as shown in Fig. 2-2. The composite and grand composite curves set the maximum energy recovery targets for the system which are used to design the HEN in the Aspen Energy Analyzer software.
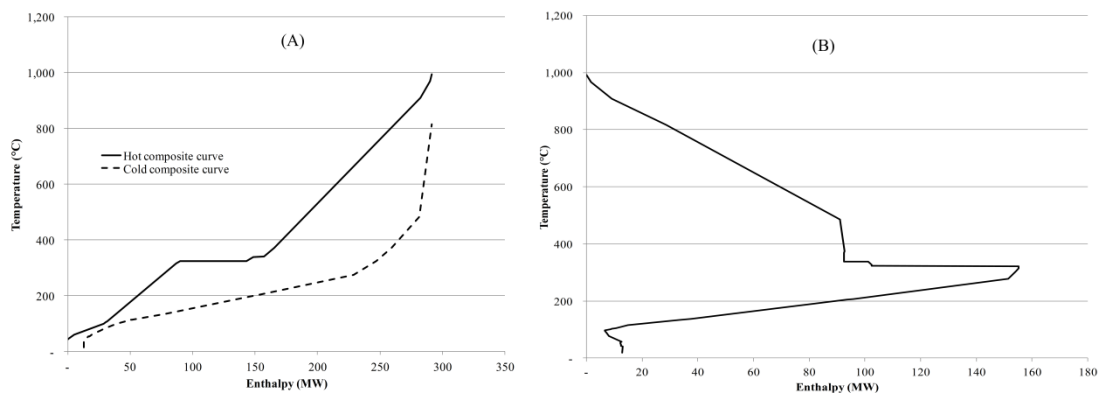
Figure 2-2. (A) Composite and (B) Grand composite curves of the process showing minimum utility requirements and maximum heat recovery targets for a ΔT_{min} of 5 °C.

For the HEN design the choice of ΔT_{min} is usually a trade-off between capital and utilities costs as an increase in ΔT_{min} means less heat exchanger area and thus less capital cost, but more utilities costs because less heat is recovered by process to process heat exchange; the opposite occurs with a decrease in ΔT_{min}. As regards this analysis, ΔT_{min} values of 5 $^{\circ}$C, 10 $^{\circ}$C and 15 $^{\circ}$C were considered with the resulting composite curves showing that the process is a threshold problem meaning that there is no net hot utility requirement. Thus for a reduction in ΔT_{min} values from 15 $^{\circ}$C to 5 $^{\circ}$C there was no improvement in operating costs savings but an incremental improvement in capital costs. However, a ΔT_{min} of 5 $^{\circ}$C was chosen as it represents a conservative capital cost estimation of the HEN. Results from NREL thermochemical biomass to ethanol design reports [9,21] show that the HEN is typically a small fraction of the overall capital costs of thermochemical plants thus it is expected that the capital cost increments due to the selection of a 5 $^{\circ}$C ΔT_{min} for the HEN will not have a significant impact on the overall capital cost of the plant.

2.2.3 Economic analysis

The economics of this process were determined based on an "n^{th} plant" assumption (in other words, the learning curve associated with building new plants of this type have been surmounted). A discounted cash flow rate of return (DCFROR) analysis is used to determine the MBSP of the plant. The MBSP is the selling price of butanol over the plant's life time at which the net present value (NPV) is zero. Capital cost estimates were based on a combination of literature data, particularly from the NREL reports [9,21], and Aspen Capital Cost Estimator$^{®}$ software. Reported values from literature were scaled using the capacity power law expression, $\frac{Cost_2}{Cost_1} = (\frac{Capacity_2}{Capacity_1})^m$, with m varying from 0.48 to 0.87, and adjusted to 2012 U.S. dollars using the Chemical

Engineering Plant Cost Index. The economic assumptions for this analysis are shown in Table 2-3.

Fixed operating costs are calculated using correlations from Seider et al. [35], and include line items such as labour related operations, maintenance, operating overhead, property tax and insurance. The variable operating costs used for this analysis are detailed in Table 2-4. The prices shown in the table (except diesel, for which the average 2012 price is shown) are converted to 2012 dollars using a reported inorganic index from the U.S. Bureau of Labour Statistics [36]. The market price of diesel in 2012 is based on the U.S. Energy Information Administration (EIA) average price for 2012 [37]. The wood feedstock cost of $75.01/ dry tonne is a combination of Idaho National Laboratory's 2012 targeted cost of $46.37/ dry ton (51.11/ dry tonne) for total feedstock logistics (from harvest through insertion to the gasifier reactor inlet) and NREL total cost of grower payment adjusted to 2012 dollars ($23.90/ dry tonne) using the inorganic index [9,36,38]. This cost also accounts for the capital and operating costs associated with the biomass feed preparation and drying section.

Table 2-3. Economic parameters and indirect costs basis used in the analysis

Economic Parameter	Basis
Cost year for analysis	2012
Plant financing by equity/debt	50%/ 50% [39]
Internal rate of return (IRR)	10% after tax [24]
Term for debt financing	10 years [24]
Interest rate for debt financing	8% [24]
Plant life/analysis period	30 years [24]
Depreciation method	Straight Line depreciation 10 years for general plant and utilities
Income tax rate	35% [24]
Plant construction cost schedule	3 years (20% Y1, 45% Y2, 35% Y3) [40]
Plant decommissioning costs	$0
Plant salvage value	$0
Start-up period	3 months [24]
Revenue and costs during start-up	Revenue = 50% of normal Variable costs = 75% of normal Fixed costs = 100% of normal [24]
Inflation rate	2.14% [39]
On-stream percentage	90% (7,884 hours/year)
Land	6.5% of Total Purchased Equipment Cost (TPEC) [35]
Royalties	6.5% of TPEC [35]
Working capital	5% of Fixed Capital Investment (excluding land) [24]
Indirect costs	
Engineering and supervision	32% of TPEC [41]
Construction expenses	34% of TPEC [41]
Contractor's fee and legal expenses	23% of TPEC [41]
Contingencies	20.4% of TPEC [9]

In this analysis the income from the electricity and mixed alcohols co-products help offset the MBSP of the plant. Electricity (industrial) is priced at $0.0654/kWh following the EIA prices of December 2012 [42]. The valuation of the mixed alcohol co-product was made on its heating value relative to gasoline, and the EIA's 2012 average value of gasoline [43]. This gasoline value also corresponds to an average West Texas Intermediate (WTI) crude oil price of 85.36 $/bbl in 2012 as reported by the EIA [44]. The mixed alcohol co-product price assumed for this analysis is $0.69/L which is 90% of the calculated $0.77/L based on its heating value.

Table 2-4. Variable operating cost parameters used in the analysis

	Literature Price	2012 Price
Feedstock cost	$61.57/ton [9,38]	$75.01/dry tonne
Olivine	$172.9/ton [9]	$319.86/tonne
MgO	$365/ton [9]	$675.23/tonne
Tar reformer catalyst	$17.74/lb [9]	$55.8/kg
Alcohol synthesis catalyst	$30/kg	$30/kg
Solids disposal (Ash)	$36/tonne [41]	$70.21/tonne
Diesel fuel (plant wide)	$3.11/gal [37]	$0.83/L or $3.11/gal
Water makeup	$0.22/tonne [16]	$0.403/tonne
Boiler feed water chemicals	$1.4/lb [9]	$7.12/kg
Cooling tower chemicals	$1.00/lb [9]	$5.97/kg
LO-CAT chemicals	$408/ton sulphur produced [9]	$583.12/tonne sulphur produced
Amine makeup	$16.94/million lb acid gas removed [9]	$46.3/ million kg acid gas removed
Waste water treatment	$0.53/tonne [41]	$0.97/tonne

2.3   Results and discussion

2.3.1   Process modelling results

Fig. 2-3 shows the product yields, power, and water demand results of the plant. The process produces mixed alcohols in a similar proportion to butanol, demonstrating the importance of an economic analysis to determine the impact of this co-product on the MBSP. The butanol production rate of 10,162 kg/hr (10,890 L/hr) is linked to the CO conversion assumptions made for the alcohol synthesis section thus highlighting the importance of a sensitivity analysis to see how the production rate varies with the CO conversion and the resultant impact on the MBSP.
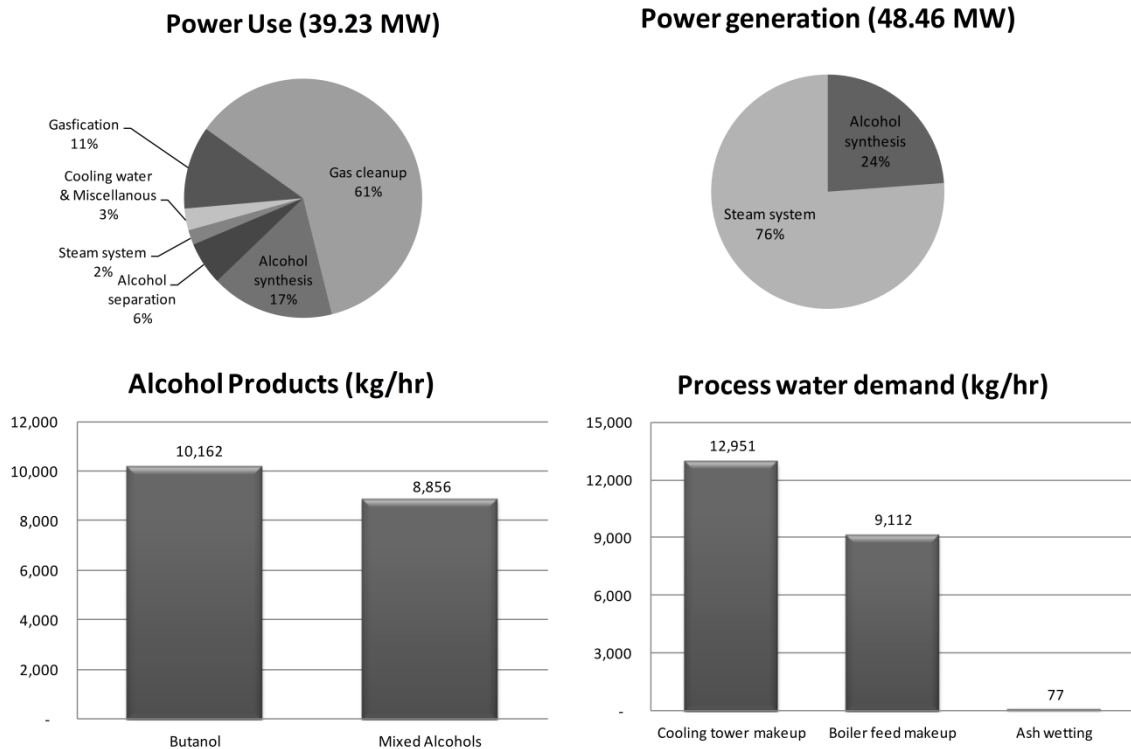
Figure 2-3. Process results of plant production, water demand, power generation and use.

Although this study was centred on butanol production, one of the benefits of carrying out the heat integration analysis is the production of excess power as a co-product, mainly as a result of extra steam generation and its subsequent expansion in the steam turbines. This net 9.23 MW power can be exported to the grid and used to offset some of the butanol production costs. As shown in Fig. 2-3, the greatest power use is attributed to the gas cleanup and conditioning section because of the large parasitic power requirement of the amine system and first syngas multicompressor.

Water use is an important environmental consideration especially in water-constrained regions. Therefore one of the design considerations taken into account for this process was the minimization of fresh water use. Water loss in the system is mainly as a result of evaporation and drift losses in the cooling tower, and thus air cooling is used to replace water cooling for processes were it is feasible (i.e. compressor interstage

cooling, steam turbine condenser and distillation column condensers). The overall water demand of the thermochemical butanol plant is 2.04 L water/ L butanol, which is comparable to the thermochemical biomass-to-ethanol process of Phillips et al [21]. Finally, as shown in Table 2-5, the plant's overall efficiency on a lower heating value (LHV) basis is 46%, with approximately 44% of the biomass energy ending up in the butanol and mixed alcohols products.

Table 2-5. Plant efficiency calculation (LHV basis)

Plant data	Units	Value
Biomass flow rate (bone dry)[*]	kg/hr	75,000
Biomass, LHV	MJ/kg	18.59
Biomass thermal energy (LHV× flowrate) [A]	MJ/hr	1,394,250
Net electricity generated [B]	MJ/hr	33,253
Mixed Alcohols prod. flowrate	kg/hr	8,857
Mixed Alcohols prod., LHV	MJ/kg	30.85
Mixed Alcohols prod. thermal energy (LHV× flowrate) [C]	MJ/hr	273,234
Butanol prod., flowrate	kg/hr	10,162
Butanol prod., LHV	MJ/kg	32.96
Butanol prod. thermal energy (LHV× flowrate) [D]	MJ/hr	334,915
% Plant efficiency [(B + C + D)/A]	**%**	**46.0**

2.3.2 Economic analysis results

The total capital investment cost of the plant is shown in Table 2-6, with Fig. 2-4 illustrating the contributions of the process areas to the total direct costs (TDC). The gas cleanup area has the highest contribution to the TDC of $58 million due to major cost items such as the tar reformer, syngas compressor and amine system. The steam system and gasification areas are the next major cost contributors respectively due to items such as the steam turbines in the former, and gasifier in the latter. A detailed breakdown of the TDC is given in the supplementary material.

---

[*] "bone dry" refers to the biomass without any moisture. It is used because the LHV and HHV basis are typically expressed as bone dry.

Table 2-6. Total Capital Investment calculation

Total Purchased Equipment cost (TPEC)		104,360,000
Installation factor		2.05
Total direct costs (TDC)	TPEC × Installation factor	**213,770,000**
engineering and supervision	32% of TPEC	33,400,000
construction expenses	34% of TPEC	35,480,000
contractor's fee and legal expenses	23% of TPEC	24,000,000
contingency	20.4% of TPEC	21,290,000
Total Indirect Costs (TIC)	TIC	**114,170,000**
Total depreciable capital (TDep)	TDep = TDC + TIC	**327,940,000**
Royalties	2% of TDep	6,560,000
Land (pure real estate)	2% of TDep	6,560,000
Fixed Capital Investment (FCI)	FCI = TDep + Royalties + Land	**341,060,000**
Working Capital (WC)	5% of FCI (excluding Land)	16,730,000
Total Capital Investment (TCI)	TCI = FCI + WC	**357,780,000**

The DCFROR analysis for the MBSP was carried out using the economic assumptions and values discussed in section 2.2.3, with details available in the supplementary material. The obtained MBSP value of $0.83/L is comparable to the minimum selling price of biochemical butanol reported in the literature as shown in Table 2-7. This wide range in prices of biochemical butanol is as a result of assumptions and key parameters related to feedstock costs, co-products prices and yields amongst others. For example, the key difference between the $2.71/L biochemical butanol value reported in the literature by Pfromm et al. [27] and the other reported values is because of a higher feedstock cost and lower butanol yield. As relates to this study, this highlights the importance of a rigorous sensitivity analysis to investigate the impact of key parameters on the thermochemical biobutanol's MBSP.

Table 2-7. Techno-economic assumptions for biochemical butanol production available in the literature

Assumptions	Qureshi et al. [26]	Kumar et al. [8]	Pfromm et al. [27]	Qureshi and Blaschek [25]
Cost year	2012	2010	2007	1999
Feedstock and feedstock cost	Wheat straw - $0.024/kg	Switchgrass - $0.04/kg	Corn - $1.853/kg	Corn - $0.71 /kg
Co-products and price				
Ethanol	$0.8/kg	$0.89/kg	$0.59/kg	$0.33/kg
Acetone	$1.3/kg	$0.81/kg	$0.92/kg	$0.33/kg
Plant capacity (tonnes butanol/year)	150,000	10,000	54,370	121,600
Butanol yield (kg butanol/kg feedstock)	0.2	0.234	0.11	0.33
Fermentation bacteria	Clostridium beijerinckii P260		Clostridium acetobutylicum	Clostridium beijerinckii BA101
Butanol price (2012 $)	$1.05/L	$0.59/L	$2.71/L	$0.87/L
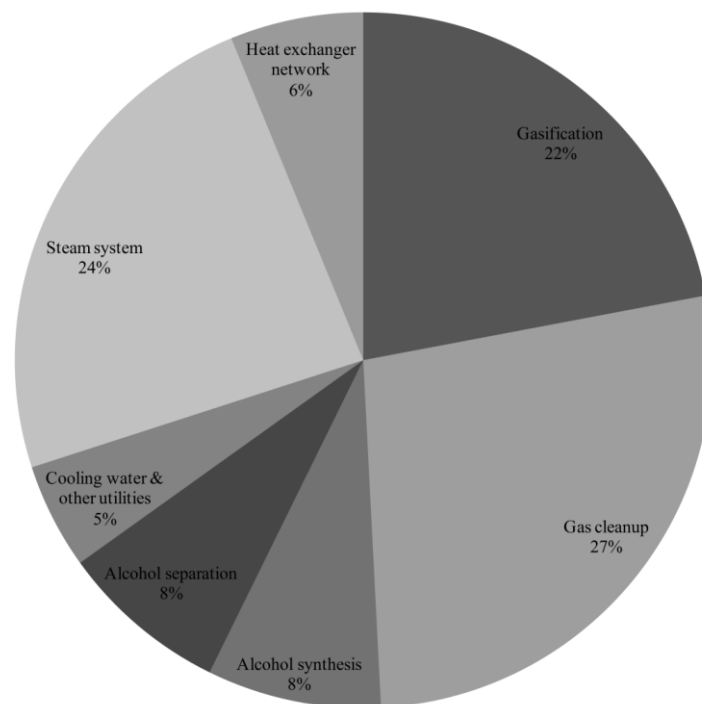
Figure 2-4. Contribution of process areas to the Total Direct Cost of $214 MM.

2.3.3 Sensitivity and uncertain scenario analysis

2.3.3.1   Sensitivity analysis

Due to inherent uncertainties in some of the key costs and parameters assumed for this study, it is important to carry out a sensitivity analysis to evaluate the impact that variations in these parameters will have on the MBSP. The results of the sensitivity analysis in Fig. 2-5 show that the internal rate of return (IRR), mixed alcohols co-product value, total depreciable capital, and feedstock costs have the greatest impact on the MBSP. The largest impact is caused by the IRR, as varying the IRR from 5% to 15% causes the MBSP to vary from $0.66 to $1.05/L. As expected, because of the significant quantity of mixed alcohols co-product produced by the plant, its valuation has a significant effect on the MBSP, second only to the IRR. Varying the selling price of the mixed alcohol co-product at approximately $\pm$22% of its base value results in an MBSP change from the base MBSP of $0.83/L to $0.67/L and $1.00/L, respectively ($\mp$20.75% of the base MBSP). A $\pm$30% change in the total depreciable capital results in an MBSP change from the base case to $0.97/L and $0.70/L, respectively ($\pm$15.72% from the base value). Since the woody biomass feedstock is the major raw material for this process, it is unsurprising that its cost also has a major impact on the MBSP. As expected, a change in the biomass feedstock cost from its base case value of $74/ dry tonne to $60/ dry tonne and $90/ dry tonne ($\pm$20% from the base value) results in a MBSP of $0.73/L and $0.94/L, respectively as there is a direct correlation between raw material cost and the MBSP. The MBSP reduces with an increase in the percentage inflation and vice versa because components of the profit (total product sales and total costs) are assumed to inflate at the same rate.
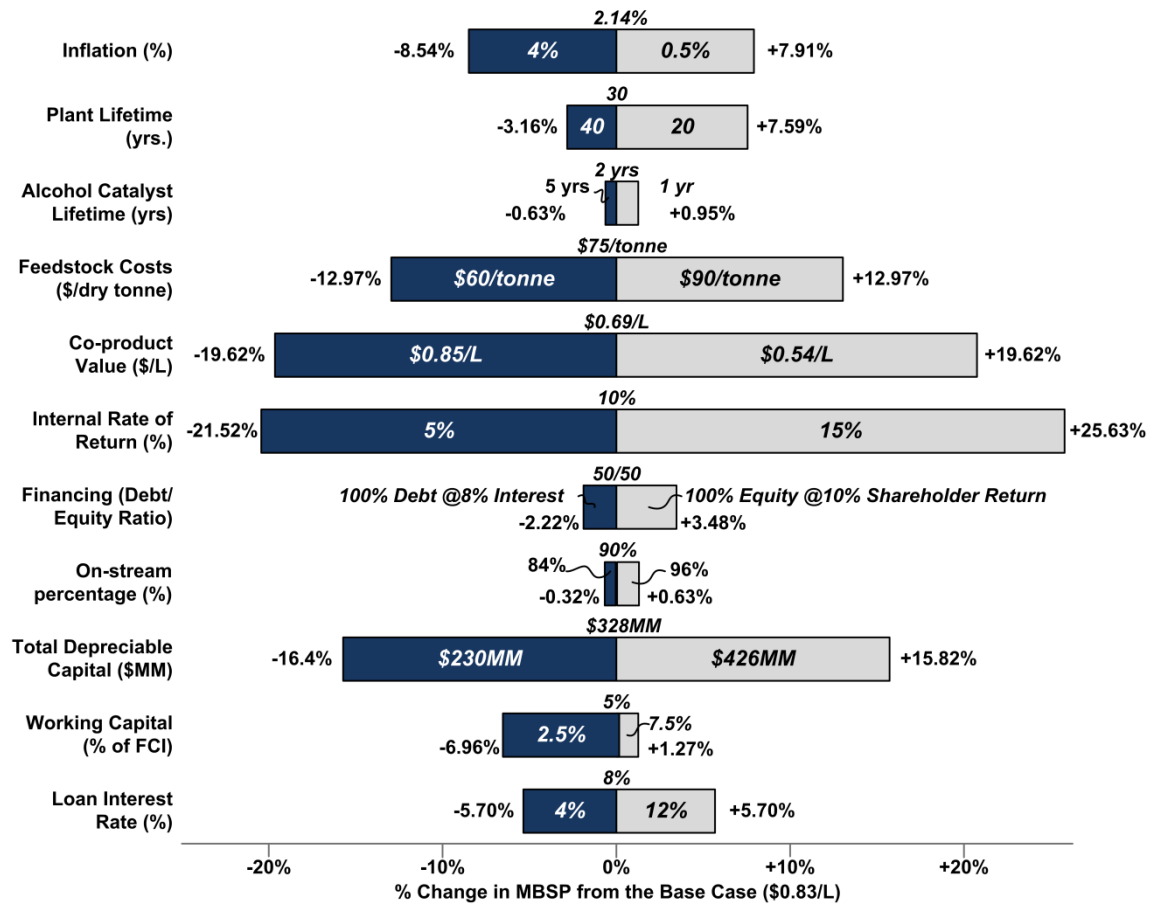
Figure 2-5. The effects of changing key parameters from their base case values on MBSP.

2.3.3.2   Impact of the catalyst conversion on the MBSP

Most of the important parameters considered in Fig. 2-5 cannot be determined until the time of plant construction (such as IRR and market prices). However, the catalyst activity (measured as the percent conversion of CO on a CO_2-free basis) has an important impact on the economics and can be improved during the early research phases. Shown in Fig. 2-6 is a sensitivity analysis on the impact of the CO conversion on the MBSP at average 2012 crude oil prices [44], increasing the catalyst conversion to 55% (which is 5% higher than the NREL target [21]) from the base case assumption of 40% had only a small (4.11%) improvement on MSBP. However when the CO conversion is reduced to 21%, the MSBP increases by 10.44% to $0.92/L. Further

analysis shows that a CO conversion as low as 18% is enough to achieve a MSBP of $1.00/L, which is competitive with reported values of ABE-derived butanol [8,25-27]. Noting that the current CO conversion of this particular catalyst is reported to be 8.5% [15], 18% is a reasonably achievable research target in the near term. Note that this target has already been achieved by high pressure modified methanol synthesis catalysts albeit at much higher pressure and temperature conditions [14]. However, 8.5% is not likely to be enough, since it results in an MSBP as high as $1.56/L.
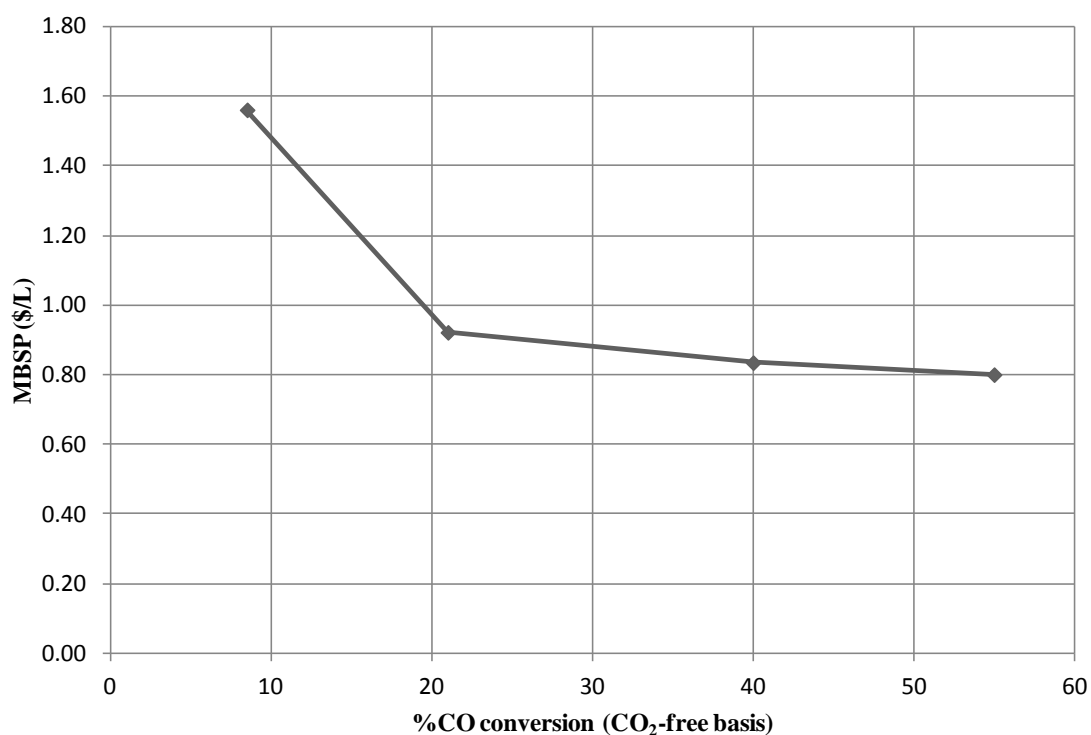
Figure 2-6. Impact of changes in CO conversion on the MBSP at average 2012 crude oil prices [44]

2.3.3.3 Impact of crude oil price changes on MBSP

In the analyses that has been presented so far, the MBSP has some correlations to gasoline prices and thus by extension, to crude oil prices. This is because this study assumes that mixed alcohols have market demands and trends similar to that of gasoline and thus the mixed alcohols have been priced relative to gasoline. It is thus of interest to

see how changes in crude oil prices impact the MBSP. In line with the assumptions for mixed alcohols, butanol can be sold as a commodity with market demands and trends similar to that of gasoline and can thus be priced as gasoline adjusted on a butanol heating value basis (BEQ gasoline).

In general, on a per litre basis the price of crude oil contributes 50 % to 70 % of retail gasoline prices with the other components of the gasoline price being taxes, refining costs, and distribution & marketing costs. For our analysis we will make use of WTI crude oil which is reported by the EIA and is generally used in the trade press as a representative for world crude oil prices. In 2012 the average WTI crude oil price was $85.355/bbl [44] representing 55.2 % of the average 2012 U.S. retail gasoline price (all grades, all formulations) [43]. This value of 55.2 % will be used in the subsequent analysis to extrapolate retail gasoline prices and thus prices for the mixed alcohols and BEQ gasoline.

The range of crude oil prices considered for this analysis represents prices which have occurred in the past decade and a half. In January 2002 WTI crude oil prices were $19.73/bbl and rose to a high of $134.02/bbl by July 2008 before dropping to $39.26/bbl by February 2009. In recent times they have shown a steady increase with April 2014 prices at $102.04/bbl [44].
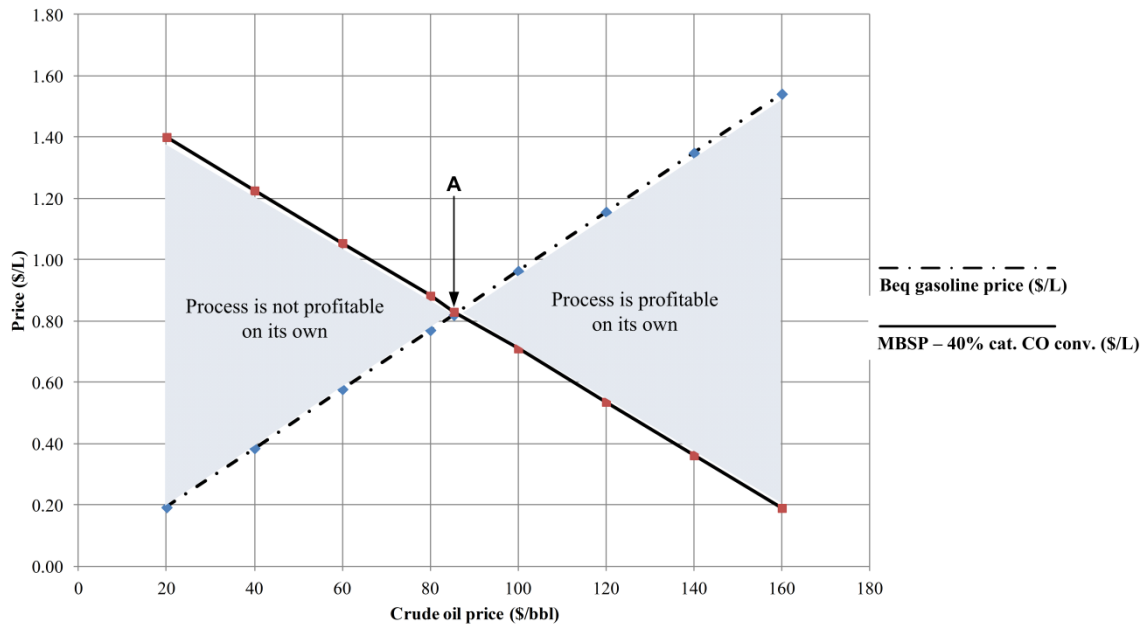
Figure 2-7. Impact of crude oil price changes on the MBSP of the base case process

Fig. 2-7 shows the impact of changes in crude oil prices on the MBSP for the base case 40 % catalyst CO conversion. Also shown is the butanol equivalent (BEQ) gasoline price which reflects how the market prices the butanol product. Point A shows the break-even value for the 40 % catalyst conversion and represents the point at which the thermochemical biobutanol process is competitive with the BEQ gasoline. This point shows that at a crude oil price of $85.36/bbl corresponding to an MBSP of $0.825/L the 40 % catalyst conversion becomes competitive with the BEQ gasoline. The shaded region to the left of point A signifies scenarios in which the MBSP is greater than the BEQ gasoline and thus the process cannot compete with the BEQ gasoline without the help of government subsidies/mandates. However, the shaded region to the right of point A represents scenarios in which the BEQ gasoline is greater than the MBSP and the process is thus profitable on its own.
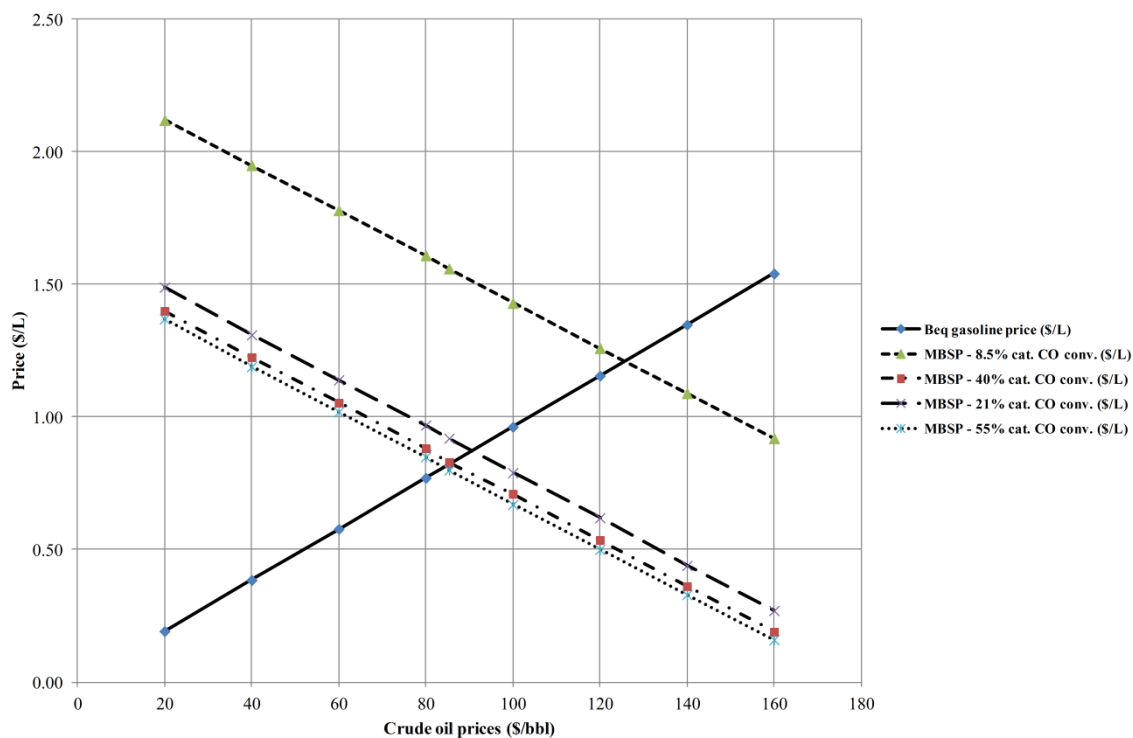
Figure 2-8. Impact of crude oil price changes on the MBSP for different catalyst CO conversions

In Fig. 2-8 the same idea as Fig. 2-7 is illustrated for the different catalyst conversions considered in section 2.3.3.2. The break-even point for the 8.5 % catalyst CO conversion reported in the literature by Herman et al. [15] is at $126/bbl corresponding to a MBSP of $1.22/L. Improving the catalyst activity to 21 % results in a break-even point of $92/bbl and MBSP of $0.86/L, while achieving a 55 % catalyst activity results in a break-even point of $84/bbl and $0.8/L. At April 2014 crude oil prices of $102.04/bbl, an MBSP of $0.98/L will be required for the process to break even. This can potentially be achievable for this particular catalyst if near term improvements for the CO to 18 % are achieved as discussed in section 2.3.3.2. If crude oil prices continue to show a steady increase and reach the historic July 2008 price of $134.02/bbl, then the process becomes profitable at the literature reported 8.5 % catalyst conversion.

Note that this analysis is true only on a purely quantitative basis, and is in line with the market assumptions made for the bioalcohols. In reality, renewable fuels have a number of uncertainties especially as regards government policies, and other potential benefits such as carbon emission reductions, fossil fuel energy savings, energy security, economic development etc. which can be difficult to quantify. Despite these uncertainties, an attempt is made in the next section to quantify the impact of the U.S. renewable fuel standard II (RFS) on the process economics.

2.3.3.4   Impact of the U.S. renewable fuel standards on the MBSP

The U.S. RFS sets required volumes of renewable fuels to be blended into the U.S. fuel supply by diesel and gasoline producers and importers (obligated parties) [45]. Each gallon of blended renewable fuel is identified by a Renewable Identification Number (RIN) which is generated by the producer or importer of the renewable fuel, and is submitted to the regulators by the obligated parties to show that they meet their Renewable Volume Obligations. After blending the renewable fuel, the RINs may be detached from the gallons of renewable fuel that generated them and sold as a commodity.

The major factors that determine the RIN value are the RFS policy, renewable fuels production in the U.S., and motor fuels demand in the U.S. [45]. These factors create a supply and demand market that drives the RIN price, thus RIN prices act as a bridge between the renewable fuels supply and the demand driven by the government mandate and can thus be seen as an incentive/subsidy for producers of renewable fuels.
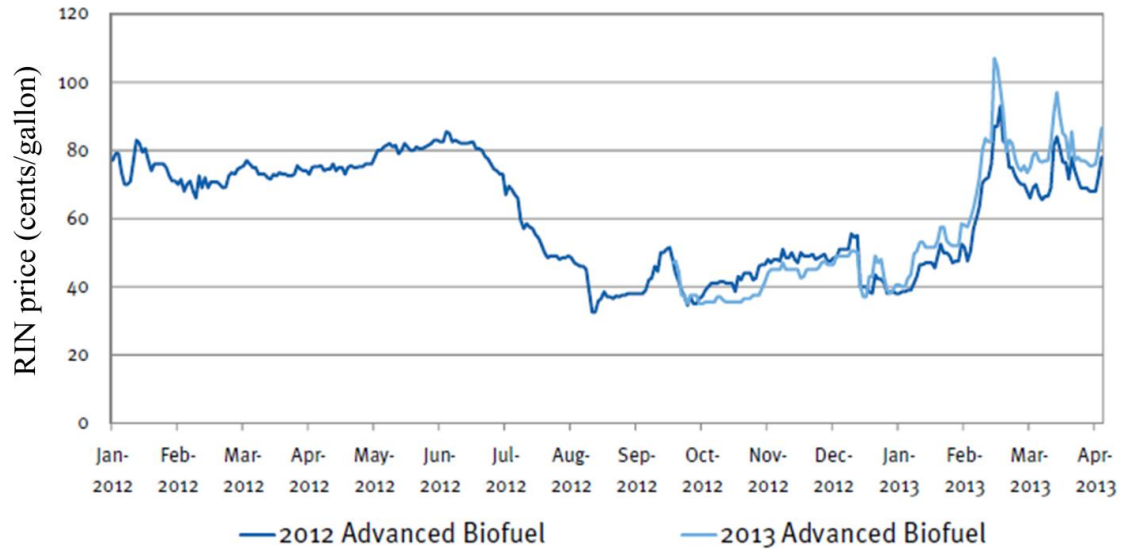
Figure 2-9. RIN prices for advanced biofuels (2012 and 2013 vintages) between January 2012 and April 2013 [46].

According to the updated U.S. RFS, biobutanol from the thermochemical lignocellulosic biomass to butanol route can be classified as an advanced biofuel. In general because the demand for these advanced biofuels far outstrips their supply, the RIN prices are quite high. Fig. 9 shows the January 2012 to August 2013 RIN prices for 2012 and 2013 advanced biofuels (the year describes the period the RIN was generated). From January 2012 to June 2012 the RIN price hovers around $0.80/gallon before dropping close to $0.40/gallon between July 2012 and January 2013 and subsequently rising to $0.80/gallon by April 2013.

The RIN price of 62 cents/gallon ($0.16/L) is an average value over the period shown in Fig. 2-9 and will be considered as a MBSP discount/subsidy in the following analysis on the impact of the advanced biofuels RIN values on the economics of the process. In general the RIN values decrease the MBSP of the process thus reducing the crude oil prices at which the process is competitive as illustrated by Fig 2-10. At the base case 40 % catalyst CO conversion the break even MBSP becomes $0.75/L (crude oil price of

$76/bbl) which is a 9.1 % reduction from the break even MBSP price of $0.825/L for the non-subsidized case discussed in section 2.3.3.3. At the 8.5 % catalyst CO conversion case the break even MBSP becomes $1.13/L (crude oil price of $117/bbl) representing a 7.4 % reduction from the equivalent non-subsidized case. These results are interesting because they demonstrate the ability of government policies to encourage investment in new technologies. In fact, from the enactment of the U.S. RFS in 2007 till the second quarter of 2012 more than $3.4 billion have been invested in advanced biofuels production by venture capitalists alone [47].
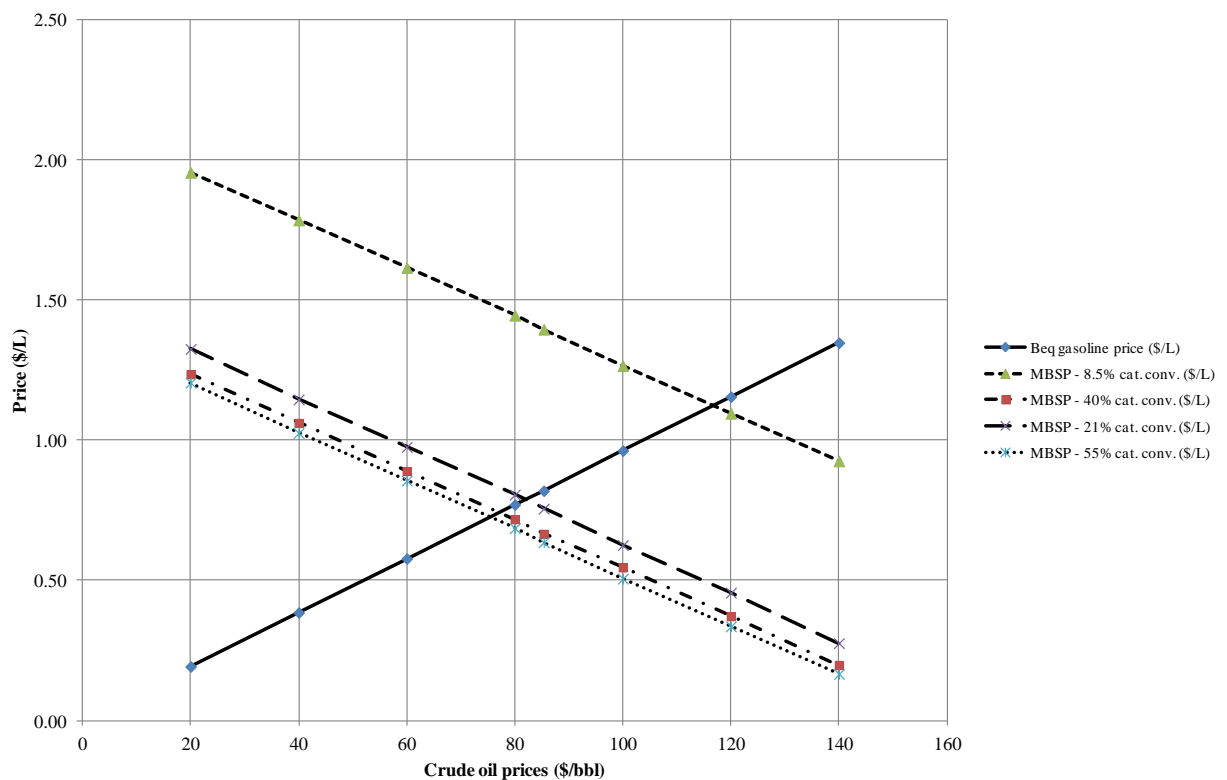
Figure 2-10. Impact of crude oil price changes on the MBSP for different catalyst CO conversions, with subsidies as relates to RIN prices accounted for.

2.3.3.5   Scenario analysis

In reality, the parameters used for the sensitivity analysis will generally vary at the same time, thus different scenarios in which the most significant parameters from the

sensitivity analysis are varied simultaneously are considered to see the impact on the MBSP. The scenarios considered are identified as: very optimistic, optimistic, base case, pessimistic and very pessimistic. For these scenarios, IRR, feedstock costs, mixed alcohol co-product value, and total depreciable capital were varied within the upper and lower limits discussed in section 2.3.3.1. Also included in the analysis is the catalyst CO conversion using the values that have been discussed in section 2.3.3.2. The results of the scenario analysis are shown in Fig. 2-11. The very optimistic case represents a scenario symbolic of a very mature technology in which long term MAS catalyst CO conversion targets have been achieved, a high demand for mixed alcohols exists, and feedstock costs are low. In this scenario the MBSP is $0.28/L with a break-even crude oil price of $29.10/bbl. At the other end of the spectrum the very pessimistic case represents a scenario similar to a 'next' plant for which no catalyst improvements have been achieved, low demand for mixed alcohols, and high feedstock costs. The MBSP for this scenario is $2.30/L with a very high crude oil price of $238.96/bbl required to break-even. However, these two scenarios will tend to have a low probability of occurring in reality. More probable will be scenarios between the optimistic to pessimistic range where the MBSP ranges from $0.55/L to $1.22/L with break-even crude oil prices ranging from $57.14/bbl to $126.75/bbl. This range is competitive with biochemical butanol prices reported in the literature [8,25-27].

Scenarios	Very optimistic	Optimistic	Base case	Pessimistic	Very pessimistic
Internal Rate of Return (%)	5	7.5	10	12.5	15
Feedstock costs ($/per dry tonne)	60.01	67.52	75.01	82.52	90.01
Mixed Alcohol co-product value ($/L)	0.85	0.77	0.69	0.62	0.54
Total depreciable Capital ($MM)	230	279	328	377	426
Catalyst % CO conversion	55	40	40	21	8.5
MBSP ($/L)	0.28	0.55	0.83	1.22	2.30
Break-even crude oil price ($/bbl)	29.10	57.14	86.23	126.75	238.96
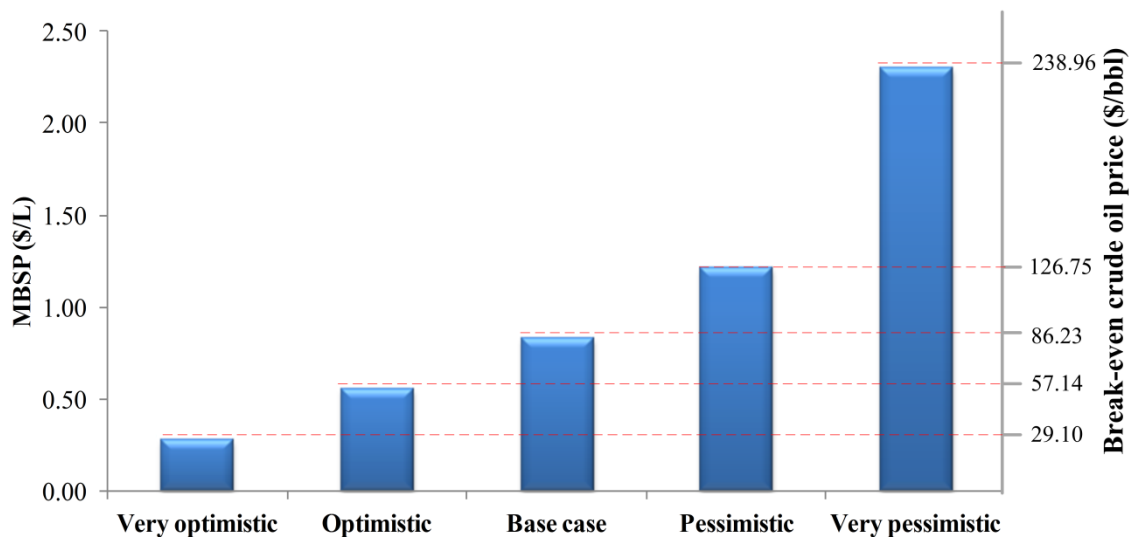
Figure 2-11. Impact of different economic scenarios on MBSP.

2.4   Conclusion

A novel biobutanol process using a thermochemical approach was designed, simulated, and its economics assessed. The determined MBSP ($0.83/L) for the base case is competitive with BEQ gasoline at crude oil prices greater than $85.36/bbl. A key assumption is the catalyst CO conversion, with the sensitivity analysis showing that a potential near term research target of doubling CO conversion results in competitive economics especially if crude oil prices stay higher than $92/bbl. In addition, the feedstock costs, IRR and mixed alcohols co-product value have the most significant impacts on the economics. It has also been shown that the application of government policies such as the U.S. RFS further improve the economics of this technology. Furthermore, thermochemical biobutanol is economically competitive with biochemical butanol even for a wide range of potential future market conditions. In future work the

potential of improving the economics of this process by consideration of cheaper feedstock, different process configurations, and process intensification will be assessed.

2.5   References

[1] Wood, M. S.; Layzell, D. B. A Canadian Biomass Inventory: Feedstocks for a Bio-based economy. *BIOCAP Canada Foundation* **2003**,18–24.

[2] U.S. Department of Energy. *U.S. Billion-Ton Update: Biomass Supply for a Bioenergy and Bioproducts Industry*; Oak Ridge National Lab: TN, August 2011.

[3] U.S. Energy Information Administration. Annual Energy Outlook 2014. http://www.eia.gov/forecasts/aeo/pdf/0383(2014).pdf (accessed May 28, 2014).

[4] International Energy Agency. World Energy Outlook 2013. http://www.worldenergyoutlook.org/media/weowebsite/2013/WEO2013_Ch06_Re newables.pdf (accessed May 28, 2014).

[5] Congress U. S. Energy independence and security act of 2007. *Public Law* **2007**, *2*, 110–140.

[6] Kumar, M.; Gayen, K. Developments in biobutanol production: new insights. *Appl. Energy* **2011**, *88(6)*, 1999–2012.

[7] Ranjan, A.; Moholkar, V. S. Biobutanol: science, engineering, and economics. *Int. J. Energy Resour.* **2012**, *36(3)*, 277–323.

[8] Kumar, M.; Goyal, Y.; Sarkar, A.; Gayen, K. Comparative economic assessment of ABE fermentation based on cellulosic and non-cellulosic feedstocks. *Appl. Energy* **2012**, *93*, 193–204.

[9] Dutta, A.; Talmadge, M.; Hensley, J.; Worley, M.; Dudgeon, D.; Barton, D.; Groenedijk, P.; Ferrari, D.; Stears, B.; Searcy, E. M.; Wright, C. T.; Hess, J. R. *Process Design and Economics for Conversion of Lignocellulosic Biomass to Ethanol*; Technical Report for National Renewable Energy Laboratory: Golden, CO, 2011.

[10] Lee, S. Y.; Park, J. H.; Jang, S. H.; Nielsen, L. K.; Kim, J.; Jung, K. S. Fermentative butanol production by clostridia. *Biotechnol. Bioeng.* **2008**, *101(2)*, 209–228.

[11] Kraemer, K.; Harwardt, A.; Bronneberg, R.; Marquardt, W. Separation of butanol from acetone–butanol–ethanol fermentation by a hybrid extraction–distillation process. *Comput. Chem. Eng.* **2011**, *35(5)*, 949–963.

[12] Nexant Inc. *Equipment Design and Cost Estimation for Small Modular Biomass Systems, Synthesis Gas Cleanup, and Oxygen Separation Equipment, Task 9: Mixed Alcohols from Syngas State of Technology*; Technical Report for National Renewable Energy Laboratory: Golden, CO, 2006.

[13] Surisetty, V. R.; Dalai, A. K.; Kozinski, J. Intrinsic Reaction Kinetics of Higher Alcohol Synthesis from Synthesis Gas over a Sulfided Alkali-Promoted Co− Rh− Mo Trimetallic Catalyst Supported on Multiwalled Carbon Nanotubes (MWCNTs). *Energy Fuels* **2010**, *24(8)*, 4130–4137.

[14] Verkerk, K. A. N.; Jaeger, B.; Finkeldei, C.; Keim, W. Recent developments in isobutanol synthesis from synthesis gas. *Appl. Catal., A* **1999**, *186*, 407–431.

[15] Herman, R. G. Advances in catalytic synthesis and utilization of higher alcohols. *Catal. Today* **2000**, *55(3)*, 233–245.

[16] Fang, K.; Li, D.; Lin, M.; Xiang, M.; Wei, W.; Sun, Y. A short review of heterogeneous catalytic process for mixed alcohols synthesis via syngas. *Catal. Today* **2009**, *147(2)*, 133–138.

[17] Surisetty, V. R.; Dalai, A. K.; Kozinski, J. Alcohols as alternative fuels: An overview. *Appl. Catal., A* **2011**, *404(1)*, 1–11.

[18] Christensen, P.; Dysert, L. R. *Cost estimate classification system- as applied in engineering, procurement, and construction for the process industries - American Association of Cost Engineers (AACE) No. 18R-97;* AACE International, November 2011.

[19] Sims, R. E.; Mabee, W.; Saddler, J. N.; Taylor, M. An overview of second generation biofuel technologies. *Bioresour. Technol.* **2010**, *101(6)*, 1570–1580.

[20] Gnansounou, E.; Dauriat, A. Techno-economic analysis of lignocellulosic ethanol: A review. *Bioresour. Technol.* **2010**, *101(13)*, 4980–4991.

[21] Phillips, S.; Aden, A.; Jechura, J.; Dayton, D.; Eggeman, T. *Thermochemical Ethanol via Indirect Gasification and Mixed Alcohols Synthesis of Lignocellulosic Biomass*; Technical Report for National Renewable Energy Laboratory: Golden, CO, 2007.

[22] Zhu, Y.; Gerber, M. A.; Jones, S. B.; Stevens, D. J. *Analysis of the effects of compositional and configurational assumptions on Product costs for the thermochemical conversion of lignocellulosic biomass to Mixed Alcohols - FY 2007 Progress report*; Pacific Northwest National Laboratory: Richland, Washington, February 2009.

[23] Dutta, A.; Bain, R. L.; Biddy, M. J. Techno-economics of the production of mixed alcohols from lignocellulosic biomass via high-temperature gasification. *Environ. Prog. Sustain. Energy* **2010**, *29(2)*, 163–174.

[24] Dutta, A.; Talmadge, M.; Hensley, J.; Worley, M.; Dudgeon, D.; Barton, D.; Groenedijk, P.; Ferrari, D.; Stears, B.; Searcy, E. M.; Wright, C. T.; Hess, J. R. Techno-economics for conversion of lignocellulosic biomass to ethanol by indirect gasification and mixed alcohol synthesis. *Environ. Prog. Sustain. Energy* **2012**, *31(2)*, 182–190.

[25] Qureshi, N.; Blaschek, H. P. Economics of Butanol Fermentation using Hyper-Butanol Producing Clostridium Beijerinckii BA101. *Food Bioprod. Process* **2000**, *78(3)*, 139–144.

[26] Qureshi, N.; Saha, B. C.; Cotta, M. A.; Sing, V. An economic evaluation of biological conversion of wheat straw to butanol: A biofuel. *Energy Conversion and Management* **2013**, *65*, 456–462.

[27] Pfromm, P. H.; Amanor-Boadu, V.; Nelson, R.; Vadlani, P.; Madl, R. Bio-butanol vs. bio-ethanol: A technical and economic assessment for corn and switchgrass fermented by yeast or Clostridium acetobutylicum. *Biomass and Bioenergy* **2010**, *34(4)*, 515–524.

[28] Okoli, C.; Adams II, T. A. Techno-economic analysis of a thermochemical lignocellulosic biomass-to-butanol process. In Proceedings of *European Symposium on Computer Aided Process Engineering (ESCAPE-24)*; Budapest, In Press.

[29] Spath, P.; Aden, A.; Eggeman, T.; Ringer, M.; Wallace, B.; Jechura, J. *Biomass to Hydrogen Production Detailed Design and Economics Utilizing the Batelle Columbus Laboratory Indirectly Heated Gasifier*; Technical Report for National Renewable Energy Laboratory: Golden, CO, 2005.

[30] *Suppliers Association (GPSA) Engineering Data book*; Gas Processors and Suppliers Association: Tulsa, OK, 2004.

[31] Burcham, M. M.; Herman, R. G.; Klier, K. Higher alcohol synthesis over double bed Cs-Cu/ZnO/Cr$_2$O$_3$ catalysts: optimizing the yields of 2-methyl-1-propanol (isobutanol). *Ind. Eng. Chem. Res.* **1998**, *37(12)*, 4657–4668.

[32] U.S. Environment Protection Agency. Modification to Octamix Waiver Regarding TOLAD MFA-10A. http://www.epa.gov/otaq/fuels/registrationfuels/notices.htm (accessed July 31, 2013).

[33] Hicks, T. G.; Wills, K. D. *Handbook of mechanical engineering calculations*; McGraw-Hill: New York, 2006.

[34] Perry, R. H.; Green, D. W. *Perry's Chemical Engineers' Handbook*; 7th ed., McGraw Hill: New York, 1997.

[35] Seider, W. D.; Seader, J. D.; Lewin, D. R. *Product & Process Design Principles: Synthesis, Analysis and Evaluation*; 3rd ed., John Wiley & Sons: New Jersey, 2009.

[36] U.S Department of Labor - Bureau of Labour Statistics. Producer Price Indexes - April 2013. http://www.bls.gov/news.release/pdf/ppi.pdf (accessed July 31, 2013).

[37] U.S Energy Information Administration (EIA - Official Energy Statistics from the U.S. Government) U.S. No 2 Diesel Wholesale/Resale Price by Refiners. http://www.eia.gov/dnav/pet/hist/LeafHandler.ashx?n=PET&s=EMA_EPD2D_PWG_NUS_DPG&f=A (accessed July 31, 2013).

[38] Searcy, E.; Wright, C.; Hess, J. R.; Westover, T. *Logistics Costs for the 2012 Conventional Woody Biomass Feedstock Supply for Thermochemical conversion*; Idaho National Laboratory memo to the U.S. Department of Energy: January 2012.

[39] Consonni, S.; Katofsky, R. E.; Larson, E. D. A gasification-based biorefinery for the pulp and paper industry. *Chem. Eng. Res. Des.* **2009**, *87(9)*, 1293–1317.

[40] Flnkenrath, M. *Cost and performance of carbon dioxide capture from power generation* (No. 2011/5); Organization for Economic Co-operation and Development (OECD): 2011.

[41] Peters, M. S.; Timmerhaus, K. D.; West, R. E. *Plant Design and Economics for Chemical Engineers*; McGraw-Hill Science/Engineering/Math: Massachusetts, 2003.

[42] U.S Energy Information Administration (EIA - Official Energy Statistics from the U.S. Government) Average Retail Price of Electricity to Ultimate Customers. http://www.eia.gov/electricity/monthly/epm_table_grapher.cfm?t=epmt_5_3 (accessed July 31, 2013).

[43] U.S Energy Information Administration (EIA - Official Energy Statistics from the U.S. Government) Petroleum & Other Liquids - U.S. All Grades All Formulations Retail Gasoline Prices. http://www.eia.gov/dnav/pet/hist/LeafHandler.ashx?n=PET&s=EMM_EPM0_PTE_NUS_DPG&f=A (accessed July 31, 2013).

[44] U.S Energy Information Administration (EIA - Official Energy Statistics from the U.S. Government) Petroleum & Other Liquids - Cushing, OK Crude Oil Future Contract 1.

http://www.eia.gov/dnav/pet/hist/LeafHandler.ashx?n=pet&s=rclc1&f=m (accessed May 28, 2014).

[45] U.S. Environmental Protection Agency - Fuels and Fuel Additives, Renewable Fuel Standard.

http://www.epa.gov/otaq/fuels/renewablefuels/compliancehelp/rfs2-aq.htm (accessed May 28, 2014).

[46] Argus White Paper: Argus RINs prices.

https://media.argusmedia.com/~/media/Files/PDFs/White%20Paper/Argus%20RINs%20Prices%202013.pdf (accessed June 6, 2014).

[47] U.S. Environmental Protection Agency. Regulation of Fuels and Fuel Additives: 2013 Renewable Fuel Standards; Final Rule. Federal Register 2013, 78(158), 49794–49830.

CHAPTER 3 Design and economic analysis of a macroalgae-to-butanol process via a thermochemical route

The contents of this chapter have been published in the following peer reviewed literature journal:

Okoli, C.O., Adams, T.A., Brigljević, B. and Liu, J.J., 2016. Design and economic analysis of a macroalgae-to-butanol process via a thermochemical route. Energy Conversion and Management, 123, pp.410-422.

3.1   Introduction

Macroalgae or seaweed is a term used to describe non-vascular large aquatic photosynthetic plants, thus they differ from microalgae which are unicellular [1,2]. Globally in 2012, seaweed production was estimated to be about 24.9 million wet-metric tonnes (85 - 90 % moisture content) with 96% coming from aquaculture production [3]. Most of the world's farmed macroalgae is produced in Asia, with 99% of the world's production coming from that region [4]. Macroalgae has traditionally been grown for use as edible food, or as a raw material from which hydrocolloids utilized in the pharmaceutical and food industries are extracted.

Recently, there has been an increased interest in growing macroalgae for use in biofuel production. This is because macroalgae, which is a feedstock for third generation biofuels, have fast growth rates with up to 4–6 harvest cycles per year. Unlike first and second generation biofuel feedstocks, macroalgae can be grown in the sea thus eliminating issues relating to land use and irrigation water [4]. Furthermore, macroalgae is preferable to microalgae (also a third generation biofuel feedstock) for biofuel production because its plant-like characteristics make it easier to harvest, and its high concentration of carbohydrates in comparison to microalgae make it a potentially better biofuel feedstock [2,5,6].

Several studies have been conducted by government research institutes around the world investigating the potential of macroalgae as a biofuel feedstock. One such preliminary study by the Energy Research Center of the Netherlands (ECN) investigated the feasibility of producing biofuels from macroalgae cultivated offshore in the North Sea [7]. The study recommended carrying out a pilot scale seaweed cultivation experiment in the North Sea to improve the technological and ecological know-how of seaweed production, and also endorses the development of biorefinery technologies for

seaweed utilization including its conversion to chemicals and fuels. The Sustainable Energy Authority of Ireland also carried out a study which concluded that priority should be given to the large scale cultivation of macroalgae to ensure sufficient feedstock for biofuel production and avoid the negative impact that could occur on marine biodiversity by exploiting wild seaweed [8]. In another study carried out in the United States (U.S.) by the Pacific Northwest National Laboratory, it was concluded that the U.S. has a high potential for producing macroalgae biomass based on the very high surface area of U.S. coastal waters and known rates of macroalgae production in other parts of the world [4]. However, the authors note that additional research into macroalgae cultivation, harvesting and conversion into fuel is needed. In South Korea, research into macroalgae biomass has been funded by the Ministry of Oceans and Fisheries since 2009 and has focused on offshore systems for large scale growth of macroalgae and their conversion to energy [9].

In the peer-reviewed literature several recent review studies have been carried out by researchers into the potential of macroalgae use for fuel or chemicals production. Lehahn et. al. [10] used a modeling approach to investigate the global potential for macroalgae growth as identify areas for growth. They estimate that 98 gigatonnes per year dry weight of macroalgae can be grown globally over a surface area of approximately 10^8 km^2 and conclude that with near-future aquaculture technologies, offshore cultivation of macroalgae has huge potential to significantly provide fuels and chemicals for humans. Another point noted by some of these review studies was that despite the potential for macroalgae based biorefineries, technological improvements in the whole supply chain of macroalgae based biorefineries (such as seaweed cultivation, harvesting and transporting, pretreatment, and fuel conversion technologies) are needed for economically feasible macroalgae fuel and chemical processes [11,5,12].

Based on the conclusions from all these studies, there is a high motivation to conduct research into the technological and economical aspects of macroalgae conversion to fuels.

Currently, research efforts into biofuels suitable for gasoline replacement have shifted focus to butanol instead of ethanol because of advantages such as lower miscibility with water, higher heating value (HHV), and better compatibility with existing gasoline engines and fuel pipeline infrastructure [13,14]. Similar to first and second generation biofuel feedstocks such as corn and agricultural residue, butanol can be produced from macroalgae using either a biochemical or thermochemical route.

The conversion of macroalgae to butanol through the biochemical route is done via the acetone, butanol and ethanol (ABE) process where species of *Clostridium* bacteria are used to convert sugars such as hexoses and pentoses to acetone, butanol and ethanol. Nikolaison et al. [15] fermented the macroalgae *Ulva lactuta* with *Clostridium* strains to produce butanol with a yield of 0.16 g butanol/ g sugars, which was lower than that of ethanol produced under similar conditions. Using Clostridium beijerinckii as the fermentation organism Van Der Wal et al. [16] obtained butanol yields of 0.23 g butanol/ g sugars from *Ulva lactuta*. Potts et al. [17] showed through a pilot study in which *Ulva lactuta* grown in Jamaica Bay, New York City was used as a fermentation substrate that a butanol yield of 0.29 g butanol/ g sugars was obtainable. This value corresponds to a 22.4 % deviation from the theoretical yield of 0.37 g butanol/g sugars [18]. Huesemann et al. [19] carried out a study of butanol fermentation from brown algae (*Saccharina*), but obtained very low butanol yields of 0.12 g butanol/g sugars. One challenge of current ABE fermentation strains is the difficulty in effectively converting some glucose-based polysaccharides, such as mannitol which constitutes up to 12 % of brown algae [7], thus leading to slow reaction rates and productivity [6,20],

thus progress in the area of metabolic engineering of fermentation organisms is required to improve butanol yields at the laboratory scale [6,11]. This has led to the conclusion that significant improvements at the laboratory scale are still required before economically feasible butanol production from fermentation of seaweed can be achieved on the industrial scale [16,21]. In fact no conceptual studies on the techno-economics of macroalgae-to-butanol processes via the biochemical route have been carried out in the peer reviewed literature.

In this regard the thermochemical route might be of considerable interest to study as past research on first and second generation biomass to butanol processes have shown that the thermochemical route has a number of more technologically mature processing steps such as the gasification, syngas cleanup and separation steps [22,23], and thus might be closer to commercial implementation than the biochemical route. However, though past work [24] has shown that economically competitive butanol can be produced from second generation biofuel feedstock using a thermochemical route, no such studies have been carried out on a macroalgae-to-butanol process in the peer reviewed literature to the best of the authors' knowledge.

As a first step in building an understanding of the process design and economics of macroalgae to butanol processes, this work will focus on developing a macroalgae-to-butanol process using a thermochemical conversion route and assessing its economics with future work focusing on the biochemical route. The research will aim to develop different design configurations for producing butanol from seaweed and address questions regarding the overall efficiency and butanol yields that are possible from these designs. Furthermore the different configurations will be compared amongst themselves and against other biofuels by using standard metrics such as the cost of CO_2 equivalent emissions (CCA) as well as the minimum butanol selling price (MBSP). These metrics

are also assessed for different market scenarios, and along with sensitivity analyses on key economic parameters help give a robust assessment on the potential for butanol production from seaweed using the thermochemical route.

3.2 Materials and Methods

3.2.1 Macroalgae

The macroalgae selected for this study is the brown macroalgae *Laminara Japonica*. *L. Japonica* is chosen for this study because it is the most widely produced macroalgae with a production rate of 5 million wet tons per year, making up 33 % of the world's yearly production [6]. Table 3-1 shows the plant gate characteristics of the *L. Japonica* that is used for this study [25], noting that the chemical composition of brown macroalgae changes somewhat depending on the season, growing habitat, and species [12,20]. In general, carbohydrates are consumed in the dark season and produced in the light season [26]. On a moisture free basis, the biochemical composition of brown macroalgae consist of 30 - 50 % minerals, 30 - 60 % carbohydrates, 10 - 13 % cellulose, 6 - 20 % proteins and 1 - 3 % lipids [27].

Table 3-1. Ultimate and proximate analysis of *L. Japonica* used in this study [25].

Ultimate analysis	wt % dry basis	Proximate analysis	wt %
Carbon	32.41	Moisture	2.79
Hydrogen	3.37	Volatile matter	70.90
Nitrogen	1.18	Fixed Carbon	3.32
Sulphur	0.31	Ash	22.99
Oxygen	39.74		
Ash	22.99		
HHV (MJ/kg)	14.05		

3.2.2 Process simulation and description

3.2.2.1 Process and simulation overview

This paper considers and assesses three design configurations for the thermochemical conversion of macroalgae to butanol. All of the design configurations adhere to a

similar approach. First, macroalgae is gasified to produce syngas (CO and H_2). The syngas is then cleaned before being sent to the mixed alcohol synthesis reactor for alcohols production, after which the alcohols are separated into the required products in an alcohols separation section. The differences in configurations arise as a result of different criteria for providing high temperature process heat, and power. In configuration 1 (also called the "self-sufficient" configuration), the plant is self-sufficient in terms of high temperature process heat and power, meaning that some of the syngas generated by macroalgae gasification is split and diverted as combustion fuel for the endothermic gasification and tar reforming processes. In other words, configuration 1 is 100% powered by renewable biomass. Configuration 2 or the "natural gas (NG) import" configuration uses NG combustion for high temperature process heat needs instead of bio-syngas combustion because NG is cheaper than seaweed per unit heating value. The disadvantage to this approach is that the use of fossil fuels reduces the "greenness" of the process and the resulting biofuel. Finally, configuration 3 (or the "NG and power import" configuration) utilizes NG for high temperature heat similar to configuration 2, and in addition imports electric power for process use instead of generating power through expansion of hot gases and steam turbines. Past work showed that the steam turbines and gas expanders can contribute up to 25 % of the capital cost of thermochemical biobutanol process [24], thus this configuration is motivated by the idea that it might be better to purchase power from the grid instead and avoid the significant capital costs required for purchasing steam turbines and gas expanders. Even though this could ultimately be somewhat more expensive over the lifetime of the process, the significantly reduced capital may be very desirable in terms of financing and risk, making the process more commercially feasible. The trade-offs between the

three configurations are the environmental considerations such as GHG emissions, amount of renewable energy used, capital and operating costs.
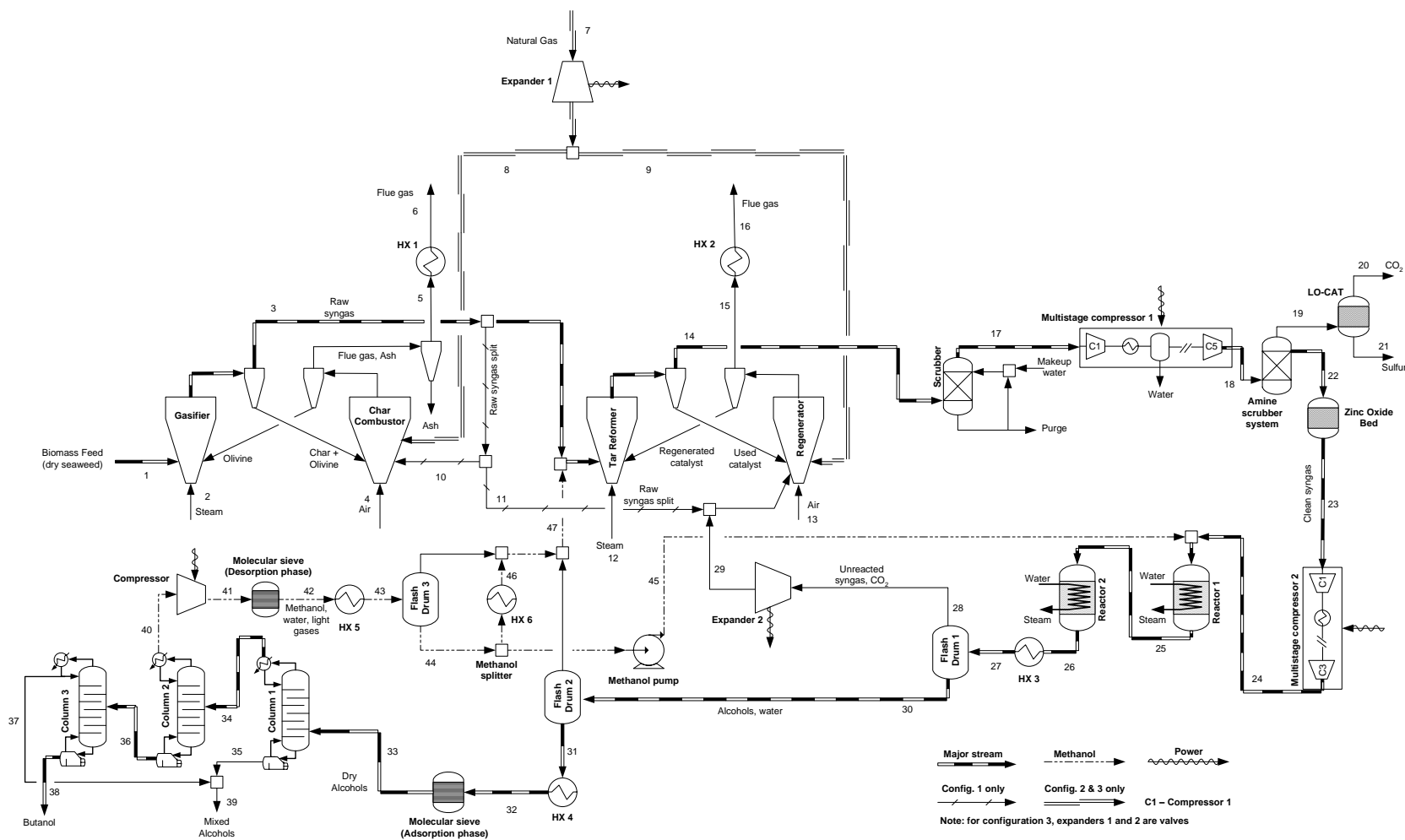
Figure 3-1. Superstructure process flow diagram of the proposed thermochemical biomass (seaweed) to butanol process showing all design options considered. Full stream conditions are provided in the Supporting Information on www.macsphere.mcmaster.ca.

Table 3-2. Major design parameters of process areas

Gasification		Gas cleanup (acid gas removal)	
Feed rate per train (gasifier inlet)	700 dry tonnes/ day	Amine used	Monoethanolamine
Parallel trains required	Two (2)	Amine concentration, wt %	35
Gasifier operating pressure	2.28 bar	Amine temperature in absorber (^{o}C)	43.33
Gasifier operating temp.	800 ^{o}C	Absorber pressure (bar)	31
Char combustor pressure	2 bar	Stripper pressure (bar)	4.12
Char combustor temp.	850 ^{o}C	Heat duty to remove CO_2 (kJ/kg)	5337
Gas cleanup (tar reforming)		**Alcohol synthesis reactors**	
Reformer operating pressure (bar)	1.86	H_2/CO ratio (reactor 1 inlet)	1.23
Reformer operating temp. (^{o}C)	910	Gas hourly space velocity (h^{-1})	5000
Reformer space velocity (h^{-1})	2,476	Reactor 1 temperature (^{o}C)	325
Tar reformer conversions (%)		Reactor 2 temperature (^{o}C)	340
Methane (CH_4)	80%	Pressure (bar)	76
Ethane (C_2H_6)	99%	CO_2 concentration (mol %)	5
Ethylene (C_2H_4)	90%	Sulphur concentration (ppmv)	0.1
Tars (C_{10+})	99%	CO conversion per-pass (CO_2 free basis)	40 mol%
Benzene (C_6H_6)	99%	Total alcohol selectivity	87.27 mol%
Ammonia (NH_3)	90%	Catalyst alcohols prod. (g/kg-catalyst/hr)	455.26
Alcohol separation (distillation columns)		**Steam system and power generation (cases 1 and 2)**	
Column 1		Turbine design	Three stage turbine
Butanol recovery in overhead	99.2 mol%	High pressure inlet conditions	58 bar, 482 ^{o}C
Pentanol recovery in bottoms	99 mol%	Medium pressure inlet conditions	12 bar, 303 ^{o}C
Total number of trays	28	Low pressure inlet conditions	4.5 bar, 210 ^{o}C
Column 2		Condenser outlet conditions	0.304 bar, saturated
Methanol recovery in overhead	99 mol%	Cooling water	
Ethanol recovery in bottoms	99 mol%	Supply temperature (^{o}C)	32
Total number of trays	48	Return temperature (^{o}C)	43
Column 3			
Propanol recovery in overhead	99.3 mol%	Alcohol separation (Molecular sieve)	
Butanol purity in bottoms	96 wt%	Inlet water content (wt %)	7.93
Total number of trays	54	Outlet water content (wt %)	0.5

This work made use of Aspen Plus V8 software to estimate the mass and energy balance for each design strategy. Physical property packages, and unit operation specifications and design criteria were selected to be consistent with the authors' previous work in which a lignocellulosic biomass to butanol process using a thermochemical route was

designed and assessed [24]. In the proceeding process description sub-sections, each plant area that has already been described in the previous work will only be briefly discussed. However, any differences in unit operations design and specification from the previous work will be noted and discussed in more detail.

A simplified process flow diagram of the process is shown in Fig. 3-1. The figure shows the key processing steps for the conversion of seaweed to butanol via gasification, syngas production, and mixed alcohol synthesis. These different areas of the process are further discussed in sections 3.2.2.2 – 3.2.2.6. The major design parameters for these process areas are also shown in Table 3-2.

3.2.2.2 Gasification

A dried macroalgae feed at 1,200 tonnes per day with characteristics as shown in Table 3-1 is sent to the gasifier in which it is indirectly gasified with low pressure steam. The wet macroalgae after collection is air dried to about 20 - 35 wt% moisture content before being transported to the biobutanol plant [28]. Further drying to the moisture content shown in Table 3-1 can be done by using waste hot flue gas heat from the biobutanol process (not modeled), using a similar procedure as discussed in Okoli and Adams [24].

The composition and higher heating value of syngas produced from biomass gasification is highly variable and is affected by a number of process parameters such as; fuel type and composition, fuel moisture content, gasification temperature, gasification pressure, gasifier bed materials and gasification agent (air, oxygen, steam) [22,29]. Thus the gasifier selection, and its operating conditions are chosen so as to meet specific syngas

requirements for downstream operations [30]. For example the syngas H_2/CO ratio for Fischer Tropsch gasoline production is about 0.6, but approximately 2.0 for methanol production [30]. Puig-Arnavat et al. [22] discusses the various types of biomass gasifiers and their syngas outputs in detail.

The gasifier design chosen for this work is a low pressure allothermal indirect circulating fluidized bed gasifier that has the product composition of its output modeled with temperature correlations from the Batelle Columbus Laboratory test facility [31]. Though this model was not originally developed for seaweed, it has been validated for a wide range of hard and soft woods, as well as for non-woody biomass such as corn stover which have high ash content, low carbon and high oxygen content just like seaweed, thus making the model robust enough to predict the outlet composition of seaweed gasification [31] in the absence of experimental data.

The gasification reactions are endothermic; as a result the required heat is supplied by circulating hot olivine from the char combustor through the gasifier. The exit from the gasifier includes the olivine as well as the gasification products (CO, H_2, CH_4, tars and solid char). Cyclones are then used to separate the gaseous products (mainly CO, H_2, CH_4 and tars) from the solids (olivine and char) which are recycled back to the char combustor. In the char combustor, the char is combusted with air thus heating the olivine. If extra heat is needed, provision is made for extra fuel to be supplied by recycling a fraction of the syngas as in configuration 1 (stream 10 in Fig. 3-1), or using NG (specifications are shown in Table 3-3) as in configurations 2 and 3 (stream 8 in Fig. 3-1).

Finally, the hot flue gas from the char combustor is used to generate steam in the steam cycle.

Table 3-3. NG specifications [32]

Component	mol %
Methane	94.9
Ethane	2.5
Propane	0.2
i-Butane	0.03
n-Butane	0.03
i-Pentane	0.01
n-Pentane	0.01
Hexanes+	0.01
Nitrogen	1.6
CO_2	0.7
Oxygen	0.02
Hydrogen	trace
HHV (MJ/m^3), dry basis	37.8
Density at STP (kg/m^3)	0.585

3.2.2.3   Gas cleanup

The goal of the gas cleanup section is to remove impurities from the raw syngas such as tars, CO_2 and sulphur that have the potential to foul downstream equipment and poison the mixed alcohol synthesis (MAS) catalyst. There are two steps in the gas cleanup section. First, secondary tar reforming is used to reform the tars, methane, and other hydrocarbons in the syngas from the gasifier. Secondary tar reforming differs from primary tar reforming in that it does not occur internally in the gasifier. Though primary tar reforming has the potential to reduce capital costs by eliminating the extra equipment needed for an external tar reformer, the technology is not commercially mature [33]. The secondary tar reformer is a circulating, heterogeneous, fluidized catalyst bed system which uses separate beds for reforming and catalyst regeneration. The reforming reactions

occur between the raw syngas and steam, and are catalyzed by a fluidizable Ni/Mg/K catalyst [31]. The reformer bed is maintained at isothermal conditions by the transfer of heat from the catalyst regenerator which is exothermic. The catalyst is separated from the reformed syngas using cyclones at the reformer exit and then transferred to the catalyst regenerator. The catalyst is regenerated by combusting the coke entrained on the catalyst, after which the heated catalyst is passed through cyclones to separate it from the combustion gases. The loop is completed when the heated catalyst is sent back to the reformer. The hot combustion gases are used to provide heat for steam generation and process heating. If the heat duty supplied from the catalyst regeneration step is insufficient, it can be supplemented by combusting a portion of the raw syngas feed from the gasifier as in configuration 1 (stream 11 in Fig. 3-1) or NG as in configurations 2 and 3 (stream 9 in Fig. 3-1), as well as unreacted syngas from downstream.

In the second step of the gas cleanup process, the hot syngas from the tar reformer is cooled before water quenching and scrubbing to remove any remaining solids, tars, and other impurities. The purge water stream is then sent to a downstream waste water treatment facility (not modeled). The cooled syngas is compressed to 30 bar in a multi-compressor prior to being sent to the amine scrubber system for acid gas removal. The amine scrubbers and the subsequent ZnO bed are used to reduce the H_2S and CO_2 concentrations in the syngas to meet the MAS catalyst specifications of < 0.1 ppm H_2S and < 6 % CO_2 [34]. The amine scrubber reduces the H_2S concentration to 10 ppm, before it is further reduced to 0.1 ppm by the ZnO bed. A LO-CAT system then takes the H_2S and CO from the amine scrubber exit, and generates elemental sulphur and CO_2.

All the technologies described here for syngas cleanup have been demonstrated commercially. Fluidizable Ni based catalysts for tar reforming have already found wide applications in the petrochemical industry for naphtha and methane reforming to syngas [35]. The LO-CAT system has been commercially implemented with more than 200 installations existing around the world for H_2S removal from gas streams as reported by Merichem company [36]. Amine scrubbing with monoethanolamine (MEA) solutions is the leading method for CO_2 and H_2S removal and is used in 75 - 90 % of commercial CO_2 capture processes [37]. Finally ZnO beds have found commercial application in a variety of syngas to chemicals processes where they are used to clean syngas streams to achieve very low H_2S concentrations [38].

3.2.2.4 Alcohol Synthesis

The cleaned syngas is compressed from 30 bar to 76 bar in a multi-stage compressor, and subsequently heated to 325°C before the reactor inlet. Prior to entering the reactor, the clean syngas is mixed with methanol and water that are recycled from the alcohol separation section. A double bed reactor configuration consisting of two reactors in series is used for the reactor system. Both fixed bed reactors contain equivalent amounts of a modified low pressure methanol synthesis catalyst ($Cs/Cu/ZnO/Cr_2O_3$ based) with the second reactor operating at 340°C [39,40]. This reactor configuration favours the production of C_1– C_3 alcohols in the first reactor because lower temperatures favour higher equilibrium amounts of methanol, while higher temperature favour the conversion of $C_1 - C_3$ alcohols to higher alcohols. According to the experimental results of Burcham et al. [40], the double bed reactor configuration produces a higher butanol yield than the

single reactor configuration and is thus potentially more favourable. The reactor products consist of $C_1 - C_4$ alcohols, water, methane, C_{5+} alcohols and other hydrocarbon products. The MAS reactions are highly exothermic, thus a shell and tube configuration is used for the reactors, with the reactions taking place in the tubes while heat removal occurs through steam generation from the shell side. This process helps maintain isothermal conditions in the reaction.

The products from the reactor are cooled to 60°C by heat exchange with process streams and cooling water. The unconverted syngas which is still at high pressure is separated from the liquid alcohols by a series of flash drums, and is expanded through a turbine to recover power in configurations 1 and 2, while it is expanded through a flash valve in configuration 3. The expanded syngas is then sent to the gas cleanup section where it is combusted in the catalyst regenerator to help meet the heat requirements of the plant, while the liquid alcohols are sent to the alcohols separation section.

3.2.2.5   Alcohol Separation

Absorbed gases are removed from the raw alcohols by flashing to 4 bar, with the gases recycled to the tar reformer. The liquid alcohols are superheated prior to being sent for dehydration in a molecular sieve. The alcohols are then separated into final products by three distillation columns in series. The main product for the distillation sequence is isobutanol which is recovered at 96 wt% purity to meet ASTM fuel specification standards [41]. Other products are C_{5+} alcohols recovered from the bottom of column 1, methanol and lighter gases recovered from the top of column 2, and ethanol and propanol

recovered from the top of column 3. Methanol recovered from the distillation columns is superheated and recycled as a sweep gas to recover adsorbed water from the molecular sieve. The methanol vapour and recovered water vapour is split and recycled to the MAS reactor to help improve the overall alcohols yield while the rest is recycled to the tar reformer to be reformed back to syngas. The bottoms product of column 1 and the distillate product from column 3 are blended to obtain a mixed alcohol co-product.

3.2.2.6 Utilities (Steam system, power generation and cooling)

A steam cycle is integrated into the design to produce high pressure (HP) steam for power generation in configurations 1 and 2, and low pressure (LP) steam for direct injection into the biomass gasifier and tar reformer in all the configurations. There is also a requirement for indirect heating using LP steam in the reboilers of the distillation columns and amine system. The steam condensate is then returned to the steam cycle in a loop. HP steam in the steam cycle is generated via heat exchange with hot process streams like the flue gases from the char combustor and catalyst regenerator, and the exothermic heat from the MAS reactors. The steam system design conditions are shown in Table 3-2.

Process power requirements for configurations 1 and 2 are met by the expansion of high pressure steam through steam turbines in series. Extra power is obtained via the expansion of unconverted syngas through a turbine in the alcohol synthesis section. In configuration 3 all power is imported from the grid; this creates a trade-off in eliminating the high cost of capital associated with purchasing and installing turbines and expanders while increasing the operating cost associated with power purchase from the grid.

The cooling requirements of all the configurations are met by the use of forced-air heat exchangers and cooling water after process stream to process stream heat exchange has been carried out. Forced-air heat exchangers are used with the aim of reducing the water demand of the process and provide cooling for the multistage compressors, distillation and amine system condensers, as well as for condensing the steam turbine exhaust.

3.2.3 Economic analysis

The objective of the economic analysis is to determine the MBSP of the different processes. The MBSP is defined as the unit selling price of butanol over the plant's life such that the net present value (NPV) is zero. It is determined through a discounted cash flow rate of return analysis, which is a useful metric for comparing all the different configurations that are modeled. The economics of a process or product usually depends on the market in which it is to be implemented or assessed. Thus, the economics for the different process designs are considered in both a U.S. market and a South Korean market scenario to reflect the two regions (North America and Asia) of interest for this work.

The estimates of capital costs for the processes are based on data from Aspen Capital Cost Estimator software and literature, especially U.S. National Renewable Energy Laboratory (NREL) reports [31,42]. The values which are obtained from the literature are scaled to the required size by using the capacity power law expression shown in equation (1),

$$\frac{Cost_2}{Cost_1} = (\frac{Capacity_2}{Capacity_1})^m \qquad (1)$$

with m varying from 0.48 to 0.87, and adjusted to 2014 U.S. dollars through the Chemical Engineering Plant Cost Index [43]. For the South Korean scenario, the capital cost is adjusted from its corresponding U.S. market value by multiplying with the purchasing power parity (PPP) between U.S. and South Korea, which is 0.78 [44]. The PPP is an economic factor that is used to adjust the exchange rate between countries so that the exchange rate reflects each country's actual purchasing power or cost of goods compared to the other country. The assumptions used for the economic analysis are summarized in Table 3-4.

Table 3-4. Economic parameters and indirect costs basis used in the analysis

Economic Parameter	Basis
Cost year for analysis	2014
Plant financing by equity/debt	50 %/ 50 % [45]
Internal rate of return (IRR)	10 % after tax [46]
Term for debt financing	10 years [46]
Interest rate for debt financing	8 % [46]
Plant life/analysis period	30 years [46]
Depreciation method	Straight Line depreciation 10 years for general plant and utilities
Income tax rate	35% [46]
Plant construction cost schedule	3 years (20% Y1, 45% Y2, 35% Y3) [47]
Plant decommissioning costs	$0
Plant salvage value	$0
Start-up period	3 months [46]
Revenue and costs during start-up	Revenue = 50% of normal Variable costs = 75% of normal Fixed costs = 100% of normal [46]
Inflation rate	1.75% [48] U.S., 1.10% [49] South Korea
On-stream percentage	90% (7,884 hours/year)
Land	6.5% of Total Purchased Equipment Cost (TPEC) [50]
Royalties	6.5% of TPEC [50]
Working capital	5% of Fixed Capital Investment (excluding land) [46]
Indirect costs	
Engineering and supervision	32% of TPEC [51]
Construction expenses	34% of TPEC [51]
Contractor's fee and legal expenses	23% of TPEC [51]
Contingencies	20.4% of TPEC [31]

The operating costs are broken down into fixed operating costs and variable operating costs. The correlations used for computing fixed operating costs are obtained from Seider et al. [50], and consist of items such as maintenance, labour related operations, operating overhead, property tax, and insurance. The variable operating costs which are used for this study are summarized in Table 3-5. The values shown are adjusted to U.S. 2014 dollars from their reference values by using an inorganic index obtained from the U.S.

Bureau of Labor Statistics [52]. Besides the sale of butanol as a product, electricity (for configurations 1 and 2 only) and mixed alcohols are sold as co-products to generate additional revenue for the plant with the price of mixed alcohols computed as 90% of the price of gasoline on an HHV equivalent basis (obtained from Aspen Plus simulations).

Table 3-5. Cost of materials and products used in the analysis

Commodity prices in 2014 U.S. dollars	U.S.	South Korea
Seaweed cost ($/dry tonne)	71.42 [53]	67.9 [54]
Olivine ($/tonne)	304.75 [31]	PPP adjusted U.S. price
MgO ($/tonne)	604.33 [31]	PPP adjusted U.S. price
Tar reformer catalyst ($/kg)	53.16 [31]	PPP adjusted U.S. price
Alcohol synthesis catalyst ($/kg)	28.58 [24]	PPP adjusted U.S. price
Solids disposal (Ash) ($/tonne)	81.28 [31]	PPP adjusted U.S. price
Water makeup ($/tonne)	0.47 [55]	PPP adjusted U.S. price
Boiler feed water chemicals ($/kg)	6.79 [31]	PPP adjusted U.S. price
Cooling tower chemicals ($/kg)	4.08 [31]	PPP adjusted U.S. price
LO-CAT chemicals ($/tonne sulphur produced)	555.5 [31]	PPP adjusted U.S. price
Amine makeup ($/ million kg acid gas removed)	44.15 [31]	PPP adjusted U.S. price
Waste water treatment ($/tonne)	1.12 [31]	PPP adjusted U.S. price
Electricity (cents/kWh)	6.63 [56]	9.98 [57]
Gasoline ($/L)	0.91 [56]	1.53 [57]
NG ($/tonne)	397 [56]	1,221 [57]

3.3   Results and Discussion

3.3.1   Process modeling results

The three different design configurations (self-sufficient, NG import, and NG & power import) were simulated in Aspen Plus so as to be able to quantify the different mass and energy flows, as well as sizes of processing units. The stream conditions which correspond to Fig. 3-1 for the three different configurations are provided in the Supplementary Material. Table 3-6 summarizes the process modeling results for the different configurations. The plant energy efficiency shown in the table is computed on an HHV basis, and is defined as the total HHV of the output products (butanol, mixed

alcohols and electricity) divided by the total HHV of the input feedstocks (seaweed, NG, and electricity). It shows the major feed and product flows of the processes, as well as net power and energy efficiency of the processes.

Table 3-6. Major flowrates and process energy efficiency

	Case 1- Self-sufficient	Case 2 - NG import	Case 3 - NG & power import
Seaweed flow rate (kg/h)	45,631	45,631	45,631
NG requirement (kg/hr)	-	5,024	5,024
Total Product yields (kg/hr)	5,921	9,730	9,730
Butanol	2,782	4,572	4,572
Mixed alcohols	3,139	5,158	5,158
% products yield per feed (mass basis)	13.0	21.3	21.3
Net Electric Power Exported (MW)	3.24	5.04	-20.4
Power generation	16.04	24.79	-
Power consumption	12.8	19.75	20.4
Biomass HHV (MW)	178.09	178.09	178.09
NG HHV (MW)	-	90.17	90.17
Butanol HHV (MW)	28.85	47.41	47.41
Mixed alcohols HHV (MW)	29.07	47.77	47.77
Total input HHV + electricity import	178.09	268.26	288.66
Total output HHV + electricity export	61.16	100.23	95.19
Plant energy efficiency (% HHV basis)	34.34	37.36	32.98

From Table 3-6 it can be seen that the use of NG as a high temperature heat source leads to an increase in the liquid product yields in configurations 2 and 3. This is because more syngas can be diverted to the MAS reactor for conversion to butanol and mixed alcohols. The table also shows that configuration 2 has a higher net power production than configuration 1, while a net power import of 20.4 MW is required for configuration 3. As a result of the higher net power production and total liquid product, the plant thermal efficiency of configuration 2 is higher than configurations 1 and 3. The requirement for power import reduces the plant thermal efficiency of configuration 3 making it have the

lowest plant energy efficiency despite the increased liquid products yield. The butanol and mixed alcohols HHVs are computed using Aspen Plus simulations. Note though that the plant energy efficiency of the designed configurations are low in comparison to similar plants which use cellulosic feedstock. For example, the plant energy efficiency of a lignocellulosic biomass-to-butanol self-sufficient process previously published by the authors is 46% on an HHV basis [24]. The main reason behind this disparity is the high ash content in *L. Japonica* seaweed (23%) as compared to the lower ash content ($< 7\%$) in cellulosic biomass. This means that there is much less carbonaceous material in seaweed for conversion to fuel and thus the lower plant energy efficiency values.

3.3.2   Economic analysis results

The economic analyses for the different process designs are carried out for a U.S. market scenario and a South Korean scenario with the results summarized in Table 3-7. Some important points stand out from the results. First of all the total capital investment (TCI) for the different processes follow the same trends for both the U.S. and South Korean scenarios: the NG import configuration has the highest TCI followed by the self-sufficient configuration, with the NG & power import configuration having the lowest TCI. The NG import configuration has the highest TCI because it has the most equipment in comparison to the other configurations, as well as the highest flows of syngas and other process streams downstream of the gasifier. This means larger equipment is needed leading to higher costs. Though the NG & power import case has larger flows through the process in comparison to the self-sufficient case, its TCI is lower because the absence of

steam turbines and gas expanders leads to less equipment and significantly lower direct costs in process sections such as the steam system and the power generation section.

As for the operating costs, the relative trends remain the same for the U.S. and South Korean scenarios; however the relative scale of the trends has changed. For the U.S. scenario, the NG & power import configuration has the highest total operating costs (TOC), followed by the NG import configuration and finally the self-sufficient configuration. This trend is because the NG & power import configuration has additional costs related to the purchase of NG and electricity, with electricity import not required for the NG import configuration, and import of power and NG not required for the self-sufficient configuration. Note that the scale of the relative differences for the U.S. scenario is much smaller than the South Korean scenario because the cost of energy (NG and electricity) is relatively much higher in South Korea than the U.S., thus the energy costs dominate the operating costs in the South Korean market scenario. This dominance of the energy costs in the South Korean scenario is clearly shown by the increase in TOC for the NG import and the NG & power import configurations in the South Korean scenario in comparison to their U.S. scenario counterparts.

The flipside of the increased energy costs in the South Korean market is that co-products such as mixed alcohols and electricity export have more value (since they are assumed to be proportional to the local gasoline price) and thus bring in more revenue in comparison to the U.S. scenario. Thus the total co-product revenues are the highest in the South Korean scenario.

In regards to the MBSP, the lower cost of capital and the higher total co-product revenues for the South Korean cases lead to lower MBSP values for the South Korean cases relative to their equivalent U.S. cases. For each case, the relative difference between the markets is attributable to the TOC. For instance, the self-sufficient plant has the largest magnitude in MBSP difference between markets because the TOC in the South Korean market is 14% lower than in the U.S. market. However, NG & power import case has the smallest MBSP difference between markets because the TOC in the South Korean market is 25% higher than the U.S. market, which is the greatest amongst all the configurations.

In general, the total co-product revenue appears to be a good indicator for the MBSP in terms of relative profitability of each case. For instance the South Korean - NG import case has the lowest MBSP because it has the highest total co-product revenue, while the U.S - self-sufficient case has the highest MBSP because it has the lowest total co-product revenue. However there are two exceptions. For the first exception, the MBSP of the U.S. - NG & power import case is lower than that of the U.S. - NG import case. This is because in the U.S. market the cost of capital dominates energy costs, thus the differences in TOC and total co-product revenue for the U.S. market for these two cases are much smaller than in their equivalent South Korean cases leading to a higher MBSP for the U.S. - NG & power import case in comparison to the U.S. - NG case. The second exception is that the MBSP of the U.S. - NG & power import case is lower than that of the South Korean - self-sufficient case. The reason behind this exception is the much lower yield in butanol product in the self-sufficient process design in comparison to the NG & power import design (see butanol yield in Table 3-6). The much lower butanol

yield in the self-sufficient case means that a much higher MBSP is required to make the NPV zero, thus the higher MBSP for the South Korean - self-sufficient case despite its higher total co-product revenue in comparison to the U.S. - NG & power import case.

The MBSP values obtained for the different case studies range from 1.97 $/L in the South Korean - NG import case to 3.33 $/L in the U.S. - self-sufficient plant case. These values are high in comparison to biobutanol obtained from cellulosic biomass sources. For example, Okoli and Adams [24] obtained an MBSP of 0.83 $/L from a self-sufficient thermochemical lignocellulosic biomass to butanol process which was designed on a similar basis to the designs discussed in this study (albeit at a larger biomass feed rate of 2,000 tonnes per day), while Qureshi et al. [58] obtained an MBSP of 1.05 $/L for a biochemical wheat straw-to-butanol process.

Table 3-7. Economic summary for case studies in U.S. and South Korea scenarios (a more detailed breakdown is provided in the supporting information)

Plant design	U.S.			South Korea		
	Self-sufficient plant	NG import	NG & power import	Self-sufficient plant	NG import	NG & power import
Capital Investment ($'000)						
Direct costs breakdown						
Gasification	38,239	38,239	38,239	29,826	29,826	29,826
Gas Cleanup	41,221	51,069	50,269	32,152	39,834	39,210
Mixed Alcohol Synthesis	4,638	6,878	1,484	3,618	5,365	1,157
Alcohol Separation	12,269	13,651	13,651	9,570	10,648	10,648
Steam system & Power Gen.	41,047	54,312	4,613	32,017	42,363	3,598
Cooling Water & Other Utilities	10,448	11,211	11,211	8,150	8,744	8,744
Total Direct Costs	147,863	175,360	119,466	115,333	136,781	93,184
Engineering & Supervision	22,128	26,863	17,055	17,260	20,953	13,303
Construction Expenses	23,511	28,541	18,121	18,339	22,262	14,135
Contractor's Fee & Legal Expenses	15,904	19,307	12,258	12,406	15,060	9,562
Contingency	14,107	17,125	10,873	11,003	13,357	8,481
Royalties	4,470	5,344	3,555	3,487	4,168	2,773
Land	4,470	5,344	3,555	3,487	4,168	2,773
Working Capital	11,399	13,627	9,066	8,891	10,629	7,072
Total Capital Investment	*243,852*	*291,511*	*193,951*	*190,205*	*227,379*	*151,282*
Operating costs ($'000/year)						
Seaweed	25,693	25,693	25,693	24,428	24,428	24,428
NG	-	13,113	13,113	-	43,942	43,942
Catalysts & Chemicals	1,268	1,695	1,722	989	1,322	1,344
Waste Stream Treatment	7,364	7,425	7,425	5,744	5,791	5,791
Water Makeup	51	35	50	40	27	39
Electricity Import	-	-	8,414	-	-	12,665
Labour Related Costs	22,377	22,377	22,377	18,734	18,734	18,734
Maintenance Costs	15,304	18,150	12,365	11,937	14,157	9,644
Operating Overheads	6,237	6,590	5,873	5,820	6,095	5,536
Property Taxes & Insurance	2,957	3,507	2,389	2,307	2,736	1,864
Total Operating Costs	*81,252*	*98,585*	*99,422*	*69,999*	*117,233*	*123,988*
Co-prod. revenues ($'000/year)						
Mixed Alcohols	19,459	31,980	31,980	32,849	53,986	53,986
Electricity Export	1,690	2,631	-	2,544	3,961	-
Total co-prod. revenue	*21,149*	*34,612*	*31,980*	*35,392*	*57,947*	*53,986*
MBSP ($/L)	3.33	2.25	2.07	2.15	1.97	2.01

3.3.3 Cost of CO₂ equivalent emissions avoided (CCA)

Due to the emission of climate changing greenhouse gases associated with fossil derived fuels, one major objective behind development of biofuels is to minimize greenhouse gas emissions from the transportation sector in a cost effective way. Thus one metric for comparing different biofuel processes is the CCA. The CCA is defined as the additional cost required to avoid the emission of a unit of GHG when a biofuel is combusted in place of a fossil fuel, thus the lower the value the better. The unit of GHG emissions is "kg of CO_2 equivalent emissions (CO_2e)". This metric is a good indicator for comparing biofuel processes to each other and to non-biofuel processes because it factors in both cost and life cycle impacts. For this work conventional gasoline is used as a baseline for computing the CCA, and this is done by using equation 2. Note that this equation is only applicable in cases where the carbon intensity of gasoline is higher than the carbon intensity of the biofuel. This is because if the carbon intensity of the biofuel process is greater than that of gasoline then it is not worth investing in that biofuel process as it does not help offset GHG emissions.

$$CCA\left(\frac{\$}{kgCO_2e}\right) = \frac{Biobutanol\ marginal\ cost\left(\frac{\$}{MJ}\right)}{GHG\ emissions\ avoided\left(\frac{kgCO_2e}{MJ}\right)} = \frac{MBSP - gasoline\ price}{CIG - CIB} \tag{2}$$

The carbon intensity of gasoline (CIG) is the total wells-to-wheels life cycle emissions, made up of the sum of the direct GHG emissions of gasoline when used in a vehicle plus the indirect GHG emissions of its entire upstream supply chain, including oil drilling, production, refining, and transportation (the contributions of all GHG related chemicals are evaluated using the IPCC 100-year metric [59]).

For each butanol process, the carbon intensity of butanol (CIB) is similarly the wells-to-wheels GHG emissions of the biofuel, including all emissions associated with its production, the indirect emissions of utilities used in the process, and the final combustion of the fuel itself. For NG, this includes indirect GHG emissions related to its production from the well and transportation of NG to the biobutanol plant, as well as direct GHG emissions from its combustion for heating purposes at the plant. More than 90 % of the NG used in South Korea is obtained from liquefied NG (LNG) imports. Thus for this analysis LNG used in South Korea is assumed to be purchased and shipped from the U.S. The upstream, liquefaction and regasification life cycle inventory (LCI) data are obtained from PACE [60], while the shipping emissions for transportation from U.S. to South Korea is obtained from Abrahams et al. [61].

For electricity, the carbon intensity includes indirect GHG emissions related to its generation and transmission to the biobutanol plant, including the production, delivery, and use of all fuels used to produce power for the electric grid, which is different for the United States and South Korea. The indirect and direct gasoline emissions are assumed to be the same for both U.S. and South Korea. Note also that all energy values reported here are assumed to be on a HHV basis with conversion factors for conventional gasoline taken from CTA & ORNL [62].

The emissions associated with harvesting seaweed (which include production, mechanical pretreatment, drying and transportation) are assumed to be the same as reported in a study of brown seaweed harvested in Norway (about 176 $kgCO_2e$/tonne dry seaweed) [63] since data for *L. Japonica* in South Korea and U.S. were not available. Furthermore, it was

assumed that all carbon in the seaweed originated from atmospheric CO_2, and thus the biogenic CO_2 uptake can be computed from the ultimate analysis of the seaweed as shown in Table 3-1. Finally, an allocation factor computed as the fraction of butanol product in the total product mix on a HHV basis (see Table 3-6) is used to allocate GHG emissions from the seaweed-to-biofuel process to butanol. A summary of all direct and indirect GHG emissions along the cradle-to-gate life cycle considered in this analysis are shown in Table 3-8.

Table 3-8. Indirect and direct GHG emissions data used for this analysis

GHG emissions (kgCO$_2$e/GJ)	U.S.	South Korea
Indirect NG emissions	8.4 [64]	26.63 [60,61]
Indirect electricity emissions	21.26 [65]	18.79 [65]
Indirect seaweed emissions (harvesting, pre-treatment and transportation)	12.53 [63]	12.53 [63]
Indirect gasoline emissions	17.36 [66]	17.36 [66]
Direct gasoline emissions	67.87 [67]	67.87 [67]

Very interesting insights are obtained by looking at the CCA, which are shown in Table 3-9. The first major insight is the very high values of CCA for the NG & power import cases in comparison to the other cases, despite the NG & power import cases being amongst the lowest in terms of MBSP. These large values are directly attributable to the indirect emissions associated with electricity import for these cases. In fact the GHG emissions from the South Korean - NG & power import case are greater than that of gasoline thus this plant should not be considered for GHG emissions avoidance purposes as it does not help offset GHG emissions. Furthermore, the low GHG emissions for the self-sufficient plant cases have led to these cases having some of the lowest CCA, with the South Korean - self-sufficient plant having the lowest CCA.

Table 3-9. Summary of CCA calculations

	U.S.			South Korea		
Plant	Self sufficient	NG import	NG + power import	Self sufficient	NG import	NG + power import
Seaweed growth (CO_2 uptake)	-1,189	-1,189	-1,189	-1,189	-1,189	-1,189
GHG emissions from upstream seaweed supply chain	176	176	176	176	176	176
GHG emissions from seaweed to butanol process	880	981	981	880	981	981
Indirect GHG emissions from natural gas	-	61.47	61.47	-	194.88	194.88
Indirect GHG emissions from electricity	-	-	35.20	-	-	31.11
Well-to-plant exit GHG emissions (kgCO$_2$e/dry tonne seaweed)	-132.83	30.35	65.55	-132.83	163.76	194.87
Well-to-plant exit GHG emissions allocated to butanol (kgCO$_2$e/GJ)	-26.76	3.73	8.48	-26.76	20.12	25.21
Direct GHG emissions from butanol use (kgCO$_2$e/GJ)	63.32	63.32	63.32	63.32	63.32	63.32
Well-to-wheel GHG emissions for butanol (kgCO$_2$e/GJ)	36.36	66.85	71.61	36.36	83.25	88.34
Total GHG emissions avoided (kgCO$_2$e/GJ)	48.87	18.38	13.62	48.87	1.98	-3.11
MBSP ($/L)	3.33	2.25	2.07	2.15	1.97	2.01
MBSP ($/GJ)	110.12	74.40	68.45	71.10	65.14	66.47
Biobutanol marginal cost ($/GJ)	85.80	50.08	44.13	30.09	24.14	25.46
CCA ($/tonneCO$_2$e)	1,756	2,724	3,239	616	12,170	*N/A

*N/A - not applicable because the well-to-wheel emissions for butanol are greater than the well-to-wheel emissions for gasoline.

The CCA for these processes are quite high, but are still in the general range of other biofuels. Ryan et al. [68] estimate the CCA for European biofuels to be between 277 - 2,524 $/tonneCO$_2$e (Euro converted to U.S. dollars using December 2014 exchange rate) while Fulton et al. [69] puts this cost at 180 - 874 $/CO$_2$e avoided for ethanol from different biomass sources. The only exception to this is ethanol from sugar cane in Brazil

which has a much more practical CCA of around 30 \$/tonneCO$_2$e [69]. This is due to the very high productivity of sugarcane crops in Brazil, and the utilization of its co-products to provide process energy, and also in most cases export electricity resulting in near zero fossil fuel requirements [68,69]. Note that even though the estimated CCA for seaweed is in range with other biofuels it is still not competitive with the CCA of 50 \$/tonneCO$_2$e recommended by policy makers in most western countries for investment in GHG emissions reduction technologies [69].

However, it is important to note that the baseline for this analysis is gasoline from conventional crude oil which has lower environmental and economic costs in comparison to unconventional oil from sources such as tar sands and shale oil. In North America, these unconventional oil sources have estimated reserves which are much greater than the estimated reserves of conventional oil, and release much more GHG emissions in the production process [70]. It has been noted in some estimates that oil from tar sands releases up to two to six times the amount of CO$_2$ released per barrel of oil produced from conventional oil [70–72]. Thus if the baseline for computation of CCA is changed from conventional gasoline to unconventional gasoline the potential for biobutanol from seaweed improves.

3.3.4   Sensitivity analysis

It is important to carry out sensitivity analysis to evaluate the impact that the variations of some of the key parameters used in this study have on MBSP and CCA. This is because of inherent uncertainties in some of the assumed values for the key costs and parameters.

A sensitivity analysis is carried out on the self-sufficient and NG import process designs for U.S. market and the self-sufficient design for the South Korea market, as these options offer the best value on CCA.

Table 3-10. Input parameters for sensitivity analysis

	U.S.	South Korea	deviation amounts
Seaweed price ($/tonne)	71.42	67.90	+/- 30 % deviation
Total direct costs ($MM)	175.36	136.78	+/- 30 % deviation
Internal Rate of Return (%)	10	10	+/- 5 units deviation
NG price ($/tonne)	397.22	1006.38	+/- 30 % deviation
Gasoline price ($/L)	0.91	1.53	+/- 30 % deviation

Table 10 shows the base case values of the varied parameters and the amounts they are perturbed. The results of the sensitivity analyses for the selected cases are shown in Figs. 2 - 4. The vertical axes show the parameters that are varied while the horizontal axes are the percentage deviation in the response variables, MBSP and CCA, from their base values. The top bars with solid fills represent the percent deviation in the CCA as a result of variations in input parameters while the bottom bars with hatched fills represent the percent deviation in the MBSP as a result of input parameters variations. Aside from gasoline price which has an indirect correlation with MBSP and CCA, there is a direct correlation between the other sensitivity input parameters and the response variables.

Some interesting points can be noted from the sensitivity analysis. First, as can be seen from Figs. 3-2 - 3-4, the CCA is more sensitive to changes in the input parameters in comparison to the MBSP, with the South Korean market case (Fig. 3-4) being generally more sensitive. Secondly, deviations in gasoline prices have the most impact on the CCA for all the cases. This impact increases from Fig. 3-2 to Fig. 3-4. For example, in Fig. 3-4

increasing the gasoline price by 30% results in an 82% reduction in the CCA, while reducing the gasoline price by 30% results in a 79% increase in the CCA. The increased sensitivity of the CCA to gasoline prices for the South Korean cases is because the revenue per unit of mixed alcohols is directly correlated to the unit price of gasoline, thus the higher gasoline prices in South Korea coupled with the lower cost of capital mean that the revenue from mixed alcohols have more impact on the MBSP and also CCA. Thus any changes in gasoline price will impact the MBSP and CCA of the South Korean cases more. In general, the South Korean case is more sensitive to operating cost and revenue items in comparison to the U.S. cases, while the U.S. cases are more sensitive to capital cost related items such as TDC and IRR. This is expected, as from the economic analysis results summarized in Table 3-7 it was shown that the energy related costs have a more dominant effect on the MBSP and CCA for the South Korean cases while the capital related costs dominate for the U.S cases.
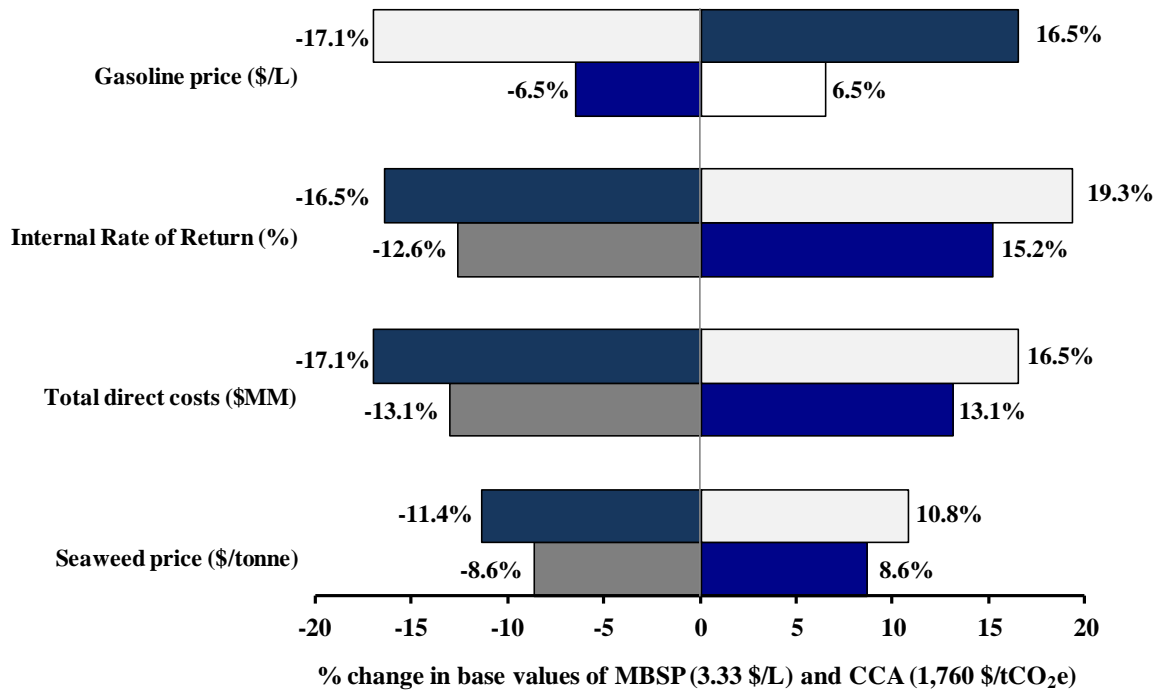
Figure 3-2. The effects of changing key parameters from their base case values on MBSP (bottom bars with hatched fill) and CCA (top bars with solid fill) of the U.S. - self-sufficient plant scenario.
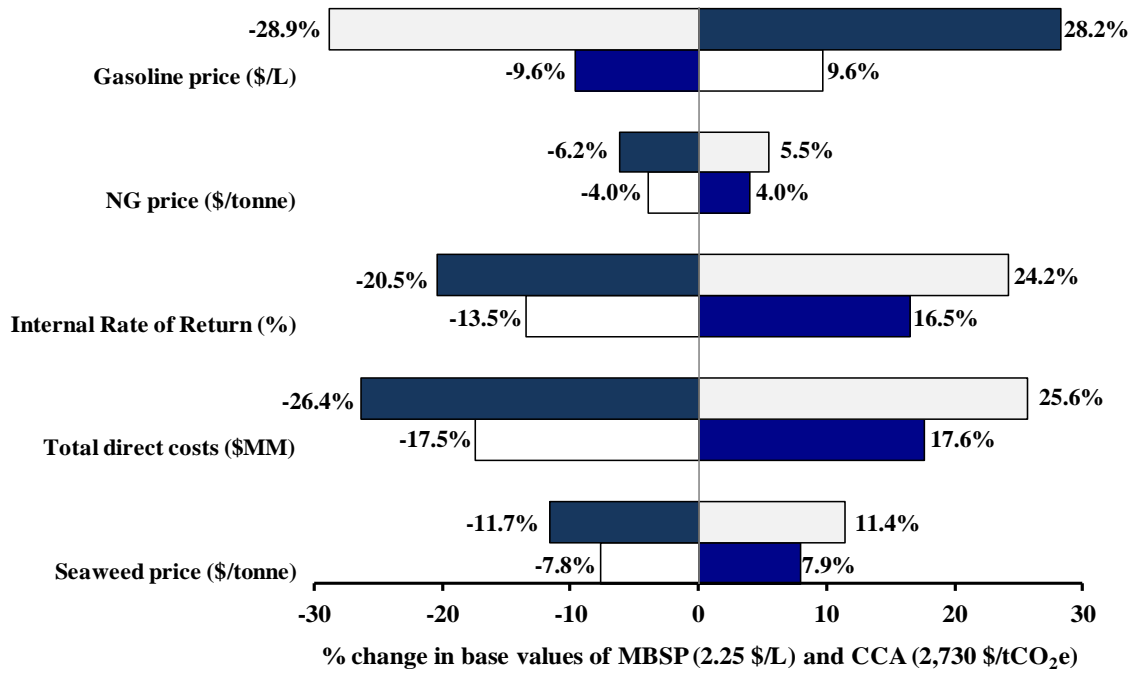
Figure 3-3. The effects of changing key parameters from their base case values on MBSP (bottom bars with hatched fill) and CCA (top bars with solid fill) of the U.S. - NG import plant scenario.
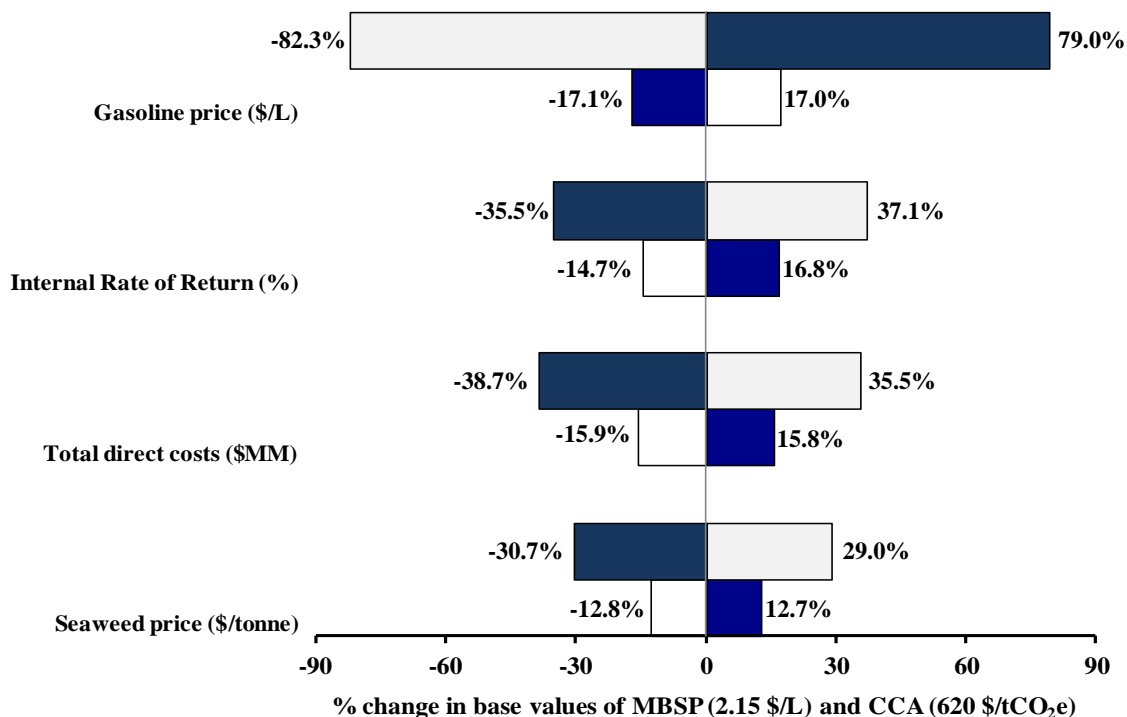
Figure 3-4. The effects of changing key parameters from their base case values on MBSP (bottom bars with hatched fill) and CCA (top bars with solid fill) of the South Korea - self-sufficient plant scenario.

3.4   Conclusions

This work is the first study (to the authors' knowledge) of the techno-economic potential of seaweed-to-biobutanol processes based on a thermochemical route. Different process configurations were designed and simulated, and their economic and environmental feasibility were assessed and quantified using metrics such as the MBSP and CCA for different market scenarios.

The MBSP results showed that the NG import and NG & power import configurations have the lowest MBSP values in their individual markets. However, when the CCA was used as a metric the self-sufficient configurations had the best values in their individual markets with the NG & power import configurations the worst.

The most significant result obtained in the sensitivity analysis is that +/- 30% deviations in gasoline prices lead to greater than -/+ 75% deviation in the CCA for the South Korean self-sufficient configuration. This is because in comparison to the U.S. market, energy related costs have a more dominant impact in the South Korean market. When MBSP is used as a metric the seaweed biomass-to-butanol process using the thermochemical route, with values ranging from 1.97 $/L to 3.33 $/L, is high in comparison to other butanol produced from cellulosic feedstock. However its CCA, which ranges from 620 - 2,720 $/tonneCO$_2$e for the best three cases is in line with that of other first and second generation biofuels, but much higher than the break-even value of 50 $/tonneCO$_2$e recommended by policy makers in western countries.

These results show that more research on the macroalgae supply chain (harvesting to processing plant) and conversion technologies is required to improve the economic and environmental potential of biobutanol from seaweed.

3.5 References

[1]   Kiran B, Kumar R, Deshmukh D. Perspectives of microalgal biofuels as a renewable source of energy. Energy Convers Manag 2014;88:1228–44. doi:10.1016/j.enconman.2014.06.022.

[2]   Ben Yahmed N, Jmel MA, Ben Alaya M, Bouallagui H, Marzouki MN, Smaali I. A biorefinery concept using the green macroalgae Chaetomorpha linum for the coproduction of bioethanol and biogas. Energy Convers Manag 2016;119:257–65.

doi:10.1016/j.enconman.2016.04.046.

[3]   FAO. Fishery and Aquaculture Statistics 2012. Rome: 2012.

[4]   Roesijadi G, Jones SB, Snowden-Swan LJ, Zhu Y. Macroalgae as a biomass feedstock: a preliminary analysis. Richland, Washington: 2010.

[5]   Chen H, Zhou D, Luo G, Zhang S, Chen J. Macroalgae for biofuels production: Progress and perspectives. Renew Sustain Energy Rev 2015;47:427–37. doi:10.1016/j.rser.2015.03.086.

[6]   Jung KA, Lim S-R, Kim Y, Park JM. Potentials of macroalgae as feedstocks for biorefinery. Bioresour Technol 2013;135:182–90. doi:10.1016/j.biortech.2012.10.025.

[7]   Reith JH, Deurwaarder EP, Hemmes K, Curvers A, Kamermans P, Brandenburg W. BIO-OFFSHORE: Grootschalige teelt can zeewieren in combinatie met offshore windparken in de Nordzee. 2005.

[8]   Bruton T, Lyons H, Lerat Y, Stanley M, Rasmussen M. A review of the potential of marine algae as a source of biofuel in Ireland. Dublin, Ireland: 2009.

[9]   Hong JW, Jo S-W, Yoon H-S. Research and development for algae-based technologies in Korea: a review of algae biofuel production. Photosynth Res 2015;123:297–303.

[10]   Lehahn Y, Ingle KN, Golberg A. Global potential of offshore and shallow waters macroalgal biorefineries to provide for food, chemicals and energy: feasibility and sustainability. Algal Res 2016;17:150–60. doi:10.1016/j.algal.2016.03.031.

[11]   Wei N, Quarterman J, Jin Y-S. Marine macroalgae: an untapped resource for producing fuels and chemicals. Trends Biotechnol 2013;31:70–7. doi:10.1016/j.tibtech.2012.10.009.

[12]   van Hal JW, Huijgen WJJ, López-Contreras AM. Opportunities and challenges for seaweed in the biobased economy. Trends Biotechnol 2014;32:231–3. doi:10.1016/j.tibtech.2014.02.007.

[13]   Kumar M, Gayen K. Developments in biobutanol production: New insights. Appl Energy 2011;88:1999–2012. doi:10.1016/j.apenergy.2010.12.055.

[14]   Ranjan A, Moholkar VS. Biobutanol: science, engineering, and economics. Int J Energy Resour 2012;36:277–323. doi:10.1002/er.

[15]   Nikolaison L, Dahl J, Bech KS, Bruhn A, Rasmussen MB, Bjerre AB, et al. Energy production from macroalgae. 20th Eur. Biomass Conf., Milan, Italy: 2012.

[16]   Van Der Wal H, Sperber BLHM, Houweling-tan B, Bakker RRC, Brandenburg W,

López-contreras AM. Production of acetone , butanol , and ethanol from biomass of the green seaweed Ulva lactuca. Bioresour Technol 2013;128:431–7. doi:10.1016/j.biortech.2012.10.094.

[17] Potts T, Du J, Paul M, May P, Beitle R, Hestekin J. The Production of Butanol from Jamaica Bay Macro Algae. AIChE 2012;31:29–36. doi:10.1002/ep.

[18] Gapes JR. The Economics of Acetone-Butanol Fermentation: Theoretical and Market Considerations 2000;2:27–32.

[19] Huesemann MH, Kuo L-J, Urquhart L, Gill GA, Roesijadi G. Acetone-butanol fermentation of marine macroalgae. Bioresour Technol 2012;108:305–9. doi:10.1016/j.biortech.2011.12.148.

[20] Suutari M, Leskinen E, Fagerstedt K, Kuparinen J, Kuuppo P, Blomster J. Macroalgae in biofuel production. Phycol Res 2015;63:1–18. doi:10.1111/pre.12078.

[21] Milledge JJ, Smith B, Dyer PW, Harvey P. Macroalgae-Derived Biofuel: A Review of Methods of Energy Extraction from Seaweed Biomass. Energies 2014;7:7194–222.

[22] Puig-Arnavat M, Bruno JC, Coronas A. Review and analysis of biomass gasification models. Renew Sustain Energy Rev 2010;14:2841–51. doi:10.1016/j.rser.2010.07.030.

[23] Woolcock PJ, Brown RC. A review of cleaning technologies for biomass-derived syngas. Biomass and Bioenergy 2013;52:54–84. doi:10.1016/j.biombioe.2013.02.036.

[24] Okoli C, Adams TA. Design and economic analysis of a thermochemical lignocellulosic biomass-to-butanol process. Ind Eng Chem Res 2014;53:11427–41.

[25] Hyung J, Chul H, Jin D. Pyrolysis of Seaweeds for Bio-oil and Bio-char Production 2014;37:121–6. doi:10.3303/CET1437021.

[26] Adams JMM, Ross AB, Anastasakis K, Hodgson EM, Gallagher JA, Jones JM, et al. Seasonal variation in the chemical composition of the bioenergy feedstock Laminaria digitata for thermochemical conversion. Bioresour Technol 2011;102:226–34. doi:10.1016/j.biortech.2010.06.152.

[27] Jensen A. Present and future needs for algae and algal products. Hydrobiologia 1993;260/261:15–23.

[28] McHugh DJ. A guide to the seaweed industry. Rome: 2003.

[29] Alauddin ZABZ, Lahijani P, Mohammadi M, Mohamed AR. Gasification of lignocellulosic biomass in fluidized beds for renewable energy development: A

review. Renew Sustain Energy Rev 2010;14:2852–62. doi:10.1016/j.rser.2010.07.026.

[30] Ciferno JP, Marano JJ. Benchmarking Biomass Gasification Technologies for Fuels, Chemicals and Hydrogen Production. 2002.

[31] Dutta A, Talmadge M, Nrel JH, Worley M, Harris DD, Barton D, et al. Process Design and Economics for Conversion of Lignocellulosic Biomass to Ethanol Process Design and Economics for Conversion of Lignocellulosic Biomass to Ethanol Thermochemical Pathway by Indirect. 2011.

[32] Union Gas. Chemical Composition of Natural Gas 2016. https://www.uniongas.com/about-us/about-natural-gas/Chemical-Composition-of-Natural-Gas (accessed January 31, 2016).

[33] Devi L, Ptasinski KJ, Janssen FJJ. A review of the primary measures for tar elimination in biomass gasification processes. Biomass and Bioenergy 2003;24:125–40. doi:10.1016/S0961-9534(02)00102-2.

[34] Nexant. Equipment Design and Cost Estimation for Small Modular Biomass Systems, Synthesis Gas Cleanup, and Oxygen Separation Equipment Task 9 : Mixed Alcohols From Syngas — State of Technology. San Francisco, California: 2006.

[35] Dayton D. A review of the literature on catalytic biomass tar destruction. Golden, Colorado: 2002.

[36] Merichem C. LO-CAT H2S removal technology. Merichem Co 2015. http://www.merichem.com/gas (accessed May 31, 2015).

[37] Rubin ES, Rao AB. A Technical, Economic and Environmental Assessment of Amine-based CO2 capture Technology for Power Plant Greenhouse Gas Contorl. Morgantown, West Virginia: 2002.

[38] Matthey J. Delivering world class hydrogen plant performance. Billingham, UK: 2013.

[39] Herman R. Advances in catalytic synthesis and utilization of higher alcohols. Catal Today 2000;55:233–45. doi:10.1016/S0920-5861(99)00246-1.

[40] Burcham MM, Herman RG, Klier K. Higher Alcohol Synthesis over Double Bed Cs - Cu / ZnO / Cr 2 O 3 Catalysts : Optimizing the Yields of 2-Methyl-1-propanol (Isobutanol) 1998:4657–68.

[41] ASTM Standard D7862-15. Standard Specification for Butanol for Blending with Gasoline for Use as Automotive Spark-Ignition Engine Fuel 2015. doi:10.1520/D7862-15.

[42] Phillips S, Aden A, Jechura J, Dayton D. Thermochemical Ethanol via Indirect Gasification and Mixed Alcohol Synthesis of Lignocellulosic Biomass Thermochemical Ethanol via Indirect Gasification and Mixed Alcohol Synthesis of Lignocellulosic Biomass 2007.

[43] CE. Economic indicators. Chem Eng 2015;122:192.

[44] World Bank. PPP conversion factor, GDP (LCU per international $). World Bank, Int Comp Progr Database 2016. http://data.worldbank.org/indicator/PA.NUS.PPP (accessed January 31, 2016).

[45] Consonni S, Katofsky RE, Larson ED. A gasification-based biorefinery for the pulp and paper industry. Chem Eng Res Des 2009;87:1293–317. doi:10.1016/j.cherd.2009.07.017.

[46] Dutta A, Talmadge M, Hensley J, Worley M, Dudgeon D, Barton D, et al. Techno-economics for conversion of lignocellulosic biomass to ethanol by indirect gasification and mixed alcohol synthesis. Environ Prog Sustain Energy 2012;31:182–90. doi:10.1002/ep.10625.

[47] Flnkenrath M. Cost and performance of carbon dioxide capture from power generation. Paris: 2011.

[48] BLS. Consumer Price Index - All Urban Consumers. United States Bur Labor Stat 2016. http://data.bls.gov/timeseries/CUUR0000SA0L1E?output_view=pct_12mths (accessed January 31, 2016).

[49] TE. South Korea Inflation Rate. Trading Econ 2016. http://www.tradingeconomics.com/south-korea/inflation-cpi# (accessed January 31, 2016).

[50] Seider WD, Seader JD, Lewin DR. Product & Process Design Principles: Synthesis, Analysis and Evaluation. 3rd ed. Hoboken, New Jersey: John Wiley & Sons; 2009.

[51] Peters MS, Timmerhaus KD, West RE. Plant Design and Economics for Chemical Engineers. Massachusetts: McGraw-Hill Science/Engineering/Math; 2003.

[52] BLS. Producer Price Indexes. News Release - Bur Labor Stat 2015. http://www.bls.gov/news.release/pdf/ppi.pdf (accessed January 31, 2016).

[53] Dave A, Huang Y, Rezvani S, McIlveen-Wright D, Novaes M, Hewitt N. Techno-economic assessment of biofuel development by anaerobic digestion of European marine cold-water seaweeds. Bioresour Technol 2013;135:120–7. doi:http://dx.doi.org/10.1016/j.biortech.2013.01.005.

[54] Woo H. Establishment of economical integrated process of macroalgal biomass.

Busan, South Korea: 2015.

[55] Fang K, Li D, Lin M, Xiang M, Wei W, Sun Y. A short review of heterogeneous catalytic process for mixed alcohols synthesis via syngas. Catal Today 2009;147:133–8. doi:10.1016/j.cattod.2009.01.038.

[56] EIA UEIA. Petroleum and other liquids data. U.S. Energy Inf Adm 2016. https://www.eia.gov/petroleum/data.cfm#prices (accessed January 31, 2016).

[57] KEEI. Monthly Energy Statistics Vol 31-08-2015. 2015.

[58] Qureshi N, Saha BC, Cotta MA, Singh V. An economic evaluation of biological conversion of wheat straw to butanol: A biofuel. Energy Convers Manag 2013;65:456–62. doi:http://dx.doi.org/10.1016/j.enconman.2012.09.015.

[59] IPCC. IPCC Fourth Assessment Report: Climate Change 2007. Intergovermental Panel Clim Chang 2007. https://www.ipcc.ch/publications_and_data/ar4/wg1/en/ch2s2-10-2.html (accessed April 19, 2016).

[60] PACE. LNG and Coal Life Cycle Assessment of Greenhouse Gas Emissions. Fairfax: 2015.

[61] Abrahams LS, Samaras C, Griffin WM, Matthews HS. Life Cycle Greenhouse Gas Emissions From U.S. Liquefied Natural Gas Exports: Implications for End Uses. Environ Sci Technol 2015;49:3237–45. doi:10.1021/es505617p.

[62] CTA, ORNL. Biomass Energy Data Book 2011: Appendix A. Cent Transp Anal Oak Ridge Natl Lab 2011. http://cta.ornl.gov/bedb/appendix_a/Lower_and_Higher_Heating_Values_of_Gas_ Liquid_and_Solid_Fuels.pdf (accessed January 31, 2016).

[63] Alvarado-Morales M, Boldrin A, Karakashev DB, Holdt SL, Angelidaki I, Astrup T. Life cycle assessment of biofuel production from brown seaweed in Nordic conditions. Bioresour Technol 2013;129:92–9. doi:http://dx.doi.org/10.1016/j.biortech.2012.11.029.

[64] Skone TJ, Littlefield J, Marriot J, Cooney G, Jamieson M, Hakian J, et al. Life Cycle Analysis of Natural Gas Extraction and Power Generation. 2014. doi:DOE/NETL-2014/1646.

[65] Itten R, Frischknecht R, Stucki M. Life Cycle Inventories of Electricity Mixes and Grid Version 1.3. Uster: 2014.

[66] Skone TJ, Gerdes K. Development of Baseline Data and Analysis of Life Cycle Greenhouse Gas Emissions of Petroleum-Based Fuels. 2008. doi:DOE/NETL-2009/1346.

[67]   EIA. How much carbon dioxide is produced by burning gasoline and diesel fuel? U.S. Energy Inf Adm 2015. http://www.eia.gov/tools/faqs/faq.cfm?id=307&t=11 (accessed February 2, 2016).

[68]   Ryan L, Convery F, Ferreira S. Stimulating the use of biofuels in the European Union: Implications for climate change policy. Energy Policy 2006;34:3184–94. doi:http://dx.doi.org/10.1016/j.enpol.2005.06.010.

[69]   Fulton L, Howes T, Hardy J. Biofuels for transport: An international perspective. Paris: 2004.

[70]   Worldwatch Institute. Biofuels for Transport: Global Potential and Implications for Sustainable Energy and Agriculture. London: Routledge; 2012.

[71]   Seljom P. Unconventional Oil & Gas Production. 2010.

[72]   Kelly K, Pershing D, Young C. Life-cycle Greenhouse Gas Analysis of Conventional Oil and Gas Development in the Uinta Basin. Univ Utah 2015. http://www.oilshalesands.utah.edu/leftnavid3page21 (accessed January 31, 2015).

CHAPTER 4 Design of dividing wall columns for butanol recovery in a thermochemical biomass to butanol process

The contents of this chapter have been published in the following peer reviewed literature journal:

Okoli, C.O. and Adams, T.A., 2015. Design of dividing wall columns for butanol recovery in a thermochemical biomass to butanol process. Chemical Engineering and Processing: Process Intensification, 95, pp.302-316.

4.1   Introduction

As a result of global efforts to reduce emissions related to fossil fuel consumption, there has been a shift of focus to produce fuels from biomass. For example, the contribution of biofuels to total road-transport fuel demand was 3 % in 2013 and is estimated to grow to 8 % by 2035 [1]. However, to encourage further increase in the uptake of biofuels, production costs have to be reduced. One way to address this challenge is to reduce biofuel processing costs by employing cutting edge process intensification technologies such as dividing wall columns (DWC).

Since its first industrial application in 1985 by BASF, there have been more than one hundred DWCs implemented in industry, highlighting its increasing popularity [2], with past research showing that DWCs can reduce the investment and energy consumption of a multicomponent distillation process by up to 30 % in comparison to conventional distillation sequences [3–5].

Though DWC technology initially found wide application for distillation of zeotropic mixtures, its use has been further extended to other areas such as extractive distillation [6,7], azeotropic distillation [7,8] and reactive distillation [7]. Also critical to this uptake of DWCs is the fact that questions surrounding the controllability and operability of 3-product and 4-product DWCs have largely been addressed [4,9–12].

One important biofuel production process which may potentially benefit from the application of DWC technology is biobutanol production. This is because biobutanol, a gasoline substitute, is gathering increasing attention due to its advantages over bioethanol [13,14]. Recently, Okoli and Adams [15] showed that the fuel can be produced at a cost of $0.83/L using a novel thermochemical process. That process used a train of conventional distillation columns in the separation section to separate an

eleven component feed into four product blends (including a fuel-grade biobutanol product), and consumed 10% of the total energy and 8% of the total direct costs of the process. However, these energy and capital costs of the separation section can potentially be improved by utilizing DWCs for biobutanol recovery instead of conventional distillation columns, leading to a reduction in production costs of the process and thus have a significant impact in improving the competitiveness of biobutanol as a gasoline replacement. This application of DWC technology has not been previously investigated for biobutanol recovery from a thermochemical process, and is an interesting area of research as past research has demonstrated the benefits of DWC applications to bioethanol, bioDME and biodiesel production processes [16,17].

One major challenge in the research of DWC applications is their design. In commercial chemical process simulators the modeling of a DWC can be a difficult task as there are no custom DWC blocks. Methods identified from literature have made use of multiple columns in process simulators to represent different sections of the DWC [18,19]. Another challenge is the large number of internal column specifications needed for a DWC. This complexity means that computational difficulties should be avoided by using appropriate short-cut methods to determine initial estimates for the variables required for rigorous simulations. Once these variables have been estimated, rigorous simulations based on tray-by-tray MESH (material, equilibrium, summation and heat) equations can be implemented in the process simulation software. One such short-cut method is the minimum energy mountain method (also called the "V_{min} diagram method"). The V_{min} diagram method is a distillation column design tool that can be adapted and used to obtain good estimates for initializing rigorous DWC simulations. It provides a graphical visualization of the minimum energy required for separation of a multicomponent zeotropic feed as a function of the feed properties [20]. The minimum

energy is represented by the normalized vapour flow in the top section of the column, with the highest peak representing the minimum theoretical energy required for separation. The concept of the V_{min} diagram was introduced by Halvorsen and Skogestad of the Norwegian University of Science and Technology (NTNU) in a series of papers in 2003 [20–22]. The method was developed based on Underwood's equations, and requires only input feed details such as feed flowrate (F), composition (z) and feed quality (q) to estimate the minimum vapour flow in the top section of the column (V_T), and distillate (D) at infinite number of trays for desired product recoveries. The method can also be used to generate initial estimates for non-ideal systems by using a process simulator and a large number of trays, typically around four times the minimum number of trays (N_{min}) [20].

Outside NTNU, this method has only been applied to the design of four-product DWCs for multicomponent aromatics mixtures [19,23] and Sun and Bi [24] to the conceptual design of three-product reactive DWCs. These papers demonstrated the efficacy of this method. However, as the number of applications of this method is limited, more independent validations are needed to demonstrate its potential.

In process design, the comparison of different design options is usually done based on identical criteria after an optimization has been carried out. Classical methods for optimizing DWCs are based on mathematical programming (which require derivative information) and fall into a class of problems known as Mixed Integer Nonlinear Programming (MINLP) problems. This is due to the presence of discrete variables such as feed location, and number of trays in different column sections, as well as the nonconvexity of the MESH equations. Javaloyes-Anton et al. [25], reviewed the application of MINLP formulations for the solutions of complex distillation columns (including DWCs), and concluded that based on the high nonlinearities of these

formulations, as well as sophisticated initialization techniques needed to obtain feasible solutions (only local optima are guaranteed as the solutions are highly dependent on the initialization points), these methods are complex and suited only for those skilled enough to adapt them for their own requirements.

An alternative, and easier to implement approach to these methods is to leverage the use of commercial process simulators and derivative-free or "black box" optimization algorithms. These derivative-free algorithms are typically population based, wherein the population contains individuals, with each individual representing a particular solution to the optimization problem. Once an algorithm termination criterion has been reached the optimization problem solution is chosen as that of the individual with the best objective function value. The advantage of these algorithms over derivative search methods is their ability to escape local optima and infeasibility regions, as well as provide multiple feasible solutions to account for real world considerations that are harder to quantify by the designer in an optimization setting. However, they are not able to guarantee that the solutions found are optimal. Though derivative-based search methods can theoretically offer local optimality guarantees, they are not easily amenable to highly complex real world problems and might be unable to find solutions which are as good as those obtained by derivative-free algorithms [25,26]. Examples of these derivative-free algorithms include genetic algorithms (GA), simulated annealing, particle swarm optimization (PSO) amongst others. In-depth discussions about these methods can be found in books, such as those written by Gendreau and Potvin [27], and Kaveh [28].

As a result of these advantages of derivative-free optimization algorithms over classical derivative search methods, the use of derivative-free optimization algorithms coupled with process simulators has found wide use in the literature for optimizing complicated

process systems [25]. Amongst many examples in literature, Leboreiro and Acevedo [26] successfully demonstrated the use of a modified GA interconnected with the Aspen Plus process simulator to optimize complex distillation sequences including a Petlyuk column. Pascall and Adams [29] made use of a PSO algorithm connected to Aspen Dynamics to optimize a novel semicontinuous system for the separation of DME from methanol and water. In that work PSO was used to optimize the controller tuning parameters of the system. The PSO algorithm coupled with Aspen HYSYS was used by Javaloyes-Anton et al. [25] for the optimal design of conventional and complex distillation processes. In their work, the PSO algorithm implemented in MATLAB handles all the discrete variables such as the feed location and the number of trays in column sections, while continuous variables (reflux ratio, boilup ratio etc.) and product purity specifications are handled at the process simulator level. An interesting feature of their work was the use of a novel acyclic DWC simulation structure proposed by Navarro et al. [30] for representing a three-product DWC in the process simulator. The use of an acyclic simulation structure over a traditional recycle structure reduces the simulation time in the process simulator, as the convergence of recycle tear streams is avoided. Despite the efficacy of their methodology, its application to DWCs was restricted to a relatively simple benzene-toluene-xylene feed.

Based on this background, the objective of this paper is to investigate the benefits of applying three-product and four-product DWC technology to the recovery of fuel-grade biobutanol from a highly non-ideal multicomponent alcohol rich feed obtained from a thermochemical biobutanol process. The novelty of our work lies in the use of a comprehensive methodology for designing the DWCs for this particular application. Firstly, we demonstrate how the V_{min} method can be used to estimate decision variables for acyclic 3-product and more complicated 4-product DWC simulation structures in

Aspen Plus. Furthermore, the PSO algorithm coupled with Aspen Plus is then used to optimize the DWCs to minimize an economic objective function. In addition, a sensitivity analysis to investigate the importance of key parameters on the structure and economics of the best DWC configuration was also performed. To the best of our knowledge, this detailed approach for assessing and quantifying the potential for the application of DWC technology to biobutanol recovery is the first of its kind.

The rest of the paper is written as follows. Section 4.2 describes the system and design configurations under study, while in section 4.3 the design methodology is explained in detail. Subsequently, the results of the designed configurations are presented and analyzed in section 4.4. Finally, conclusions are drawn in section 4.5.

4.2   System Description

4.2.1   Feed and products

The multicomponent mixture to be separated is derived from a biobutanol synthesis process [15]. In this process, lignocellulosic biomass is converted to mainly biobutanol and other mixed alcohols through a number of processing steps consisting of biomass drying, gasification, syngas cleanup, and mixed alcohol synthesis. The resulting mixture undergoes a number of pre-distillation separation steps such as flashing to remove light gases, and water adsorption over a molecular sieve. Separation by distillation, which is the subject of this study, is then used to recover biobutanol and other mixed alcohols as products. Table 4-1 shows the components and feed conditions into the distillation system, as well as the product specifications.

Table 4-1. Feed, product and fixed column data for separation system

Feed conditions			Fixed Distillation Column properties	
Temperature (°C)		65.7	Condenser pressure	1.03 bar
Pressure (bar)		2.03	Tray pressure drop	0.01 bar/tray
Total Flow (kg/hr)		53,158	Tray efficiency	0.6
Total Flow (kmol/hr)		1,278		
q (feed quality, liquid fraction)		0.9		

Component	Mole Fraction	Normal b.p. (°C)	Product cuts and specifications		Key components
Carbon Dioxide	0.004	-109.2	A	> 99.3% mole recovery of Methanol	Methanol
Propane	0.036	-43.7			
Ammonia	0.001	-33.4			
n-Butane	0.057	31.1			
Methanol	0.683	64.7			
Ethanol	0.013	78.3	B	> 99% mole recovery of Ethanol	Ethanol, Propanol
Propanol	0.062	97.2			
Water	0.012	100.0			
i-Butanol	0.118	107.7	C	96% mole purity of Butanol [31]	Butanol
n-Pentanol	0.008	137.8	D	> 99% mole recovery of Pentanol	Pentanol
n-Hexanol	0.007	157.4			

4.2.2 Design configurations

In this study, several possible design configurations will be analyzed; a base case conventional configuration and three other DWC-based configurations. The distillation columns in all of the afore-mentioned configurations are simulated using the non-random, two-liquid (NRTL) activity coefficient model with the Redlich-Kwong model for the gas phase and default binary interaction parameters provided in the simulator, Aspen Plus V8.0.

This model was chosen because it provided a good fit to experimental data for the most abundant alcohols (methanol to isobutanol) in the feed mixture (see Table 4-1). Specifically, the binary vapour liquid equilibrium (VLE) data of the methanol-isobutanol [32], ethanol-isobutanol [33], propanol-isobutanol [34], methanol-propanol [35], methanol-ethanol [36], ethanol-propanol [37] pairs were validated against experimental data. Furthermore, we note that the simulation did not detect two liquid

phases using this model for any of the columns described in this study, and that there are no azeotropes present because of the very low water content in the feed.

4.2.2.1 Base case

There are five possible sequences of conventional binary distillation columns for the separation of a multicomponent feed into four products [38]. A quick way for identifying the most promising distillation sequence for further study is to apply the marginal vapour rate method [39] to determine the sequence with the least vapour flow rate. The vapour flow through the column provides a good indicator of both the column's capital and operating costs. This is because the reboiler and condenser duties increase with increased vapour flow, and larger vapour flows lead to larger diameter columns and thus higher capital costs. Therefore distillation sequences with lower vapour loads are preferred.

The results of the marginal vapour rate method as applied to the feed conditions and key component data provided in Table 4-1 are shown in Fig. 4-1. Each configuration is designed for 99.3 mol % recovery of key components, constant column pressure of 1 atm and a reflux ratio of 1.2 times the minimum reflux ratio in each column. The vapour flow rates through each column shown in Fig. 4-1 are all normalized to the total feed flow rate. From Fig. 4-1 it can be seen that the direct sequence illustrated in Fig 4-1(a) has the least total vapour rate of 3.085. Thus this configuration is chosen as the base case for further detailed study.
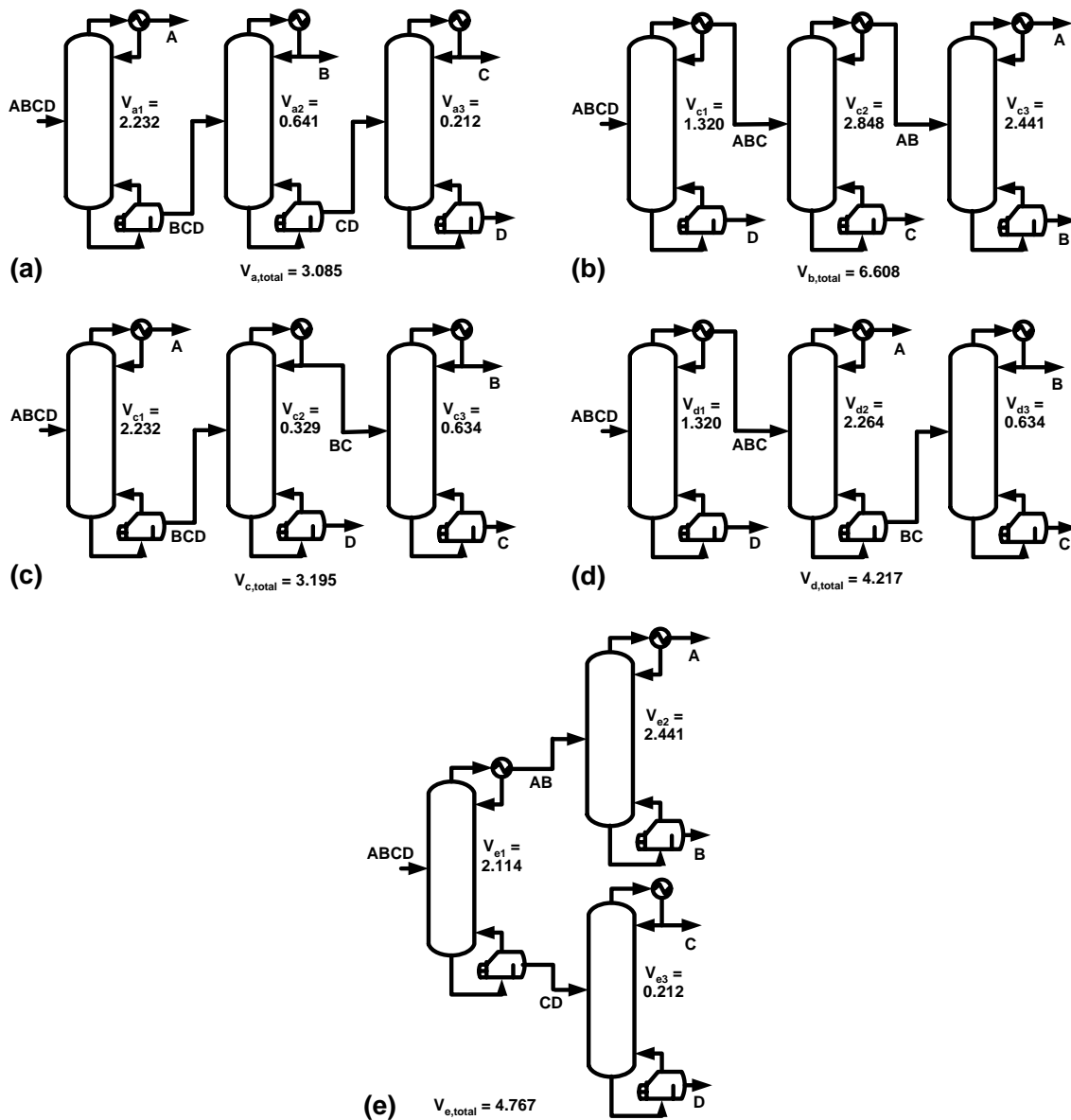
Figure 4-1. Conventional binary distillation column sequences for a four-product recovery showing marginal vapor rate results (a) Direct sequence (b) indirect sequence (c) direct-indirect sequence (d) indirect-direct sequence (e) prefactionator arrangement.

4.2.2.2 DWC configurations

A DWC is a fully thermally coupled distillation sequence in which one condenser and one reboiler are used together with a single column containing one or more longitudinal partition walls, irrespective of the number of products required [19]. In the DWC, the internal re-mixing of streams which occurs in conventional columns is avoided,

minimizing the entropy of mixing and thus energy required for separation of components [19]. The use of a single shell, reboiler and condenser to perform multicomponent (three or more components) separations in a DWC means that capital and energy costs of a distillation process can potentially be reduced.

Figs. 4-2 - 4-4 show three DWC configurations to be analyzed in this study. In Fig. 4-2 a DWC configuration with a conventional column for methanol recovery in direct sequence with a ternary product DWC is shown, while Fig. 4-3 shows a DWC configuration with a ternary product DWC in direct sequence with a butanol recovery column. Finally, Fig. 4-4 (a) shows a quaternary product DWC based on the Kaibel configuration i.e. using only a single partition wall [40]. The Kaibel configuration generally has a higher energy requirement than a 4- product Petlyuk configuration (Fig. 4-4 (b)) for the same quaternary product separation. However, the Kaibel column is preferred for practical implementation because it is easier to design, construct and operate, while the 4-product Petlyuk configuration has mechanical design, operational and control uncertainties that are yet to be overcome [19,41]. Therefore, the 4-product Petlyuk configuration is not chosen for this study.
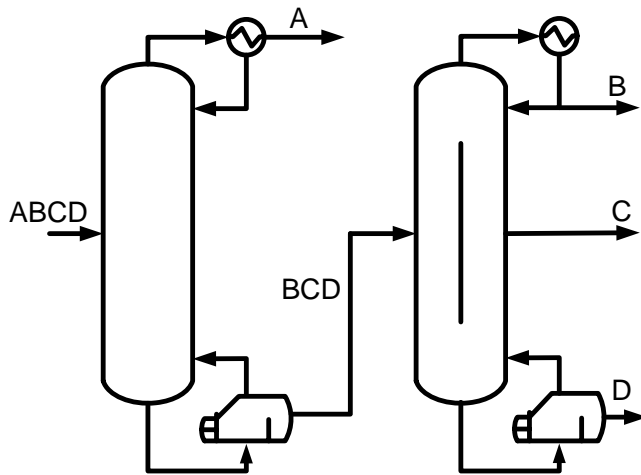
Figure 4-2. DWC configuration 1. Methanol recovery column and 3-product Petlyuk DWC.
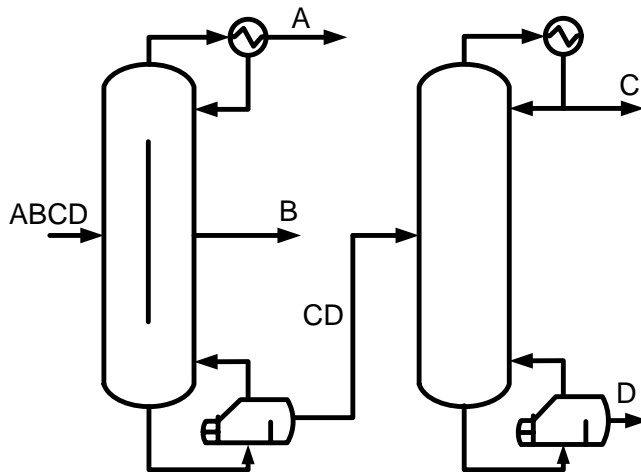
Figure 4-3. DWC configuration 2. 3-product Petlyuk DWC and butanol recovery column.
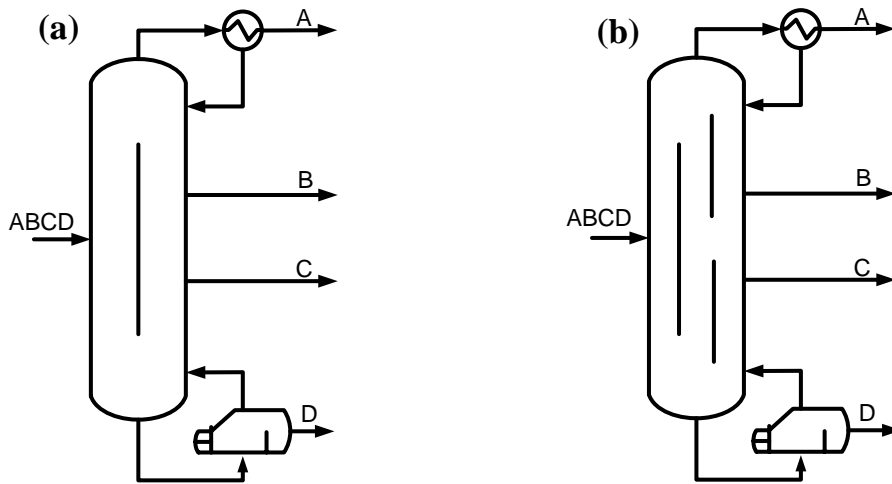
Figure 4-4. 4-product DWC using (a) the Kaibel configuration; (b) the 4-product Petlyuk configuration. The 4-product Petlyuk configuration is not used in this study except to help synthesize the Kaibel configuration.

4.3   Methodology

4.3.1   DWC simulation structure in process simulator

In process simulators, the traditional simulation strategy for DWCs is to represent the DWC structure as conventional columns in sequence connected by liquid-vapour recycle streams at the top and bottom of the column. This structure is also known as a recycle structure and is illustrated in Fig. 4-5 (a) for a ternary product DWC. In this structure, the first distillation column models the prefractionator section of the DWC, while the second column models the product sections of the DWC. In Aspen Plus, for example, each column in the model would be one RadFrac block. There are a number of disadvantages to this method; all related to the presence of recycle streams. The convergence of recycle streams when using the sequential modular mode of process simulators such as Aspen Plus is done through tear streams, thus at each iteration the columns and tear streams have to be converged leading to longer simulation times and a proneness to non-convergence. This is undesirable for scenarios where a flowsheet will

undergo a large number of runs and robustness is a key criteria, such as when linked to an external optimization algorithm.
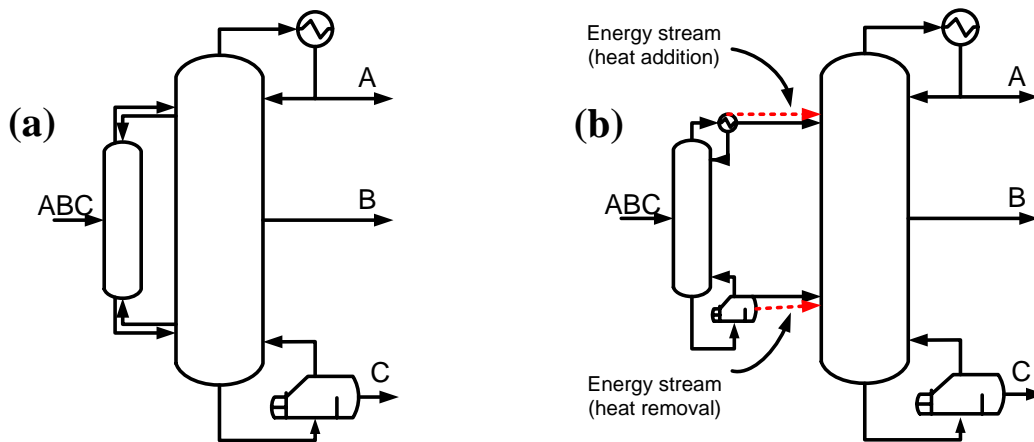
Figure 4-5. Two column structure options for the simulation of a ternary DWC: (a) recycle structure (b) acyclic structure

An alternative model structure for DWC simulation is the acyclic structure proposed by Navarro et al. [30], illustrated in Fig. 4-5 (b) for a ternary product DWC. In their work, the authors replace the material recycle streams present in the recycle DWC structure with material and energy streams. The top of the first column (prefractionator) is connected to the rectifying section of the second column (main column) with a vapour material stream at its dew point and an energy stream with the same energy that would have been removed if a partial condenser was used to provide reflux to the prefractionator. Furthermore, the bottom of the prefractionator is connected to the stripping section of the main column with a liquid material stream at its bubble point and an energy stream with the same energy that that would have been added if a reboiler was used to provide vapour to the first column. The acyclic structure avoids the problems associated with the presence of recycle streams in the recycle structure and thus simulates faster with easier convergence.

4.3.2 DWC initialization (minimum energy mountain (V_{min}) diagram method)
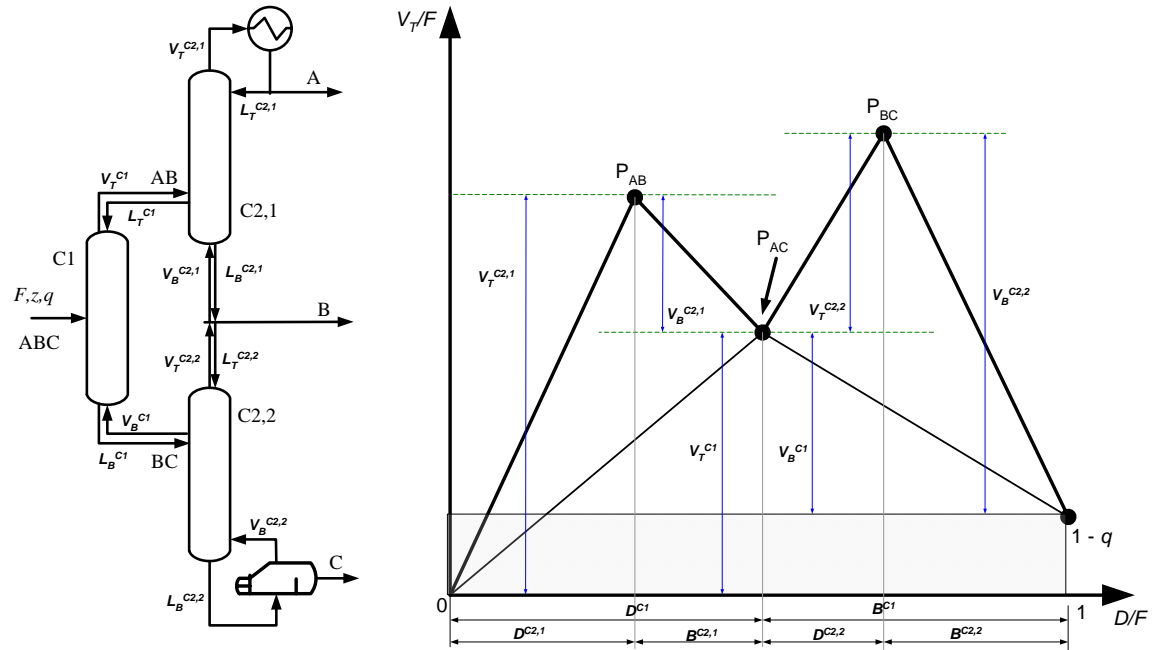
Figure 4-6. Example of column sections of a ternary DWC, and the V_{min} diagram

The V_{min} diagram method is used to generate good initial estimates of the design parameters for the DWCs discussed in this work using the following steps:

1. Select key components and their required recoveries (99.3 mol % is used in this study) for the given feed properties. For example from Table 4-1, for the separation between cut A and cut B, methanol is the light key (LK) component while ethanol is the heavy key (HK) component.

2. Calculate V_T/F and corresponding D/F values for all possible LK and HK splits between key components in a binary distillation column at constant pressure using at least $4N_{min}$ equilibrium stages at the specified recoveries. For example, to split a mixture of ABC in a single binary distillation column, there are three possible splits. (1) A/B, meaning that A is recovered in the distillate and B in the bottoms to the desired recoveries; (2) B/C, meaning B (and therefore A) in the distillate and C in the bottoms; and (3) A/C, meaning that A is in the distillate and C is in the bottoms to the desired

recoveries, with portions of B recovered in both. For each of these three cases, the distillate-to-feed ratio (D/F) and vapour-to-feed ratio (V_T/F) required to achieve the desired recoveries specified in step 1 (V_T is the vapour flow rate at the top of the column) are computed in a process simulator by assuming that the number of equilibrium stages is $4N_{min}$. For this study, a DSTWU model in Aspen Plus is used to compute N_{min} for each possible split, based on the classic Fenske equation. Then the DSTWU model is run a second time using $4N_{min}$ equilibrium stages to compute the feed location, D/F and reflux ratio. Next, this information is used as an initial guess for the more rigorous RadFrac model with $4N_{min} - 2$trays (tray efficiency is used) and the same feed location, but where the D/F and reflux ratio as predicted by DSTWU are used only as initial guesses for the design specification tool which varies D/F and the reflux ratio to achieve the desired product recoveries. The final values for D/F and V_T/F as computed by RadFrac are plotted on the V_{min} diagram as shown in Figure 4-6, where points P_{AB}, P_{BC} and P_{AC} correspond to the solutions for the A/B, B/C, and A/C splits, respectively. Note, for quaternary systems, there would be six points instead of three, corresponding to splits of A/B, A/C, A/D, B/C, B/D, and C/D.

3. Using V_T and D computed from step 2 for each split in a binary distillation column, the corresponding liquid flow from the top of the column (L_T), the liquid flow from the bottom (L_B), the vapour flow from the bottom (V_B), and the bottoms flow rate (B) can be computed using the material balance equations (1) – (4):

$$L_T = V_T - D \tag{1}$$

$$L_B = L_T + qF \tag{2}$$

$$V_B = V_T - (1-q)F \tag{3}$$

$$B = F - D \tag{4}$$

These flows are depicted graphically in Fig. 4-6 for the column sections of a ternary DWC.

4. The corresponding operating variables such as reflux ratios (*RR*) and boilup ratios (*BR*) which are useful for initializing the DWC simulation structure can then be computed using equations (5) – (6), while the side flowrate(s) can be calculated via an appropriate material balance.

$$RR = L_T /D \tag{5}$$

$$BR = V_B /B \tag{6}$$

4.3.3 Derivative-free Optimization algorithm

The PSO algorithm is a derivative-free optimization technique inspired by nature. The algorithm mimics the way a swarm of birds (particles) locate a best landing place. In the algorithm, the velocity and position of each particle in a swarm is updated iteratively based on its (i) past velocity and position (ii) personal best position at each iteration (iii) global best position (swarm's best) at each iteration. The algorithm is terminated once a stopping criterion is satisfied, and the global best position is subsequently outputted as the optimum. Adams and Seider [42] demonstrated the effectiveness of the PSO algorithm for the practical optimization of complex chemical distillation processes. Apart from its effectiveness, it is also chosen for this work because it is easy to implement and use with commercial simulation software, and has few tuning parameters.

For this work a discrete version of the PSO algorithm in which discrete decision variables are treated as continuous variables for use in the PSO algorithm, but rounded to the nearest integer (or discrete value) when used to evaluate the objective function (that is, to run the simulation) [43]. Furthermore, the positions of the particles are

initialized using a Latin hypercube sampling method to enable adequate sampling of the search space.

4.3.4 Objective function

Table 4-2. Additional data for capital and utility costs calculations

Distillation columns (default values from Aspen Plus V8.0)	
Tray type: sieve tray	
Tray spacing, s: 0.609 m (24 inches)	
Column height, H (m) = 3 + ($NT \times s$); where NT = number of trays	
Flooding approach: 80 % [44]	
Utility costs	
Natural gas [45]	$2.51/MMBtu
Electricity [46]	$0.0491/kWh
Water makeup and treatment [47]	0.002 cents /U.S. gal
Steam, computed cost (10 bar MP steam, 185 °C)	$2.14 /GJ
Cooling water, computed cost (30 − 45 °C)	$0.278 /GJ

The basis of comparison of the design configurations is the total annualized cost (TAC) of each design, which is minimized as the objective function of the PSO algorithm. The TAC for each column is a sum of the operating cost per year and annualized capital cost of the column, assuming an annualization period in years. The operating cost is the cost of the utilities (steam and cooling water) needed to provide the required heating and cooling duties to the column reboiler and condenser. These costs are estimated using the method described by Towler and Sinnott [47] in which the prices of steam (medium pressure) and cooling water are directly related to the prices of natural gas, electricity and water (see Table 4-2 for references).The capital cost is dependent on the column diameter, number of trays, and heat exchanger areas. Correlations for computing the costs of the reboiler, condenser, and sieve trays are obtained from Seider et al. [38], while cost correlations for the column are obtained from Rangaiah et al. [48]. Dejanovic et al. [9] recommends that the sieve trays in the dividing wall section of the DWCs should be about 1.2 times the cost of conventional sieve trays. Instead, it was assumed that the cost is 1.5 times the cost of conventional sieve trays as a conservative estimate. These sieve trays are specially constructed with partition walls for use in DWCs with

non-welded walls. Dejanovic et al. [9] notes that they are becoming more popular in DWCs as they allow much more design and implementation flexibility. The material of construction is assumed to be carbon steel for all capital cost computations. The computed capital cost is subsequently annualized by multiplying with an annualization factor (F) using equation (7), where i is the fractional interest rate per year, and n is the annualization period in years. The values of i and n are set at 0.1 (or 10 %) and 5 years respectively as recommended by Smith [49].

$$F = \frac{i(1+i)^n}{(1+i)^n - 1} \tag{7}$$

In order to consistently compare the predicted costs of the DWC systems in this work to the costs of the conventional continuous distillation sequences, the cost year for the analysis is December 2012 with an operating time of 8,000 h/yr for all cases. Other data for the computation of the capital and utility costs are shown in Table 4-2.

4.3.5 Two tier simulation - optimization implementation algorithm
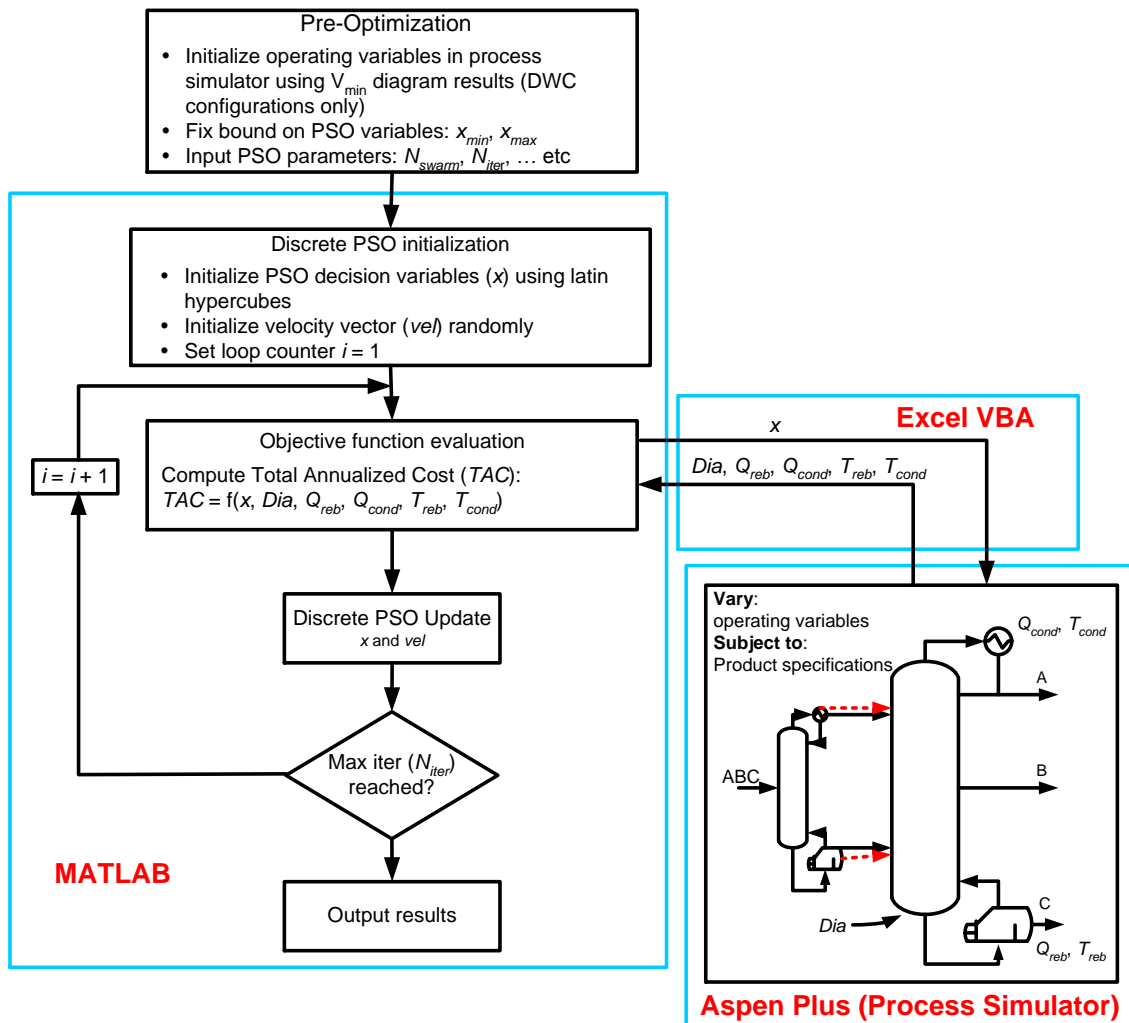
Figure 4-7. Illustration of the implemented algorithm

The proposed design methodology is implemented as illustrated in Fig. 4-7. The objective is to determine the optimal structure (feed location, total number of trays) and operating conditions (*RR*, *BR*) of the distillation columns that minimize the TAC while achieving product specifications. The implementation starts at the pre-optimization stage. For the DWC configurations, the V_{min} method is used to determine the initial values for the operating variables of the acyclic DWC simulation structure (equilibrium-based RadFrac models in Aspen Plus are used to represent the columns). Subsequently, input parameters and bounds on the decision variables of the PSO algorithm are fixed. Each decision variable, N_j, represents the number of trays in the *j*th section of the

product column. Where j is a subset of J (the total number of sections in the product column). An additional decision variable for the DWCs only is N_{J+1}, which represents the tray number of the feed location into the prefractionator. These values are then inputted into MATLAB.

For the DWC configurations, the number of trays from the V_{min} computations are used to determine the upper bounds of the number of trays in each column section for the PSO algorithm using a heuristics approach. First, the upper bounds are fixed from the V_{min} results. For example, for DWC configuration 1, the upper bound of the number of trays in N_I is fixed at N_{feed} from column section C2,1 from the V_{min} results (see Fig 4-13 for decision variable, and Table 4-4 for V_{min} results). The upper bound on N_{II} is fixed at $N_{trays} - N_{feed}$ from column section C2,1 i.e. the bottom half of the column. In addition the upper bound on N_{III} is fixed at N_{feed} from column section C2,2, while the upper bound on N_{IV} is fixed at $N_{trays} - N_{feed}$ from column section C2,2. Finally, in runs where the particles get stuck at the upper bound, these bounds are increased. The bounds can also be tightened to reduce the search space.

The PSO algorithm implementation in MATLAB then proceeds as follows; first, the decision variables of the PSO algorithm are initialized using a Latin hypercube sampling technique applied to the search space created by the bounds on the decision variables. Once the initialization of the decision variables is complete, their values are then passed to the Aspen Plus based process simulator via an Excel VBA interface. The information received from Excel VBA is used to specify the structure and feed location of the distillation columns in the process simulator. Note again that the decision variables of the PSO algorithm are discrete, and so although the variables are treated as continuous in the PSO algorithm, they are rounded to the nearest integer before passing them to Aspen Plus. Furthermore, the distillation columns in Aspen Plus are set up to

meet recovery or purity specifications of key components in product streams (distillate, bottom, and side streams as shown in Table 4-1) by varying operating variables such as reflux ratios, boilup ratios and flowrates of side streams. Thus, Aspen Plus handles all the operational constraints. Furthermore, the tray efficiencies (shown in Table 4-1) are also accounted for in the distillation column structure set up in Aspen Plus. The simulation is then run in Aspen Plus which returns information to MATLAB (via the Excel VBA interface) such as column diameter (Dia), reboiler and condenser duties (Q_{reb} and Q_{cond}), and reboiler and condenser temperatures (T_{reb} and T_{cond}) needed to compute the TAC. The TAC is then evaluated using the column structure information from the PSO algorithm and information from the process simulator. Based on the results of the TAC computation, the PSO decision variables are updated and passed to the process simulator via the Excel VBA interface. This process between MATLAB, which houses the PSO algorithm and TAC objective function, and Aspen Plus process simulator continues iteratively until an algorithm termination criteria is met i.e. a certain number of iterations has been completed by the PSO algorithm. In addition, a large penalty coefficient is used to penalize the objective function in cases of infeasible or failed runs of the process simulator (runs ending with errors). For all the cases studied in this work ten particles are chosen for the PSO algorithm, with the number of iterations (per particle) set to be one hundred.

4.4 Results and discussion

4.4.1 V_{min} diagram results

4.4.1.1 V_{min} diagram results for DWC in configuration 1

Table 4-3. Properties of the feed into the DWC of configuration 1

Feed conditions		
Temperature (°C)	120.3	
Pressure (bar)	2.06	
Total Flow (kg/hr)	18,776	
Total Flow (kmol/hr)	284	
q (feed quality)	0.86	
Mole Fraction, z (-)	Product cuts	Key components
Methanol	0.021	B	Propanol
Ethanol	0.056		
Water	0.055		
Propanol	0.276		
Butanol	0.527	C	Butanol
Pentanol	0.036	D	Pentanol
Hexanol	0.029		

In configuration 1, methanol and lighter gases (cut A) have been removed at the top of the conventional column, and the resulting bottoms are sent to the DWC. The properties of the resulting feed into the DWC are shown in Table 4-3.

Fig. 4-8 shows the column sections and the resulting V_{min} diagram for the DWC in configuration 1. The highest peak occurs at P_{BC}, meaning that the separation between cuts B and C is the most difficult and thus requires the most energy. This is expected, as amongst the key components shown in Table 4-3 the boiling points of propanol and butanol are the closest and will thus be the most difficult separation in comparison to the others.
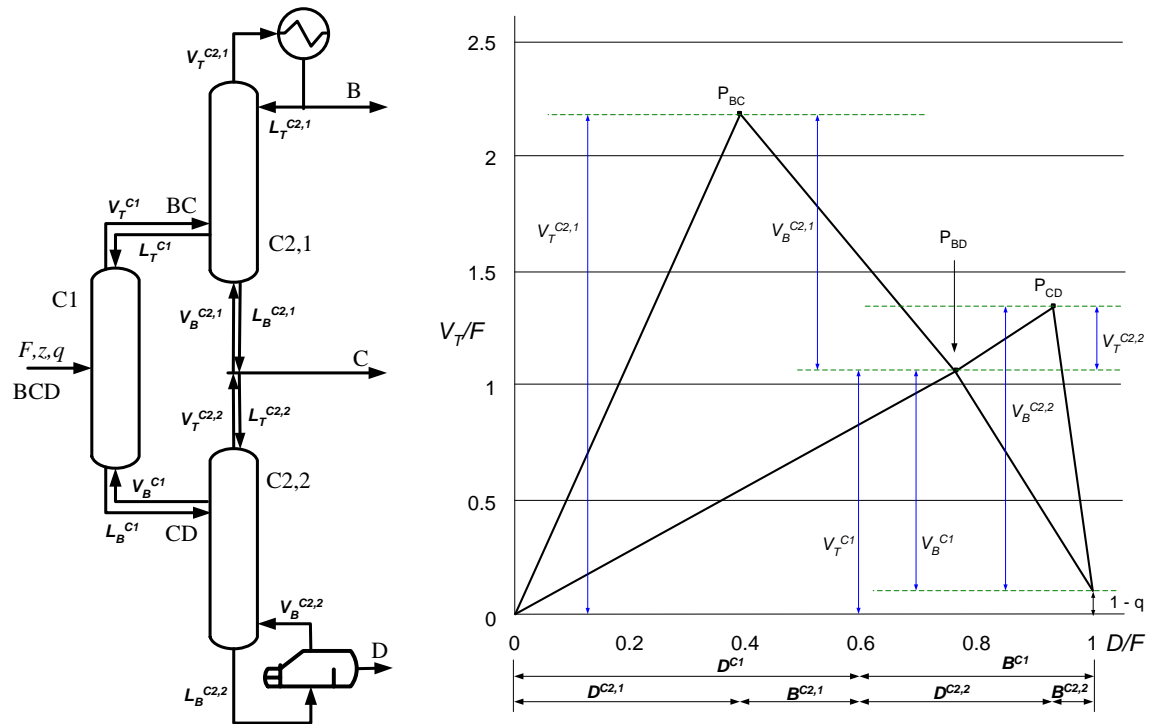
Figure 4-8. column sections and V_{min} diagram results (not drawn to scale) for DWC configuration 1

The V_{min} diagram results are then used with equations $1 - 6$ to calculate all the flows in the column sections illustrated in Fig. 4-8, and to subsequently compute the reflux ratios, boilup ratios, and side flowrate required for initializing the acyclic DWC structure. Table 4-4 shows the results of these calculations for normalized flows (based on the feed flowrate).

For initializing the operating variables in the acyclic DWC structure the required values for the product column are $RR^{C2,1}$, $BR^{C2,2}$ and side stream flowrate (sum of $D^{C2,2}$ and $B^{C2,1}$). While for the prefractionator, RR^{C1} and BR^{C1} are used.

Table 4-4. Calculated material balance results for the V_{min} diagram in Fig. 4-8 (all flows are normalized).

Sections	C2,1	C2,2	C1
N_{trays}	100	40	28
N_{feed}	50	20	14
Specified from V_{min} diagram			
V_T	2.2266	0.1945	1.1333
V_B	1.0933	1.1895	0.9950
D	0.4107	0.1406	0.7909
B	0.3802	0.0684	0.2091
Calculated			
L_T	1.8158	0.0539	0.3424
L_B	1.4734	1.2579	1.2041
RR	4.4207	0.3831	0.4329
BR	2.8757	17.3826	4.7588

4.4.1.2 V_{min} diagram results for DWC in configuration 2

The properties of the feed into the DWC in configuration 2 are shown in Table 4-1. However, cut C now comprises of pentanol and hexanol, as butanol and all components heavier than it are recovered in the bottom of the column. The column sections and resulting V_{min} diagram results are illustrated in Fig. 4-9. The highest peak is P_{AB}, which represents the energy required for the separation of cuts A and B, for which methanol is the light key from cut A and ethanol is the heavy key from cut B.
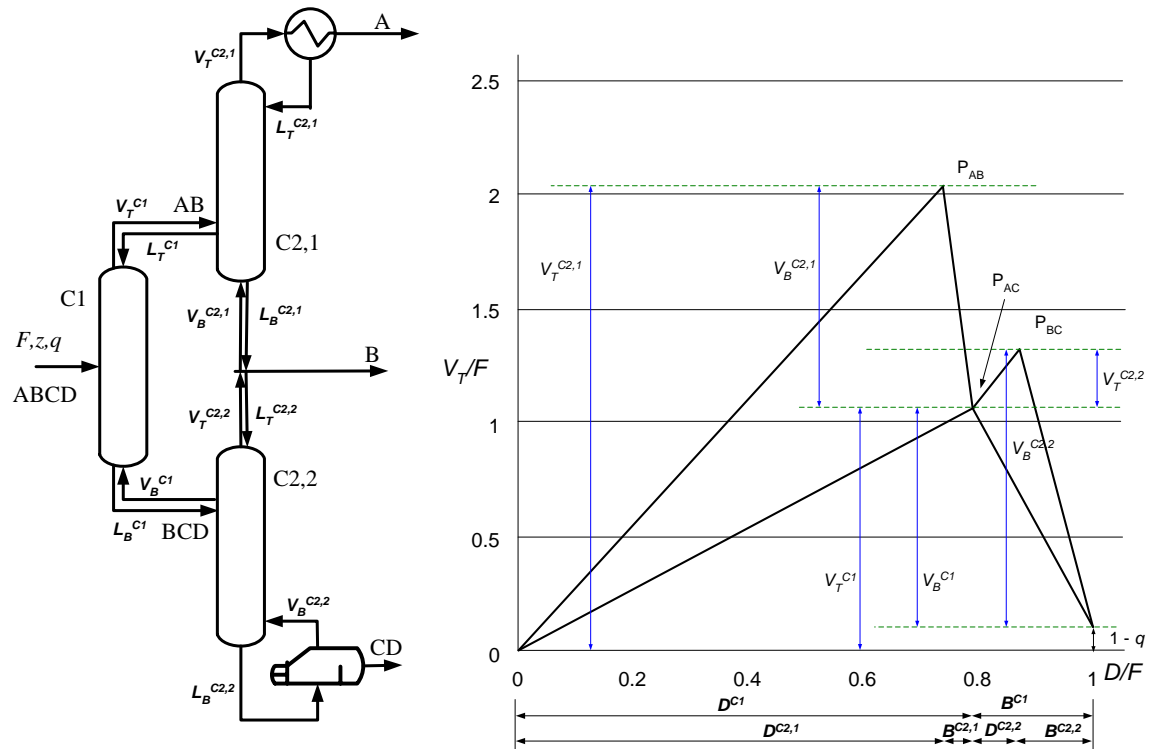
Figure 4-9. Column sections and V_{min} diagram results (not drawn to scale) for DWC configuration 2.

Table 4-5 shows the results of the calculations based on equations $1 - 6$. The selection of *RR* and *BR* values for initializing the acyclic DWC structure, as well as the calculation of the side stream flowrate is the same as that described in section 4.4.1.1.

Table 4-5. Calculated material balance results for the V_{min} diagram in Fig. 4-9 (all flows are normalized).

Sections	C2,1	C2,2	C1
N_{trays}	108	99	40
N_{feed}	47	45	18
Specified from V_{min} diagram			
V_T	2.0192	0.2255	1.0256
V_B	0.9936	1.1531	0.9276
D	0.7753	0.0772	0.7902
B	0.0149	0.1326	0.2098
Calculated			
L_T	1.2439	0.1484	0.2354
L_B	1.0085	1.2857	1.1374
RR	1.6044	1.9220	0.2979
BR	66.7094	8.6957	4.4215

4.4.1.3 V_{min} diagram results for DWC in configuration 3

The properties of the feed into the DWC in configuration 3 are shown in Table 4-1. The methodology described in section 4.3.2 for generating the V_{min} diagram is sufficient for Petlyuk configurations, as is the case in configurations 1 and 2. However, for the Kaibel configuration used in configuration 3, an additional step is taken to generate the V_{min} diagram from its corresponding 4-product Petlyuk configuration (see Fig. 4-4). This is because unlike the Petlyuk configuration, the prefractionator of the Kaibel configuration does not perform the easy split between products A and D, but performs the more difficult split between products B and C [50].

The procedure for generating the V_{min} diagram of the Kaibel configuration from its corresponding Petlyuk configuration is illustrated in Fig. 4-10, and is done using the graphical method described by Halvorsen and Skogestad [50], which is again based on the Underwood equations.

Figure 4-10. Illustration of V_{min} diagrams (Kaibel and Petlyuk) for a 4-product DWC

First the V_{min} diagram for the 4-product Petlyuk configuration is generated using the methodology described in section 4.3.2. The resulting V_{min} diagram is shown with the solid lines in Fig. 4-10, with peaks at P_{AB}, P_{BC}, and P_{CD}. The point P_{BC} is shared by both the 4-product Petlyuk and Kaibel configurations, as the prefractionator in the Kaibel column performs the split between B and C. To obtain approximate locations for peaks P'_{AB} and P'_{CD}, draw lines parallel to $P_{AD}P_{AB}$ and $P_{AD}P_{CD}$ (shown in Fig. 4-10 as dashes) from P_{BC} to intersect at the vertical lines through P_{AB} and P_{CD}. The intersection of these parallel lines from P_{BC} with the vertical lines through P_{AB} and P_{CD} give the peaks P'_{AB} and P'_{CD} respectively for the Kaibel configuration.

By applying the procedure discussed above, the V_{min} diagram result for configuration 3 can be obtained, and is shown in Fig. 4-11. The broken lines outline the V_{min} diagram of the Kaibel configuration, while the solid lines show the V_{min} diagram of the corresponding 4-product Petlyuk configuration. The highest peak occurs at P'_{AB} which as mentioned before is the separation between methanol in cut A, and ethanol in cut B.

The middle section (C2x) of the product column in the Kaibel column performs the sharp B/C split [51]. However, as this has already been performed in the prefractionator, the number of trays in this section is computed as the minimum number of trays using the Fenske equation.
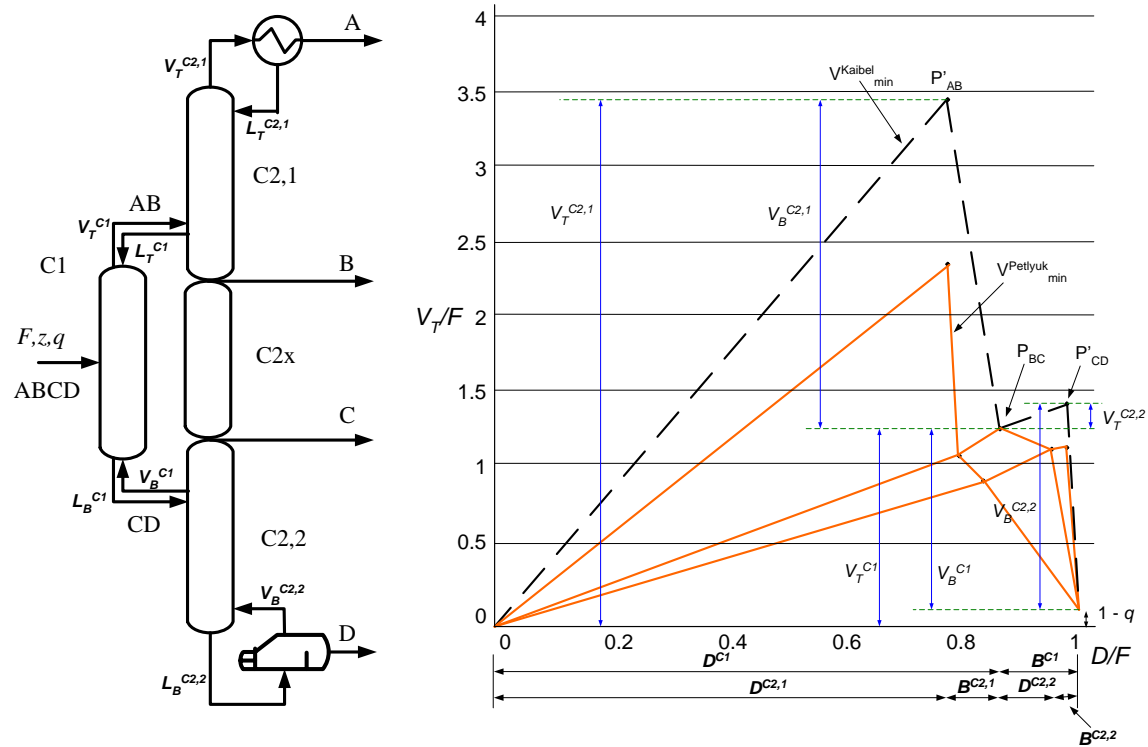
Figure 4-11. Column sections and V_{min} diagram results (not drawn to scale) for DWC configuration 3. Kaibel column (broken lines) and Petlyuk column (solid lines) are shown.

The material balance calculations for the V_{min} diagram are shown in Table 4-6.

Table 4-6. Calculated material balance results for the V_{min} diagram in Fig. 4-11 (all flows are normalized)

Sections	C2,1	C2,2	C1
N_{trays}	108	99	40
N_{feed}	47	45	18
Specified from V_{min} diagram			
V_T	3.4375	0.1864	1.2511
V_B	2.1864	1.3404	1.1540
D	0.7753	0.1168	0.8674
B	0.0921	0.0158	0.1326
Calculated			
L_T	2.6622	0.0695	0.3837
L_B	2.2784	1.3561	1.2866
RR	3.4337	0.5950	0.4424
BR	23.7443	84.9916	8.7021

For initializing the operating variables in the acyclic DWC structure the required values for the product column are $RR^{C2,1}$, $BR^{C2,2}$ and side stream flowrates ($D^{C2,2}$ and $B^{C2,1}$). While for the prefractionator, RR^{C1} and BR^{C1} are used. Note that unlike in the other DWC configurations, there are two side stream flowrates in configuration 3.

4.4.2 Optimization results (optimal structures)

4.4.2.1   Base case
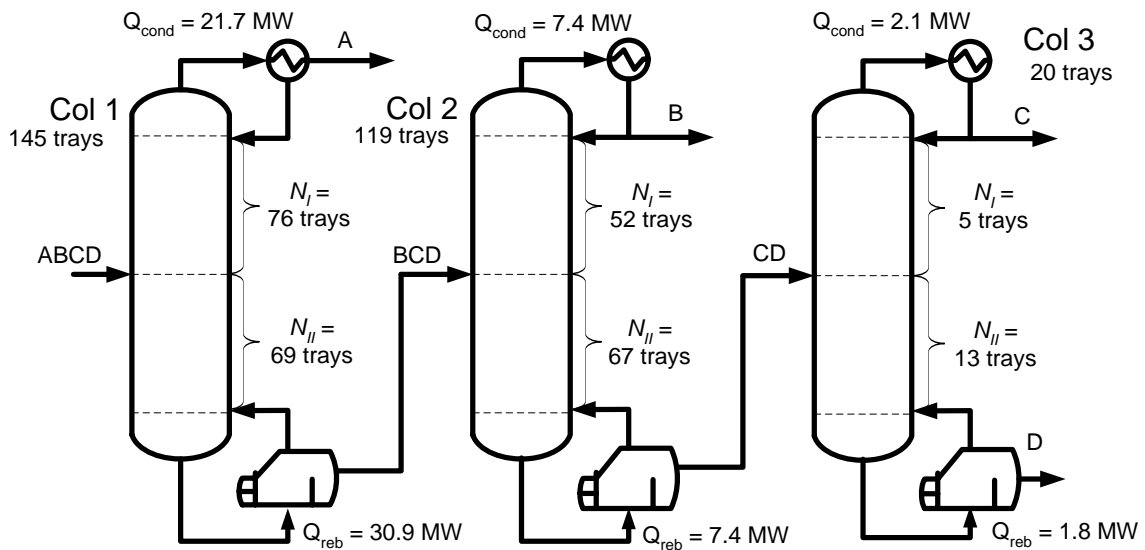
Figure 4-12. Base case showing the optimal structure of the columns, and condenser and reboiler duties

The base case is set up using the data shown in Table 4-1 with the results of its optimal structure shown in Fig. 4-12. For the base case each column is optimized individually. Each column is divided into 2 column sections with the number of trays in each column section as decision variables (N_I and N_{II}). Furthermore, the bounds of each decision variable were kept between 4 and 80 for the optimization. In addition, it should be noted that the PSO was re-run using a variety of different sets of initial conditions for the swarm, but the algorithm always converged on the same optimum result. The results show that the first column which recovers methanol and lighter components (cut A) in the distillate is the largest, both in terms of number of trays, and condenser and reboiler duties. The higher energy requirement in this column can be explained by the larger flowrate into the first column, the large amount of methanol in the feed (68.3 mol %), and the close boiling point between methanol and ethanol (HK component in cut B). All

these make recovering > 99.3 % mole recovery of methanol in the distillate difficult and more energy intensive in comparison to the other columns. Note also that though this column is tall, at approximately 91.3 m, it is below 110 m (about 175 trays) which is the maximum height recommended for distillation columns [41].

4.4.2.2 DWC configurations 1 and 2

Figure 4-13. Model for DWC configuration 1 showing (a) simulation structure, with PSO variables and bounds (b) optimal structure of the equivalent DWC design with the condenser and reboiler duties, liquid split ratio (r_L) and vapor split ratio (r_V)

In DWC configuration 1, the first column is a conventional methanol recovery column with specification and results as discussed for column 1 of the base case in section 4.4.2.1. The output of that column, with feed properties as shown in Table 4-3, is subsequently fed into the 3-product DWC. In comparison to a conventional column, there are additional operating and structural variables for minimizing the TAC of the DWC. This is because of the presence of a side stream in the DWC, as well as the interconnection between the prefractionator and product columns of the DWC. In the

process simulator, five operating variables need to be specified for simulating the acyclic DWC structure. These are the RR, BR and side stream flowrate of the product column, as well as the RR and BR of the prefractionator. The initialization of these variables is done using the results of the V_{min} method shown in section 4.4.1.1. In the process simulator setup the operating variables of the product column are varied to meet the specifications of the product streams (RR for B, side stream flowrate for C, and BR for D). This leaves the two operating variables of the prefractionator as degrees of freedom which can be varied to minimize the reboiler duty. However, in this study we simplify the process simulator setup and leave the values of RR and BR of the prefractionator at their V_{min} result values. To optimize the 3-product DWC structure, five independent discrete variables are used as shown in Fig. 4-13 (a) with their respective bounds. Variables N_I - N_{IV} relate to the number of trays in the sections of the product column, while variable N_V relates to the feed location at the prefractionator. In reality the prefractionator of the DWC is in fact located in the product column; thus a simplifying assumption is that the number of trays in the prefractionator is equivalent to the number of trays in the corresponding part of the product column i.e. the summation of variables N_{II} and N_{III}. This assumption means that an over-separation will be performed on one side of the dividing wall. However, the approach is still very reasonable as the most difficult separations determine the height of the DWC. The resulting optimal structure after optimization is shown in Fig. 4-13 (b).

In DWC configuration 2, the DWC column is placed before a conventional column for butanol recovery. Apart from the difference in feed properties into the DWC column, its process simulation setup and optimization is similar to that of the DWC column in configuration 1. The structure setup and optimal structure for configuration 2 are shown in Fig. 4-14.
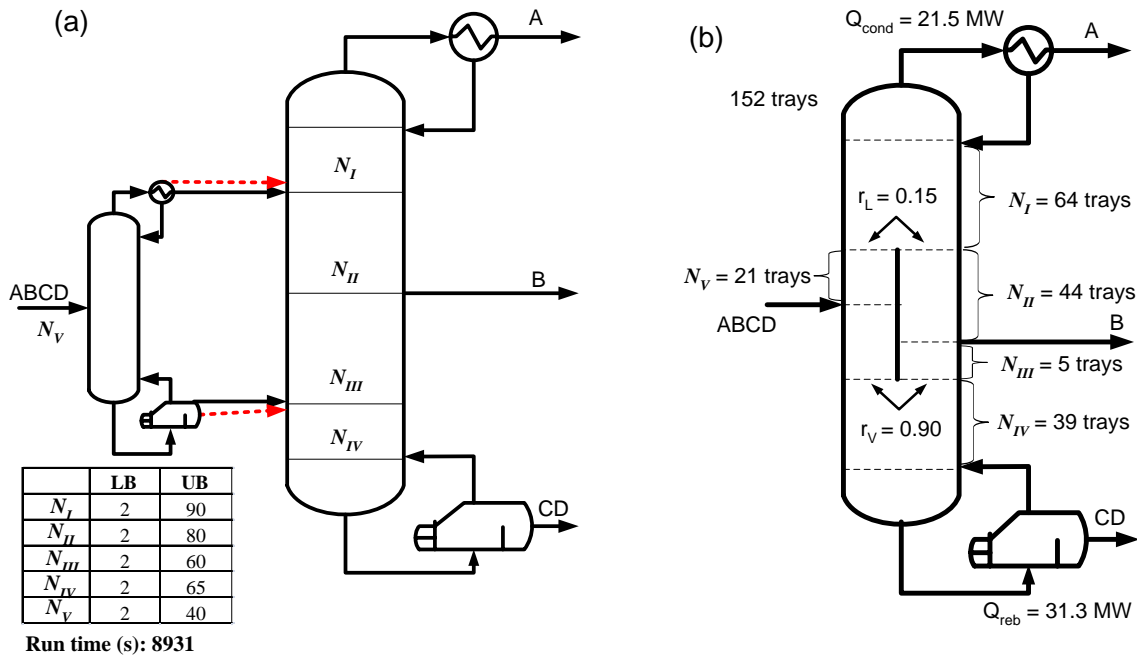
Figure 4-14. Model for DWC configuration 2 showing (a) simulation structure, with PSO variables and bounds (b) optimal structure of the equivalent DWC design with the condenser and reboiler duties, liquid split ratio (r_L) and vapor split ratio (r_V)

4.4.2.3 DWC configuration 3

In configuration 3, a 4-product DWC based on a Kaibel configuration is used. The additional product in this configuration means that in comparison to the 3-product DWC an extra operating variable needs to be specified for the operation of the column, and an extra discrete variable for optimizing the structure. The extra operating variable is the side stream flowrate of the additional side product, while an additional discrete variable is added to represent the column section between the two side products. Similar to the 3-product DWC configurations, the prefractionator operating variables are kept constant at their V_{min} values while the product column's operating variables are varied to meet product specifications during the process simulation. The number of trays in the prefractionator is given as the summation of variables N_{II} - N_{IV}, with the assumption that the number of trays in the prefractionator is equal to the number of trays in the

equivalent sections of the product column also being maintained. Fig. 4-15 shows the structure setup and optimal structure.
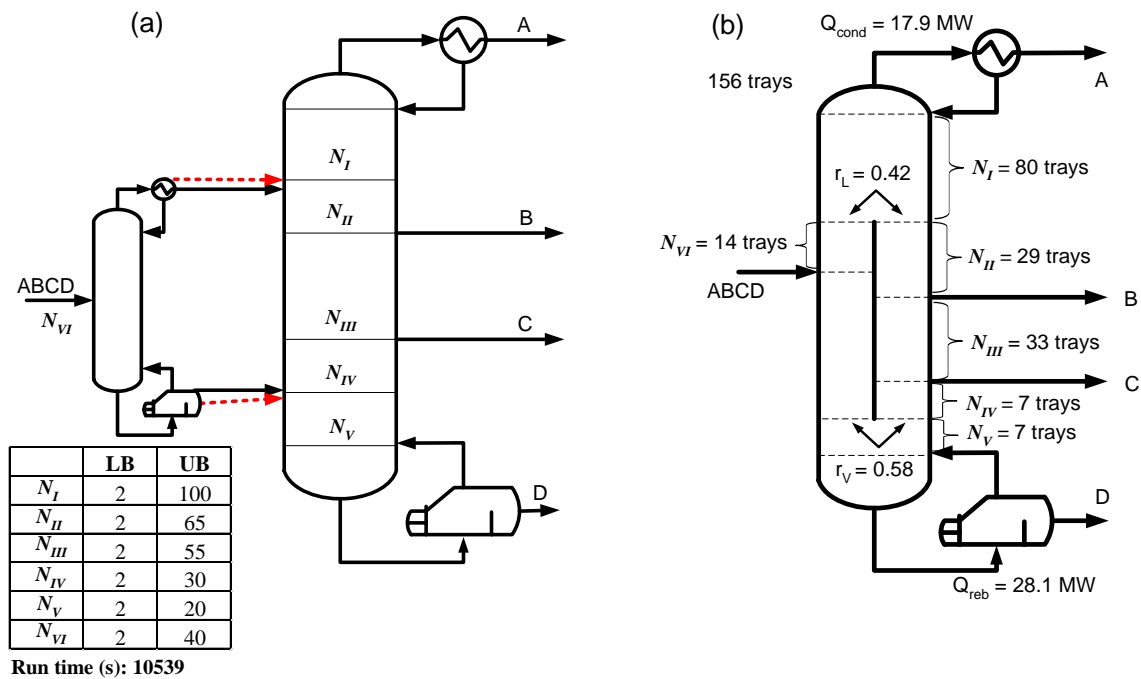
Figure 4-15. DWC configuration 3 showing (a) simulation structure, with PSO variables and bounds (b) optimal structure of the equivalent DWC design with the condenser and reboiler duties, liquid split ratio (r_L) and vapor split ratio (r_V)

4.4.3 Optimization results (economics)

The economic results of all the cases studied are shown in Table 4-7. As can been seen, configurations 1 to 3 all have better economic results than the base case, with the least amount of savings experienced for configuration 1. This is because the methanol recovery column, which is the column with the most significant cost in the base case, also contributes to configuration 1. In configuration 3, the advantages of implementing all product recoveries in one DWC column is quite clear, as savings in TAC of up to 28 % in comparison to the base case are obtained. These savings are mainly as a result of huge savings (31 %) in operating costs obtained in this configuration. These results highlight the big potential that DWCs have in replacing conventional columns in the

separation section of the thermochemical biobutanol process. It is also conceivable that similar savings might be obtainable for other biofuel applications.

Table 4-7. Operating cost, capital cost and TAC results for all cases studied

Base case			
	Op. Cost (k$/yr)	Cap. Cost (k$)	TAC (k$/yr)
Methanol recovery column	2,075	1,550	2,484
Ethanol/propanol recovery column	513	681	693
Butanol recovery column	126	165	170
Total	2,714	2,396	3,346
Configuration 1			
	Op. Cost (k$/yr)	Cap. Cost (k$)	TAC (k$/yr)
Methanol recovery column	2,075	1,550	2,484
3-product DWC	579	755	778
Total	2,654	2,305	3,262
Savings with respect to base case	*2.2%*	*3.8%*	*2.5%*
Configuration 2			
	Op. Cost (k$/yr)	Cap. Cost (k$)	TAC (k$/yr)
3-product DWC	2,098	2,053	2,640
Butanol recovery column	126	165	170
Total	2,225	2,218	2,810
Savings with respect to base case	*18.0%*	*7.4%*	*16.0%*
Configuration 3			
	Op. Cost (k$/yr)	Cap. Cost (k$)	TAC (k$/yr)
4-product DWC	1,878	2,033	2,414
Savings with respect to base case	*30.8%*	*15.2%*	*27.9%*

4.4.4 Sensitivity analysis on best configuration (configuration 3)

As has been seen from the results obtained in the prior section, the best configuration for the separation is configuration 3, the four-product DWC. In this section, a sensitivity analysis on the results of configuration 3 is carried out on some of the key economic assumptions made in this work such as the depreciation time, interest rate, utility price and cost of the sieve trays in the dividing wall section, to see the effect of these parameters on the TAC and the column structure (number of trays). These results are shown graphically in Fig. 4-16, with the TAC trends shown with solid lines, and the number of trays trends shown with the hashed trend lines. The relationship between the

TAC and number of trays versus the interest rate is shown in Fig. 4-16 (a). Increasing the interest rate increases the TAC, as the cost of borrowing capital becomes higher, while the opposite occurs when the interest rate is reduced. However, the number of trays in the column remains the same. In Fig. 4-16 (b), a plot of the change in TAC and number of trays with respect to annualization time is shown. As can be seen, an increase in annualization time from the base case results in a decrease in TAC and vice versa with a decrease in the annualization time. The increased annualization time means that capital cost repayments are spread over a longer time period, thus reducing the annualization factor and the contribution of the capital cost to the TAC, the opposite occurs when the annualization time is reduced. Note that the exponential relationship between the TAC and annualization time is a result of the exponential relationship between the annualization factor and annualization time as can be seen in equation (7).

The change in the number of trays follows a trend which is opposite to the change in TAC. This is because with an increase in annualization time, the cost of borrowing capital becomes cheaper thus favouring columns with more trays. In Fig. 4-16 (c), the TAC and optimal number of trays are plotted against the utility price. The values on the x-axis of this figure are percentage changes in utility (steam and cooling water) price from the base case values, with 100 % representing the base case. The plot shows that a linear direct relationship exists between the TAC and utility price as expected based on the equations discussed in section 4.3.4. The change in the number of trays with respect to the utility price also follows a linear trend. This is because as the operating cost is increased, taller columns are favoured and vice versa when the operating cost is reduced.

Finally, the TAC and number of trays are plotted against the cost factor assumed for the sieve trays in the dividing wall section of the DWC. As is seen in Fig. 4-16 (d), the

relationship between the TAC and sieve tray factor is linear. Increasing the tray factor means that the sieve trays are more expensive for the DWCs thus causing an increase in the TAC, and vice versa when the tray factor is reduced. However, the change in the number of trays with respect to the tray factor is linear but opposite to the TAC. This is because smaller columns are favoured when the cost of the sieve trays, and thus capital cost are increased. It should be noted that noise in the data is due to suboptimal results generated by the PSO, since the number of iterations was restricted to 100 for each case.
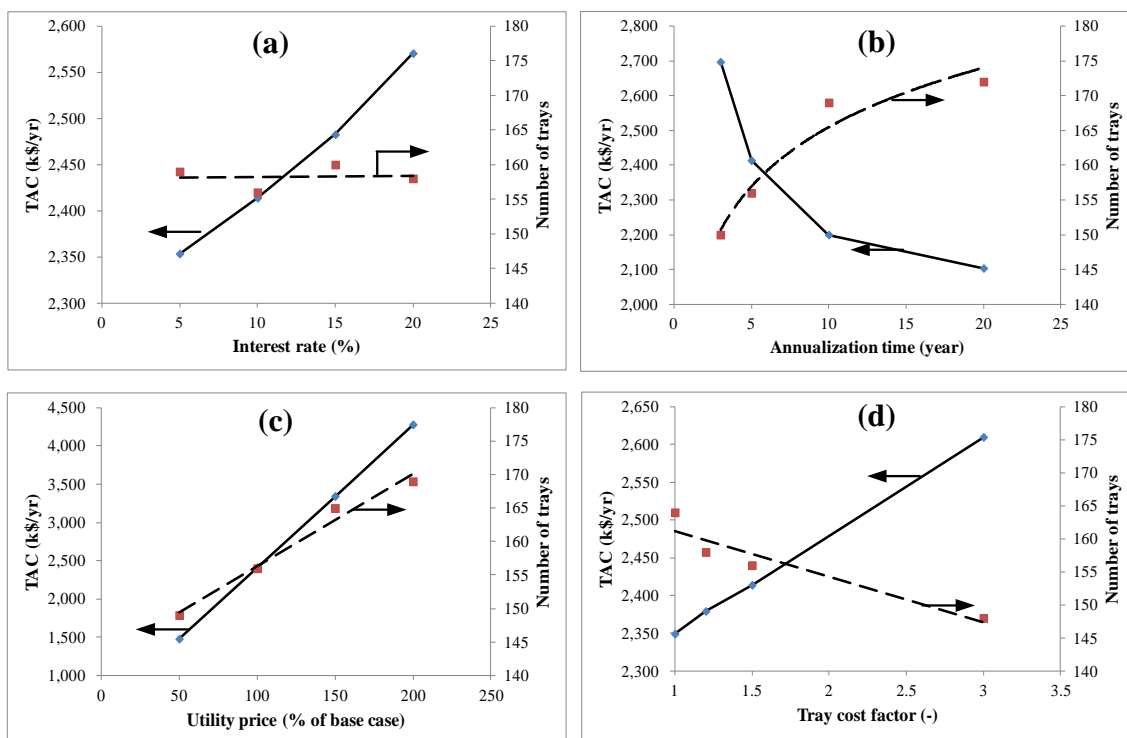
Figure 4-16. Sensitivity analysis on results of best configuration (configuration 3)

4.5   Conclusion

This work has looked at the design of DWC configurations for application to the separation section of a thermochemical biobutanol process. A general methodology based on the use of shortcut methods for column initialization, and a two-tier simulation - optimization strategy was discussed and used for design of the DWCs. The results show that all the DWC configurations provide cost savings in comparison to a base case

configuration of three conventional columns in direct sequence. Furthermore, the four - product DWC provides the most savings, with up to 31 % savings in operating costs, and 28 % savings in TAC. Note that these savings are reasonable and in line with the general savings reported for DWCs in other cases. Therefore, it can be concluded that the implementation of DWC technology in a thermochemical biobutanol process can lead to cost savings and thus improvements in the overall economics of the process. In future work the authors intend to carry out a full system study to quantify how the use of DWC configurations impact on the production cost of biobutanol from the thermochemical route.

4.6 References

[1] International Energy Agency. World Energy Outlook 2013. 2013.

[2] Yildirim Ö, Kiss A a., Kenig EY. Dividing wall columns in chemical process industry: A review on current activities. Sep Purif Technol 2011;80:403–17. doi:10.1016/j.seppur.2011.05.009.

[3] Agrawal R, Fidkowski ZT. Are Thermally Coupled Distillation Columns Always Thermodynamically More Efficient for Ternary Distillations ? 1998;5885:3444–54.

[4] Rewagad RR, Kiss A a. Dynamic optimization of a dividing-wall column using model predictive control. Chem Eng Sci 2012;68:132–42. doi:10.1016/j.ces.2011.09.022.

[5] Asprion N, Kaibel G. Dividing wall columns: Fundamentals and recent advances. Chem Eng Process Process Intensif 2010;49:139–46. doi:10.1016/j.cep.2010.01.013.

[6] Kiss A a., Ignat RM. Innovative single step bioethanol dehydration in an extractive dividing-wall column. Sep Purif Technol 2012;98:290–7. doi:10.1016/j.seppur.2012.06.029.

[7] Kiss A a. Distillation technology - still young and full of breakthrough opportunities. J Chem Technol Biotechnol 2014;89:479–98. doi:10.1002/jctb.4262.

[8] Sun L-Y, Chang X-W, Qi C-X, Li Q-S. Implementation of Ethanol Dehydration Using Dividing-Wall Heterogeneous Azeotropic Distillation Column. Sep Sci Technol 2011;46:1365–75. doi:10.1080/01496395.2011.556099.

[9] Dejanović I, Matijašević L, Olujić Ž. Dividing wall column—A breakthrough towards sustainable distilling. Chem Eng Process Process Intensif 2010;49:559–80. doi:10.1016/j.cep.2010.04.001.

[10] Kiss A a., Bildea CS. A control perspective on process intensification in dividing-wall columns. Chem Eng Process Process Intensif 2011;50:281–92.

doi:10.1016/j.cep.2011.01.011.

[11]   Ling H, Luyben WL. New Control Structure for Divided-Wall Columns. Ind Eng Chem Res 2009;48:6034–49. doi:10.1021/ie801373b.

[12]   Dwivedi D, Strandberg JP, Halvorsen IJ, Skogestad S. Steady state and dynamic operation of four-product dividing-wall (Kaibel) columns: Experimental verification. Ind Eng Chem Res 2012;51:15696–706. doi:10.1021/ie301432z.

[13]   Kumar M, Gayen K. Developments in biobutanol production: New insights. Appl Energy 2011;88:1999–2012. doi:10.1016/j.apenergy.2010.12.055.

[14]   Ranjan A, Moholkar VS. Biobutanol: science, engineering, and economics. Int J Energy Resour 2012;36:277–323. doi:10.1002/er.

[15]   Okoli C, Adams TA. Design and economic analysis of a thermochemical lignocellulosic biomass-to-butanol process. Ind Eng Chem Res 2014;53:11427–41.

[16]   Kiss A a. Novel applications of dividing-wall column technology to biofuel production processes. J Chem Technol Biotechnol 2013;88:1387–404. doi:10.1002/jctb.4108.

[17]   Kiss A a., Ignat RM. Enhanced methanol recovery and glycerol separation in biodiesel production - DWC makes it happen. Appl Energy 2012;99:146–53. doi:10.1016/j.apenergy.2012.04.019.

[18]   Ghadrdan M, Halvorsen IJ, Skogestad S. Optimal operation of Kaibel distillation columns. Chem Eng Res Des 2011;89:1382–91. doi:10.1016/j.cherd.2011.02.007.

[19]   Dejanović I, Matijašević L, Halvorsen IJ, Skogestad S, Jansen H, Kaibel B, et al. Designing four-product dividing wall columns for separation of a multicomponent aromatics mixture. Chem Eng Res Des 2011;89:1155–67. doi:10.1016/j.cherd.2011.01.016.

[20]   Halvorsen IJ, Skogestad S. Minimum Energy Consumption in Multicomponent Distillation. 1. Vmin Diagram for a Two-Product Column. Ind Eng Chem Res 2003;42:596–604.

[21]   Halvorsen IJ, Skogestad S. Minimum Energy Consumption in Multicomponent Distillation. 2. Three-Product Petlyuk Arrangements. Ind Eng Chem Res 2003;42:605–15. doi:10.1021/ie0108649.

[22]   Halvorsen IJ, Skogestad S. Minimum Energy Consumption in Multicomponent Distillation. 3. More Than Three Products and Generalized Petlyuk Arrangements. Ind Eng Chem Res 2003;42:616–29. doi:10.1021/ie0108651.

[23]   Kiss A a., Ignat RM, Flores Landaeta SJ, De Haan AB. Intensified process for aromatics separation powered by Kaibel and dividing-wall columns. Chem Eng Process Process Intensif 2013;67:39–48. doi:10.1016/j.cep.2012.06.010.

[24]   Sun L, Bi X. Shortcut method for the design of reactive dividing wall column. Ind Eng Chem Res 2014;53:2340–7. doi:10.1021/ie402157x.

[25]   Javaloyes-Antón J, Ruiz-Femenia R, Caballero J a. Rigorous Design of Complex Distillation Columns Using Process Simulators and the Particle Swarm Optimization Algorithm. Ind Eng Chem Res 2013;52:15621–34. doi:10.1021/ie400918x.

[26] Leboreiro J, Acevedo J. Processes synthesis and design of distillation sequences using modular simulators: a genetic algorithm framework. Comput Chem Eng 2004;28:1223–36. doi:10.1016/j.compchemeng.2003.06.003.

[27] Gendreau M, Potvin J-Y. Handbook of Metaheuristics Vol. 2. New York: Springer; 2010.

[28] Kaveh A. Advances in Metaheuristic Algorithms for Optimal Design of Structures. New York: Springer; 2014.

[29] Pascall A, Adams T a. Semicontinuous separation of dimethyl ether (DME) produced from biomass. Can J Chem Eng 2013;91:1001–21. doi:10.1002/cjce.21813.

[30] Navarro M a., Javaloyes J, Caballero J a., Grossmann IE. Strategies for the robust simulation of thermally coupled distillation sequences. Comput Chem Eng 2012;36:149–59. doi:10.1016/j.compchemeng.2011.06.014.

[31] ASTM Standard D7862-15. Standard Specification for Butanol for Blending with Gasoline for Use as Automotive Spark-Ignition Engine Fuel 2015. doi:10.1520/D7862-15.

[32] Ramakrishnan K, Sabarethinam PL. Isobaric vapor-liquid equilibrium data. Chem Ind Dev 1977;11:19–22.

[33] Resa JM, Gonzalez C, Goenaga JM, Iglesias M. Density, Refractive Index, and Speed of Sound at 298.15 K and Vapor−Liquid Equilibria at 101.3 kPa for Binary Mixtures of Ethyl Acetate + 1-Pentanol and Ethanol + 2-Methyl-1-propanol. J Chem Eng Data 2004;49:804–8.

[34] Mozzhukhin AS, Mitropol'skaya VA, Serafimov LA, Torubarov AI, Rudakovskaya TS. Liquid-vapor phase equilibriums in binary mixtures of some oxygen-containing substances at 760 mm. mercury. Zhurnal Fiz Khimii 1967;41:227–32.

[35] Kojima K, Tochigi K, Seki H, Watase K. Determination of vapor-liquid equilibrium from boiling point curve. Kagaku Kogaku Ronbunshu 1968;32:149–53.

[36] Kurihara K, Nakamichi M, Kojima K. Isobaric vapor-liquid equilibria for methanol + ethanol + water and the three constituent binary systems. J Chem Eng Data 1993;38:446–9.

[37] Ochi K, Kojima K. Vapor-liquid equilibrium for ternary systems consisting of alcohols and water. Kagaku Kogaku Ronbunshu 1969;33:352.

[38] Seider WD, Seader JD, Lewin DR. Product & Process Design Principles: Synthesis, Analysis and Evaluation. 3rd ed. Hoboken, New Jersey: John Wiley & Sons; 2009.

[39] Modi AK, Westerberg AW. Distillation column sequencing using marginal price. Ind Eng Chem Res 1992;31:839–48.

[40] Kaibel G. Distillation columns with vertical partitions. Chem Eng Technol 1987;10:92–8.

[41] Olujić Ž, Jödecke M, Shilkin a., Schuch G, Kaibel B. Equipment improvement trends in distillation. Chem Eng Process Process Intensif 2009;48:1089–104. doi:10.1016/j.cep.2009.03.004.

[42] Adams T a., Seider WD. Practical optimization of complex chemical processes with tight constraints. Comput Chem Eng 2008;32:2099–112. doi:10.1016/j.compchemeng.2008.02.007.

[43] Boubaker S, Djemai M, Manamanni N, M'Sahli F. Active modes and switching instants identification for linear switched systems based on Discrete Particle Swarm Optimization. Appl Soft Comput 2014;14:482–8. doi:10.1016/j.asoc.2013.09.009.

[44] Wankat PC. Separations in chemical engineering: equilibrium staged separations. New York: Elsevier; 1988.

[45] EIA UEIA. Henry Hub Gulf Coast Natural Gas Spot Price 2012. http://www.eia.gov/dnav/ng/hist/rngwhhdW.htm.

[46] IESO IESO. Hourly Ontario Energy Price 2012. http://www.ieso.ca/Pages/Power-Data/default.aspx.

[47] Towler G, Sinnott R. Chemical engineering design: principles, practice and economics of plant and process design. 2nd Edition. Massachusetts: Butterworth-Heinemann; 2012.

[48] Rangaiah GP, Ooi EL, Premkumar R. A Simplified Procedure for Quick Design of Dividing-Wall Columns for Industrial Applications. Chem Prod Process Model 2009;4:1–42. doi:10.2202/1934-2659.1265.

[49] Smith R. Chemical process design and integration. Chichester: John Wiley & Sons; 2005.

[50] Halvorsen IJ, Skogestad S. Minimum Energy for the four-product Kaibel-column. AIChE Annu. Meet. Conf. Proc., San Francisco, California: American Institute of Chemical Engineers; 2006, p. 216d/1–216d/8.

[51] Ghadrdan M, Halvorsen IJ, Skogestad S. A Shortcut Design for Kaibel Columns Based on Minimum Energy Diagrams. In: Pistikopoulos EN, Georgiadis MC, Kokossis AC, editors. 21st Eur. Symp. Comput. Aided Process Eng. - ESCAPE 21, Porto Carras, Greece: Elsevier B.V.; 2011, p. 356–60.

CHAPTER 5 Design and assessment of advanced thermochemical plants for second generation biobutanol production considering mixed alcohols synthesis kinetics

5.1   Introduction

Biofuels are increasingly seen by policy makers globally as an important strategy to help address the challenges posed by climate changing greenhouse gas (GHG) emissions. This is highlighted by the continual increase in global biofuels production. For example biofuels contributed 3 % to total road-transport fuel demand in 2013, with this value expected to hit 8 % by 2035 [1]. Key to achieving this potential for biofuels is the utilization of second generation biofuel feedstocks which are primarily cellulosic/lignocellulosic terrestrial biomass such as wood chips and grasses. Second generation biofuel feedstock are preferred over first generation biofuel feedstock (derived from corn and other food crops) because unlike first generation biofuel feedstock they are significantly less competitive with food production for land and their feedstocks are or can be made widely available. In fact, the U.S. Congress Renewable Fuel Standard (RFS) mandates a minimum production of 21 billion gal/year of cellulosic/lignocellulosic biofuels by 2022 [2]. They aim to achieve this by both technological improvements of biomass to biofuel processes, as well as improved production and supply of biomass. As a positive step towards achieving the U.S. RFS mandate, the U.S. Department of Energy and the U.S. Department of Agriculture collectively champion a goal of developing a biomass supply chain which by 2030 is able to produce 1 billion tons per year of biomass, solely to be used for second and third generation biofuels production [3].

In terms of the biofuels of choice, researchers into second generation biofuels are increasingly looking at biobutanol as a preferable option to bioethanol as a gasoline replacement in automobiles because it offers advantages over bioethanol such as a

higher energy content, lower water miscibility, and better compatibility with existing internal combustion engines and pipeline networks [4,5].

There are two routes for the production of butanol from second generation biomass feedstocks, namely the biochemical route and the thermochemical route. The biochemical route proceeds mainly through the acetone-butanol-ethanol (ABE) fermentation process which was developed in UK in 1912 and was a commercial route for acetone and butanol production from first generation biofuel feedstock (such as corn and potatoes) up until the 1950s before the advent of petrochemical derived butanol [6,7]. In this route, bacteria species (mainly species of *Clostridia*) are used to ferment the sugars in biomass into butanol. Despite its long history the ABE process faces a number of key challenges such as the difficulty in handling second-generation biofuel feedstocks such as forest residue because of their high lignin content which is difficult to break down by fermentation organisms [8]; low productivity of the fermentation process [6]; and the very challenging downstream separation process because of the low concentration of the product in the fermentation broth [6,9,10]. Review papers by researchers further discuss these challenges and mention that research efforts into metabolic engineering to improve fermentation bacteria strains and novel reactor and separation technologies can help address these challenges in the future [6,7,10–12]. However these challenges mean that production of second generation biobutanol through the biochemical route is not commercially ready [13].

One of the major pathways for the production of biobutanol from the thermochemical route is the mixed alcohol synthesis (MAS) process. In this process, biomass is gasified to produce mainly carbon monoxide (CO) and hydrogen (H_2), together called syngas. The syngas from biomass also contains impurities which are removed in a syngas cleanup step before being sent to a MAS reactor in which the syngas is catalytically

converted to butanol and other alcohols. The MAS catalysts used in this process can be subdivided into four groups namely, modified high-pressure methanol synthesis catalysts, modified low-pressure methanol synthesis catalysts, modified Fischer-Tropsch catalysts, and alkali-doped molybdenum catalysts [14,15]. Of major interest for butanol production are the modified methanol synthesis catalysts because they have better selectivity to butanol than the other catalyst groups [15]. The thermochemical route has a number of advantages over the biochemical route such as the ability to handle lignin-rich second generation biofuel feedstocks because of the ease of gasifying the carbon rich lignin into syngas, and an easier separation step because the mixed alcohols are at a high concentration in the liquid feed to the downstream separation section. The major disadvantage of the thermochemical route is the low CO conversion of current catalysts, with research currently ongoing into improvements in MAS catalysts [14,16,17]. Furthermore, this route requires capital-intensive equipment thus might not be economically feasible at small processing scales.

Despite the merits of second generation biobutanol, quantitative metrics are required to demonstrate both its economic and environmental potential. In this regard only very few studies exist in the peer reviewed literature for both the biochemical and thermochemical routes [18–21]. Qureshi et al. [18] assessed the techno-economics of the biochemical conversion of wheat straw to *n*-butanol using the ABE fermentation process based on a *Clostridium beijenrickii* fermentation bacteria specie. The plant capacity was 150,000 tonnes of butanol/year with assumptions such as a 20 % mass yield of butanol to sugars, feedstock cost of 24 $/tonne, and co-products price of 800 $/tonne for ethanol and 1,300 $/kg for acetone. The result of the analysis was that butanol can be produced at 1.05 $/L in 2012 dollars. Kumar et al. [20] studied the techno-economics of switchgrass to *n*-butanol via the ABE biochemical route. The plant

was designed to produce 10,000 tonnes of butanol/year with an assumed mass yield of 23.4 % butanol per sugars. Switchgrass was assumed to be purchased at 40 $/tonne, with co-products ethanol sold at 890 $/kg and acetone sold at 810 $/kg. This results in a butanol production price of 0.59 $/L, in 2012 dollars. Tao et al. [19] analyzed the techno-economics of *i*-butanol production from corn stover via the biochemical route using an improved strain of *Escherichia coli* bacteria. The plant was designed to process 2,000 dry tonnes of feedstock with assumptions such as 65 $/dry tonne feedstock and butanol yield of 31.45 g butanol/g sugars resulting in a butanol production price of 0.78 $/L in 2007 dollars. The assumption around butanol yield is an important one to note for this study, as it is 85 % of the theoretical butanol yield of 37 g butanol/g sugars [22], a very high value in comparison to the other studies reviewed. Furthermore, this conversion is quite futuristic as fermentation using this *E. coli* bacteria strain has not even been demonstrated in bench scale studies [19]. The study addressed the uncertainty around the selected butanol yield by carrying out sensitivity analysis with results showing that in the butanol yield range of 20 - 24 g butanol/g sugars (55 - 65 % of the theoretical butanol yield) which is typical of other biochemical butanol studies, the butanol production price is 1.20 - 1.02 $/L in 2007 dollars. These analyses highlight the importance of taking into consideration techno-economic assumptions made on feedstock costs, co-product prices, cost year of analysis, and butanol product yields, among other factors when butanol production price results are assessed.

For second generation biobutanol production via the thermochemical route, Okoli and Adams [21] is the only techno-economic study in the peer-reviewed literature. The authors design a 2,000 tonnes per day of wood chips production plant that converts syngas from the gasification section to butanol and other mixed alcohols over a modified low-pressure methanol synthesis catalyst. The MAS reactor is modeled using

simple yield and conversion data of the modified low-pressure methanol synthesis catalyst from Herman [23]. Furthermore, the CO to alcohols conversion was set at a 40 % (CO_2-free basis), which was motivated by U.S. National Renewable Energy Laboratory (NREL) future targets of 50 % CO conversion (CO_2-free basis) for MAS catalysts [24] but has not yet been achieved in practice. The resulting butanol production price was 0.83 $/L in 2012 dollars. Due to the simplistic and futuristic catalyst assumptions, a sensitivity analysis was carried out on the CO conversion of the catalyst which showed that at the literature reported CO conversion value of the catalyst at 8.5 % [23], the butanol selling price is 1.56 $/L in 2012 dollars. It might be much better for butanol production to make use of modified high-pressure methanol synthesis catalysts, which have been shown in literature to achieve CO conversions of greater than 18%, though at much higher temperature and pressure conditions [21].

As very little techno-economic studies have been carried out on second generation biobutanol and on the thermochemical route in particular, more studies are required in other to get a better economic and environmental understanding of the process. Thus this current work aims to improve on the study carried out by Okoli and Adams [21]. First, the simplistic MAS reactor model using a futuristic catalyst is replaced with a detailed kinetic model using a high-pressure modified methanol synthesis catalyst that has been demonstrated at the pilot scale [25]. This change depicts a more realistic representation of the process, and allows the impact of different design decisions, such as the impact of unreacted syngas recycle choices on the butanol production, to be evaluated. Furthermore, this study also improves on Okoli and Adams [21] by assessing other novel process configurations which consider the impact of high temperature utility and power importation on both the economic and environmental feasibility of second generation biobutanol production using metrics such as the minimum butanol selling

price (MBSP), and cost of CO_2 equivalent emissions avoided (CCA). The CCA is an important environmental metric for assessing GHG emission reduction technology as it informs biofuel technology decision makers how much financial cost is incurred to reduce GHG emissions when a particular biofuel technology is implemented over a fossil based fuel. To the best of the authors' knowledge this metric has not been appropriately studied nor quantified in the peer reviewed literature for second generation biobutanol.

Another area identified for improvements is the separation section in which a conventional distillation sequence is used for butanol recovery. Potential exists for improvements of this section by utilizing process intensification technology based on dividing wall columns (DWCs) instead of conventional distillation columns. The use of DWCs can potentially be significant as prior research has shown that DWCs can improve operating and capital costs of conventional distillation sequences by up to 30 % [26,27]. However, these savings have never been investigated on a plant-wide level for biofuel applications, and thus this work also aims to quantify these savings for thermochemical second generation biobutanol applications.

5.2   Methods

5.2.1   Biomass feedstock and plant size

Forest biomass can come from a variety of sources such as: trees that are of harvestable age but are not useful for lumber, trees killed by disturbances (such as fire, diseases or insects), harvest residues, and trees from plantations grown specifically to provide biomass for conversion to bioenergy. Furthermore, industrial forest processes such as harvesting and milling operations as well as pulping processes provide additional sources of biomass i.e. sawdust, bark and chips, and lignin-rich "black liquors". The thermochemical conversion route is preferred over the biochemical route for the

conversion of forest biomass because of the high-lignin content of forest biomass [8]. This is because fermentation bacteria used for biochemical routes find great difficulty in converting lignin which typically has to be removed in pre-treatment processes, while in the thermochemical route the carbon rich lignin is easily converted to syngas through the gasification process. Thus for biochemical biofuel routes agricultural residues have been the preferred feedstock because of their lower lignin content in comparison to forest resources [8].

The forest biomass used as the base case for this study is wood chips obtained from pine trees. The plant gate ultimate and proximate analyses used to model it are shown in Table 5-1.

The plant is designed to handle a gasifier inlet flow of 2,000 tonnes per day (10 wt % moisture content) of wood chips. This is a reasonable size for the plant leveraging on other second generation biofuel studies [8,28] as well as the availability of forest resources (existing and unexploited) in U.S. put at 334 million dry tonnes in 2005 [3].

Table 5-1. Ultimate analysis of pine wood chips used in this study [8].

Ultimate analysis	wt % moisture free basis
Carbon	50.94
Hydrogen	6.04
Nitrogen	0.17
Sulphur	0.03
Oxygen	41.9
Ash	0.92
HHV (MJ/kg)	19.99
LHV (MJ/kg)	18.59
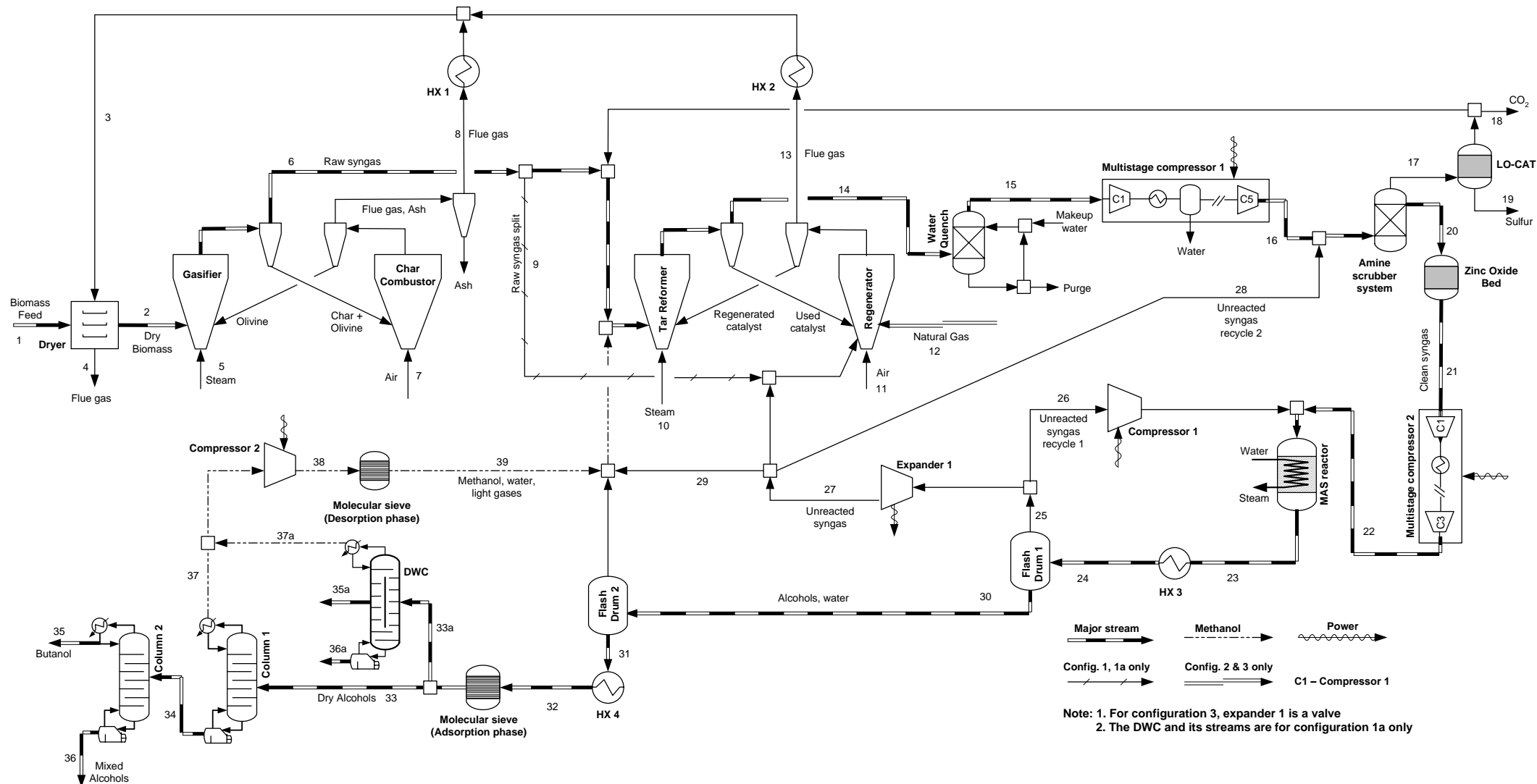
Figure 5-1. Process flow diagram of the proposed thermochemical biomass-to-butanol process superstructure. See supporting information at www. macsphere.mcmaster.ca for stream conditions.

5.2.2 Process simulation overview

In this work, three major configurations for the production of butanol from woody biomass are designed and assessed. The general process flow for all the designs is as follows: first, woody biomass is gasified to produce syngas, which is then cleaned before being used for alcohols production in the MAS reactor. The alcohols are then separated downstream of the MAS reactor into butanol and a mixed alcohols co-product.

The three configurations are differentiated by their requirements for the provision of high temperature process heat, and power. Configuration 1, which is also called the "self-sufficient" configuration, is designed such that the plant does not utilize any external sources of hot utilities, including high temperature heat, and power, thus it is totally powered by renewable biomass. This design requirement means that any extra high temperature heat required by processes such as the endothermic tar reforming process is met by combusting a portion of the syngas from the gasifier. Furthermore, an adaptation of configuration 1 called "configuration 1a", in which a DWC is used in place of a conventional column for alcohols separation is also considered. In configuration 2, referred to as the "natural gas (NG) import" configuration, combustion of NG is used for the provision of high temperature process heat in place of biomass syngas combustion because the cost per unit of heating value of NG is lower than that of biomass. The argument against this approach is that the "greenness" of the biofuel is reduced as a result of the fossil fuel input. The final configuration (configuration 3) also called the "NG and power import" configuration, uses NG for high temperature heat as is done in configuration 2. However, electricity is also imported for process use instead of power

generation through expansion of hot gases in turbines. This configuration is motivated by past work which showed that costs associated with turbines can contribute as much as 25 % of the capital costs of a thermochemical biobutanol process [21], thus power importation from the grid though increasing the operating costs of the plant might help reduce the upfront capital costs. These decisions behind the three different configurations can be assessed by considerations such as GHG emissions, renewable energy usage, capital and operating costs.

All the design configurations considered in this work are simulated in Aspen Plus V8.4 software so as to estimate their mass and energy balances. The selection of physical property packages, and unit operation specifications were done to be consistent with Okoli and Adams [21], in which a second generation biobutanol plant via a thermochemical route was designed and assessed. However, major differences between this work and that work arise in the design of the gas cleanup, alcohol synthesis, and separation sections as a result of the kinetic MAS reactor model and different MAS catalyst used for this work, as well as considerations regarding NG use, power importation and the unreacted syngas recycle configuration. These differences will be discussed in more detail in the proceeding sections.

5.2.3 Process description

In Figure 5-1 a simplified process flow diagram superstructure is used to illustrate the design configurations considered. It shows all the major steps required for the conversion of woody biomass to butanol including gasification, syngas cleanup, mixed alcohols synthesis, and alcohols separation. These processing steps are further discussed in

proceeding sub-sections, with Table 5-2 showing the major design parameters for these steps.

Table 5-2. Major design parameters of process areas

Gasification		Gas cleanup (acid gas removal)	
Feed rate per train (gasifier inlet)	1000 tonnes/ day	Amine used	Monoethanolamine
Parallel trains required	Two (2)	Amine concentration, wt %	35
Gasifier operating pressure	2.28 bar	Amine temperature in absorber (°C)	43.33
Gasifier operating temp.	800 °C	Absorber pressure (bar)	31
Char combustor pressure	2 bar	Stripper pressure (bar)	4.12
Char combustor temp.	850 °C	Heat duty to remove CO_2 (kJ/kg)	5337
Gas cleanup (tar reforming)		Alcohol synthesis reactor	
Reformer operating pressure (bar)	1.86	Gas hourly space velocity (h^{-1})	5000
Reformer operating temp. (°C)	910	Reactor temperature (°C)	440
Reformer space velocity (h^{-1})	2,476	Pressure (bar)	120
Tar reformer conversions (%)		Inlet CO_2 concentration (wt %)	< 5
Methane (CH_4)	80%	Inlet sulphur concentration (ppmv)	< 0.1
Ethane (C_2H_6)	99%	Steam system and power generation	
Ethylene (C_2H_4)	90%	Turbine design	Three stage turbine
Tars (C_{10+})	99%	High pressure inlet conditions	58 bar, 482 °C
Benzene (C_6H_6)	99%	Medium pressure inlet conditions	12 bar, 303 °C
Ammonia (NH_3)	90%	Low pressure inlet conditions	4.5 bar, 210 °C
		Condenser outlet conditions	0.304 bar, saturated
Alcohol separation (distillation columns)		Alcohol separation (distillation columns)	
Conventional column 1		Dividing wall column (configuration 1a only)	
Propanol recovery in overhead	99.3 mol%	Methanol recovery in overhead	97.4 mol%
Butanol recovery in bottoms	99.3 mol%	Butanol purity in side stream	96 mol%
Number of trays	56	Pentanol recovery in bottoms	92.4 mol%
Conventional column 2		Number of trays (wall section)	23
Butanol purity in overhead	96 mol%	Number of trays (main section)	45
Pentanol recovery in bottoms	99 mol%		
Number of trays	20	Cooling water system	
Alcohol separation (Molecular sieve)		Supply temperature (°C)	32
Outlet water content (wt %)	0.5	Return temperature (°C)	43

5.2.3.1   Feed handling and drying

Biomass with characteristics as shown in Table 5-1 is received at the plant gate with 30 wt % moisture content [8]. It is subsequently dried in a biomass dryer to 10 wt % using hot flue gas from the char combustor and catalyst regenerator via the steam generation system. Note that though the biomass drying process is modeled in all the simulations to enable accurate and complete mass and energy balance information for the steam generation system, it is assumed that the costs upstream of the gasifier inlet are accounted for in the cost of biomass. This assumption is in line with the feedstock supply and cost model of the Idaho National Laboratory (INL) which accounts for the logistical, capital, and operating costs associated with feed delivery, handling and drying of the biomass to the up to the gasifier inlet [8]. The temperature for the flue gas leaving the steam generation section (stream 3 in Figure 5-1) is adjusted to ensure that the biomass is dried to 10 wt % moisture content and that the humidified flue gas leaves the system above its dew point temperature. In Aspen Plus this is done by using a simple custom model that calculates the heat duty required to dry the biomass and the corresponding temperature and humidity change of the flue gas stream.

5.2.3.2   Gasification

The dried biomass with 10 wt % moisture content is fed to the gasifier, where it is gasified with low-pressure steam to produce syngas. The gasifier used for this study is a low-pressure allothermal indirect circulating fluidized bed gasifier whose output product composition is modeled with temperature correlations from the Batelle Columbus Laboratory test facility as reported by Dutta et al. [8]. The gasification system is made up

of two beds, the gasifier and the char combustor. In the gasifier bed, the overall gasification reaction process is endothermic, thus the required heat is supplied by circulating heated olivine from the char combustor into the gasifier making the gasification system adiabatic. The products from the gasification process are mainly CO, H_2, CH_4, tars and solid char. The olivine, which is an inert, also exits from the gasifier alongside the products. The gaseous products are separated from the olivine and char with a cyclone, with the solids recycled back to the char combustor while the raw syngas is sent to the gas cleanup section. In the char combustor, the char is combusted with air thereby producing hot combustion gases and ash as well as heating up the olivine. The olivine, ash, and hot combustion gases exit from the char combustor and are separated from each other through a series of cyclones. The hot olivine is recycled back to the gasifier, while the hot combustion gases are used to generate steam in the steam system and dry the biomass before it enters the gasifier.

5.2.3.3 Gas cleanup

After gasification, a gas cleanup step is necessary to remove impurities in the raw syngas, as these impurities such as tars, sulphur and CO_2 can foul process equipment and poison the MAS catalyst. The gas cleanup step comprises of tar reforming, syngas quenching, and amine scrubbing. The raw syngas is first sent to the tar reformer, where unreacted tars, methane, and other hydrocarbons are reformed to CO and H_2. The tar reformer is a circulating, heterogeneous, fluidized catalyst bed system that is made up of a reforming bed and a catalyst regeneration bed. In the reforming bed, the endothermic reforming reactions which is catalyzed by a fluidizable Ni/Mg/K catalyst take place between steam

and raw syngas [8]. The tar reforming catalyst is separated from the syngas through a cyclone at the reformer exit and sent to the catalyst regenerator. The catalyst regeneration occurs in the exothermic catalyst regenerator by combusting entrained coke on the catalyst, after which the regenerated catalyst is separated from the hot flue gases and sent back to the tar reformer, thus completing the loop. The heat requirement of the reformer bed, which is maintained at isothermal conditions, is supplied by heat transfer from the hot flue gases produced in the exothermic catalyst regenerator. Furthermore, the hot combustion gases stream also has its heat recovered for steam generation and biomass drying. If there is insufficient heat supply from the catalyst regenerator to the tar reformer, this can be addressed by combusting unreacted syngas from downstream, and a portion of the raw syngas feed from the gasifier as is done in configuration 1 (stream 9 in Figure 5-1) or by using heat from combusted NG as in configuration 2 and 3 (stream 12 in Figure 5-1). The NG specifications used are shown in Table 5-3.

Table 5-3. NG specifications [29]

Component	mol %
Methane	94.9
Ethane	2.5
Propane	0.2
i-Butane	0.03
n-Butane	0.03
i-Pentane	0.01
n-Pentane	0.01
Hexanes plus	0.01
Nitrogen	1.6
CO_2	0.69
Oxygen	0.02
Hydrogen	trace
HHV (MJ/kg)	52.87
LHV (MJ/kg)	47.64

The syngas from the tar reformer is cooled to 60 °C before it is quenched and water scrubbed to remove remaining particulate matter, tars, and other impurities. The purge water stream is sent for treatment to an off-site waste water treatment facility, while makeup water is also added. The cooled syngas is compressed to 30 bar in a five-stage compressor before being sent for H_2S and CO_2 (acid gas) removal in the amine scrubber system. The amine scrubbers as well as the subsequent ZnO bed are used to remove acid gas in the syngas so it meets the MAS catalyst specifications of less than 0.1 ppm H_2S and less than 5 wt % CO_2 [15]. The H_2S and CO from the amine scrubber exit are sent to a LO-CAT$^®$ system where elemental sulphur and CO_2 are generated [15]. A portion of the generated CO_2 can be recycled back to the tar reformer to regulate the H_2/CO ratio of the tar reformer exit syngas. Increasing CO_2 in the feed to the tar reformer favours the reverse reaction of the water-gas shift reaction, shown in equation (1), leading to a reduction in H_2 and an increase in CO, while the forward reaction is favoured if CO_2 is reduced in the tar reformer feed.

$$CO + H_2O \leftrightarrow CO_2 + H_2 \qquad (1)$$

5.2.3.4 Alcohol Synthesis

The clean syngas from the syngas cleanup section is compressed to 120 bar in a multi-stage compressor and then heated to 440 °C before being passed into the MAS reactor. The MAS reactor is an isothermal fixed bed reactor which uses a modified high pressure methanol synthesis catalyst (K-promoted Zn/Cr/O catalyst) [25]. The reactor products consist mainly of $C_1 - C_4$ alcohols, water, methane, C_{5+} alcohols and other hydrocarbon

products. The reactor products are cooled to 43 °C by heat exchange with process streams and cooling water, then using a series of flash drums the unconverted syngas and other light gases are separated from the liquid alcohols. A portion of the unconverted syngas, which is still at high pressure, is recompressed and recycled back to the MAS reactor while the rest is expanded to 30.4 bar through a turbine to recover power in configurations 1 and 2, and through a flash valve in configuration 3. A portion of this expanded stream is recycled to the acid gas removal section to remove CO_2 before being sent back to the MAS reactor, while the remaining stream is expanded (through a turbine in configurations 1 and 2, and a flash valve in configuration 3) to 2.3 bar and sent to the indirect tar reforming system where it is either reformed in the tar reforming bed or combusted in the catalyst regenerator to help meet the heat requirements of the plant. The liquid alcohols stream is then sent to the alcohols separation section.

One major improvement of this work over past work [21] is the use of a kinetic model to predict the production of butanol and other alcohols from the MAS reactor. This allows the impact of varying operating conditions such as feed composition, feed flowrate, temperature, pressure etc. on the reactor products, particularly butanol, to be predicted. The kinetic model used to predict the mixed alcohols production over the high pressure modified methanol synthesis catalyst was developed by Beretta et al. [25] of the Snamprogetti SpA research laboratories and the Polytechnic University of Milan using data from both laboratory and pilot scale experiments. Their work provides data on the whole set of reactions for mixed alcohols synthesis, and the accompanying rate expressions and kinetic parameter estimates, and is adapted for use in this study through

model regression of kinetic parameters to improve alcohols prediction. Note that the kinetic model is a lumped parameter model that accounts for the effects of reactant and product concentrations, reactor pressure, and temperature on the MAS reactor output predictions.

The reacting system is reduced to a selected number of components and pseudo-components as follows, CO, H_2, CO_2, H_2O, methanol, ethanol, propanol, isobutanol, C_{4+} higher alcohols, methane and C_{2+} hydrocarbons. For further simplicity in this work, the C_{4+} higher alcohols are approximated as pentanol and the C_{2+} hydrocarbons as ethane. The mixed alcohols reaction scheme is shown in equations (2) - (10):

$$CO + 2H_2 \leftrightarrow CH_3OH \tag{2}$$

$$CO + H_2O \leftrightarrow CO_2 + H_2 \tag{3}$$

$$2CH_3OH \rightarrow C_2H_5OH + H_2O \tag{4}$$

$$CH_3OH + C_2H_5OH \rightarrow C_3H_7OH + H_2O \tag{5}$$

$$CH_3OH + C_3H_7OH \rightarrow iC_4H_9OH + H_2O \tag{6}$$

$$2CH_3OH + C_3H_7OH \rightarrow C_5H_{11}OH + 2H_2O \tag{7}$$

$$2CH_3OH \rightarrow (CH_3)_2O + H_2O \tag{8}$$

$$CO + 3H_2 \rightarrow CH_4 + H_2O \tag{9}$$

$$2CO + 5H_2 \rightarrow C_2H_6 + 2H_2O \tag{10}$$
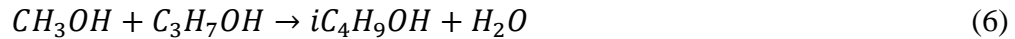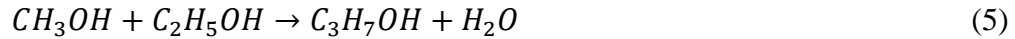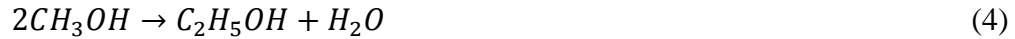
From the reaction set it can be seen that methanol is the key building block for the production of higher alcohols. In addition, methanol production from CO and H_2 is

considered reversible and chemical equilibrium limited. Furthermore, CO and H_2 react to also produce methane and ethane, while the water gas shift reaction accounts for the formation of CO_2 which is equilibrium limited. Finally, the model also accounts for the production of other oxygenated organic compounds such as dimethyl ether (equation 8).

In Aspen Plus a plug flow reactor (RPlug) model is used to model the MAS reactor, with the reaction set, rate expressions and kinetic parameters implemented using the Aspen Plus Langmuir Hinshelwood Hougen Watson and power law kinetic models. More details of the kinetic model study carried out for this work are available in the appendix.

For simulation simplicity, the operating temperature, pressure and gas hourly space velocity (GHSV) of the MAS reactor are fixed. The GHSV is fixed at 5,000 h^{-1} based on values reported in other methanol and alcohols production studies [8,24], while the temperature and pressure are set at the upper bound (440 °C) and mid range value (120 bar) of the experiment test range reported by Beretta et al. [25]. From the experiments by Beretta et al. [25], it is known that butanol yield is maximized at higher temperatures and pressure, and lower GHSV, therefore the choice of temperature and pressure is done with the idea of maximizing the production of butanol from the MAS reactor while limiting the costs associated with operation at high pressures such as the capital cost of reactors and compressors, and the energy penalty associated with syngas compression to high pressures. The selection of temperature and pressure used in this work is thus seen as a good compromise. Other variables that significantly affect the MAS reactor product yield

such as the selected unreacted syngas recycle scheme and H_2/CO ratio are determined using an optimization framework that will be discussed in the results section.

5.2.3.5 Alcohol Separation

The raw mixed alcohols stream from the alcohol synthesis section is flashed to 4 bar to remove absorbed gases which are subsequently recycled to the tar reformer in the gas cleanup section. The liquid alcohols are then superheated before being dehydrated by passing through a molecular sieve which adsorbs water [30]. The dehydrated alcohols are cooled down to a liquid state at 45 °C before they are separated into final products through two conventional distillation columns in series. In column 1, methanol, ethanol, propanol and any remaining light gases are removed in the distillate while butanol and higher alcohols (C_{5+}) are removed in the bottoms. In column 2, butanol is recovered in the distillate at $\geq$ 96 wt% purity to meet ASTM fuel specification standards [31], while the C_{5+} are recovered in the bottoms and can be sold as a mixed alcohols co-product. The methanol rich liquid distillate from column 1 is compressed and recycled to the molecular sieve where it is used as a sweep gas to recover adsorbed water from the molecular sieve in its desorption phase. As the molecular sieve is cyclic, two molecular sieves are used in parallel such that one is always adsorbing while the other is desorbing. The methanol and recovered water vapour stream is recycled back to the tar reformer, where it is reformed back to syngas, as an analysis showed that recycling back to the MAS reactor reduced the catalyst selectivity to butanol (though not significantly).

The DWC used in configuration 1a in place of the two conventional distillation columns is a ternary product DWC designed using a methodology discussed in the authors' past work [27]. A summary of the design is shown in Table 5-2.

5.2.3.6   Utilities (steam system, power generation and cooling)

Steam production is necessary in all the assessed configurations to help meet process heating requirements, for power generation, and for direct process needs. In the design of configurations 1, 1a and 2, high pressure (HP) steam is produced for power generation, while low pressure (LP) steam is produced in all the configurations for direct injection into the biomass gasifier and tar reformer. Furthermore, LP steam is used for indirect heating in the reboilers of the distillation columns and amine system. Heat exchange between water and hot process streams like the flue gases from the char combustor and catalyst regenerator, as well as the exothermic heat from the MAS reactors are used to generate HP steam, while LP steam is produced when the HP steam is expanded through steam turbines, to produce work as in configurations 1, 1a, and 2, or through an expansion valve as in configuration 3. Further power is produced in configurations 1, 1a, and 2 by the expansion of high pressure unconverted syngas through turbines in the alcohol synthesis and gas cleanup sections. It is reiterated here that all the power requirements for configuration 3 are met by importing power from the grid, thus creating a trade-off between eliminating the high cost of capital associated with purchasing turbines and expanders, and increasing the operating costs associated with purchasing grid power.

All configurations have their cooling requirements met by using forced-air heat exchangers and cooling water after process stream to process stream heat exchange has

been carried out. The idea behind using forced-air heat exchangers is to reduce the water demand of the processes by replacing cooling water in the provision of cooling for the amine system condensers and steam turbine exhaust. Aspen Plus calculator blocks utilizing correlations from literature [32,33] are used to compute the power requirements of the forced-air heat exchangers for the simulations.

5.2.4 Economic analysis

An economic analysis using the MBSP serves the purpose of providing a metric to assess the economic merits of the various plant configurations with respect to themselves as well as to other second generation biobutanol processes and conventional gasoline. The economic analysis was done an "*nth-plant*" basis, meaning that the learning curve associated with building new plants of this type has been surmounted. The MBSP is the unit selling price of butanol over the plant's lifetime for which the net present value (NPV) is zero. A discounted cash flow rate of return analysis is used to compute the MBSP and takes into consideration capital and operating costs of the processes as well as other assumptions of economic parameters which are detailed in Table 5-4.

Table 5-4. Economic parameters and indirect costs basis used in the analysis

Economic Parameter	Basis
Cost year for analysis	2014
Plant financing by equity/debt	50 %/ 50 % [34]
Internal rate of return (IRR)	10 % after tax [35]
Term for debt financing	10 years [35]
Interest rate for debt financing	8 % [35]
Plant life/analysis period	30 years [35]
Depreciation method	Straight Line depreciation 10 years for general plant and utilities
Income tax rate	35% [35]
Plant construction cost schedule	3 years (20% Y1, 45% Y2, 35% Y3) [36]
Plant decommissioning costs	$0
Plant salvage value	$0
Start-up period	3 months [35]
Revenue and costs during start-up	Revenue = 50% of normal Variable costs = 75% of normal Fixed costs = 100% of normal [35]
Inflation rate	1.75% [37]
On-stream percentage	96% (8,410 hours/year)
Land	6.5% of Total Purchased Equipment Cost (TPEC) [38]
Royalties	6.5% of TPEC [38]
Working capital	5% of Fixed Capital Investment (excluding land) [35]
Indirect costs	
Engineering and supervision	32% of TPEC [39]
Construction expenses	34% of TPEC [39]
Contractor's fee and legal expenses	23% of TPEC [39]
Contingencies	20.4% of TPEC [8]

Data used for estimating the capital costs of the various process units are based on mass and energy results of converged Aspen Plus simulations, cost data from Aspen Capital Cost estimator software and literature sources, particularly U.S. NREL reports [8,24]. Literature reported values are scaled to the required size by using the capacity power law expression as shown in equation (11), with m varying from 0.48 to 0.87. The resulting

cost (*Cost2*) is adjusted to 2014 U.S. dollars by using the Chemical Engineering Plant Cost Index [40].

$$\frac{Cost_2}{Cost_1} = (\frac{Capacity_2}{Capacity_1})^m \tag{11}$$

Table 5-5. Cost of materials and products used in the analysis

Commodity prices in 2014 U.S. dollars	
Wood chips cost ($/tonne)	75.01 [21]
Olivine ($/tonne)	304.75 [8]
MgO ($/tonne)	604.33 [8]
Tar reformer catalyst ($/kg)	53.16 [8]
Alcohol synthesis catalyst ($/kg)	28.58 [21]
Solids disposal (Ash) ($/tonne)	81.28 [8]
Water makeup ($/tonne)	0.47 [16]
Boiler feed water chemicals ($/kg)	6.79 [8]
Cooling tower chemicals ($/kg)	4.08 [8]
LO-CAT chemicals ($/tonne sulphur produced)	555.5 [8]
Amine makeup ($/ million kg acid gas removed)	44.15 [8]
Waste water treatment ($/tonne)	1.12 [8]
Average 2014 U.S. industrial electricity price (cents/kWh)	6.63 [41]
Average 2014 U.S. conventional retail gasoline price ($/L)	0.91 [41]
Average 2014 U.S. industrial NG price ($/tonne)	259.27 [41]

Operating costs can be grouped into fixed and variable operating costs. Fixed operating costs are calculated by using correlations from Seider et al. [38], and include items such as maintenance, operating overhead, labour related operations, property tax and insurance. On the other hand variable operating costs include items such as feedstock costs, cooling water costs etc. which vary with production rates. The values of the variable operating costs used for this study are shown in Table 5-5. All the values shown

in the table have been adjusted to 2014 U.S. dollars from their reference values by using an inorganic index obtained from the U.S. Bureau of Labor Statistics [42]. In addition to the sale of butanol as a product, mixed alcohols and electricity (for configurations 1, 1a, and 2) are sold as co-products to generate additional revenue with the selling price of mixed alcohols calculated as 90 % of the price of gasoline on an HHV equivalent basis.

5.2.5 Cost of CO$_2$ equivalent emissions avoided (CCA) analysis

The reduction of GHG emissions in the transportation sector is one of the major objectives driving policy for the use of biofuels as a replacement for fossil derived fuels in vehicles. However, there is usually a cost associated with reducing the amount of GHG emissions that has to be considered, as on an energy density basis fossil fuels are usually cheaper to produce than biofuels. This cost can be evaluated using the CCA metric, which is defined as the marginal cost required to avoid the emission of a unit of GHG emissions when a biofuel is combusted as a replacement for a fossil derived fuel. The unit of GHG emissions is "tonne per CO$_2$ equivalent emissions (CO$_2$e)". The lower the CCA, the better the biofuel is for reducing GHG emissions to the environment. In addition, the CCA serves as a good way to compare biofuel processes to each other and to other GHG emission reduction technologies because it factors in both cost and life cycle impacts. The CCA is computed in this study by using equation (12), and conventional gasoline as a baseline.

$$CCA\left(\frac{\$}{tonne\,CO_2e}\right) = \frac{Biobutanol\ marginal\ cost\left(\frac{\$}{GJ}\right)}{GHG\ emissions\ avoided\left(\frac{tonne\,CO_2e}{GJ}\right)} = \frac{MBSP - gasoline\ price}{CIG - CIB} \qquad (12)$$

The carbon intensity of gasoline (CIG) is its total wells-to-wheels life cycle emissions per unit of energy. It is made up of the sum of the direct GHG emissions from combustion of gasoline in a vehicle, and the indirect GHG emissions of its entire upstream supply chain including oil drilling, production, refining, and distribution. The carbon intensity of biobutanol (CIB) is also the wells-to-wheels life cycle emissions of biobutanol per unit of energy which includes all indirect GHG emissions associated with upstream biomass production, the indirect GHG emissions of utilities used in the plant (NG and electricity for example), and the direct GHG emissions from the combustion of biobutanol in a vehicle. For this analysis all GHG related chemicals are evaluated using the IPCC 100-year metric [43]. A summary of all direct and indirect GHG emissions data along the wells-to-wheels life cycle considered in this work are shown in Table 5-6 for a U.S. based plant. Note that butanol combustion in a vehicle was estimated by assuming 100% conversion of all carbon atoms into CO_2.

Table 5-6. Breakdown of GHG emissions data used in this study. All values are in units of gCO_2e per GJ functional unit.

Description	Value
Feedstock production and harvest [44]	1,800
Land use changes, cultivation [44]	-
Feedstock transportation [44]	1,000
Feedstock pre-processing [44]	2,000
Well-to-gate GHG emissions for biomass wood chips	*4,800*
Butanol dispensing [45]	179
Butanol distribution and storage [45]	1,458
Butanol combustion in vehicle (this work)	63,430
Gate-to-wheel GHG emissions for biobutanol	*65,067*
Feedstock Extraction [45]	8,495
Feedstock Transportation [45]	935
Land use changes, cultivation [45]	2
Fuel Production [45]	12,968
Gas leaks and flares [45]	2,643
Fuel dispensing [45]	138
Fuel distribution and storage [45]	575
Gasoline combustion in vehicle [46]	67,870
Well-to-wheel GHG emissions for gasoline	*93,626*
Well-to-gate GHG emissions for NG [47]	*8,400*
Well-to-gate GHG emissions for electricity [48]	*21,260*

5.3   Results and discussion

5.3.1   Particle swarm optimization of recycle configurations

The selection of the percentage of unreacted syngas stream to be recycled directly back to the MAS reactor, to the amine absorber or to the tar reforming system is not an arbitrary decision. Recycling directly back to the MAS reactor is the best option to improve the butanol yield from the MAS reactor, but the amount that can be recycled is constrained by the requirement to have less than 5 wt % of CO_2 in the reactor feed, as greater than this amount of CO_2 poisons the catalyst [15]. The next option to recycle to the amine absorber

in the gas cleanup section allows CO_2 to be removed to meet the MAS reactor CO_2 specification, albeit with a penalty of high recompression costs as the syngas flowrate through the multi-stage compressor is increased. Finally, recycling back to the tar reforming section allows higher hydrocarbons formed in the MAS reaction process to be reformed back to syngas, and/or the unreacted syngas combusted in the catalyst regenerator to help meet the heat requirements of the process. The downside of this is that it reduces the butanol yield.

The determination of the optimal unreacted syngas recycle configuration can thus be set up as an optimization problem. A simple objective function used for this study was to maximize the contribution margin of the biobutanol plant, where the contribution margin is defined as the operating revenue minus the variable operating cost. The constraints used in the optimizer are feasibility constraints to ensure that the simulation runs without errors and mass and energy is conserved, a MAS reactor feed constraint to limit the amount of CO_2 in the reactor feed stream to less than 5 wt %, and a butanol product purity constraint to have greater than 96 mol % purity of butanol. Another decision variable included in the optimization is the syngas H_2/CO ratio at the MAS reactor inlet, because experimental studies by Beretta et al. [25] showed that butanol yield from the MAS reactor is optimal when the H_2/CO ratio is in the range of 0.5 to 1.0.

Mathematically, the optimization problem is formulated as follows:

Maximize Contribution Margin

Decision variables:
1. RF1: Fraction of unreacted syngas recycled to the MAS reactor - (stream 26/ stream 25) of Figure 5-1.

2. RF2: Fraction of unreacted syngas recycled to the amine absorber - (stream 28/ stream 27) of Figure 5-1.

3. H-C: H_2/CO ratio of syngas at the tar reformer exit - stream 14 of Figure 5-1.

Inequality constraints:
1. CO_2 in MAS reactor feed ≤ 5 wt %

2. Purity of butanol in butanol product stream ≥ 96 mol %

Equality constraints:
1. Contribution margin = Revenue − Variable Operating Cost (VOC)

2. Revenue = butanol product flowrate × butanol selling price + mixed alcohols product flowrate × mixed alcohols selling price + electricity exported × electricity selling price

3. VOC = [biomass feed flowrate × biomass purchase price + NG flowrate × biomass purchase price + electricity exported × electricity selling price] × 1.05

4. Material and energy balance equations of process flowsheet

The selling prices of butanol and mixed alcohols are calculated based on their HHV adjusted gasoline prices (90 % of that value in the case of mixed alcohols). The prices used for biomass, NG, gasoline and electricity in the optimization are given in Table 5-3. Note also that the variable operating cost (VOC) calculation is increased by 5 % to account for miscellaneous VOC items such as makeup water, catalyst refills etc.

A particle swarm optimization (PSO) algorithm was used for this analysis. The PSO algorithm is a nature-inspired derivative-free optimization technique that has found wide use in the peer-reviewed literature for optimizing complicated process systems or systems with no gradient information available, such as Aspen Plus sequential modular flowsheets. Although PSO cannot guarantee that it will find the global optimum, the

global optimum is not strictly required in this case. In-depth discussions about PSO and other similar derivate-free optimization algorithms can be found in books, such as those written by Gendreau and Potvin [49], and Kaveh [50].

The PSO optimization framework used here is adapted from the authors' previous work on optimizing DWCs in Aspen Plus [27] in which MATLAB (which executes the PSO algorithm) is linked to the Aspen Plus simulation file using an Excel Visual Basic for Applications interface. The decision variables are calculated by the PSO algorithm in MATLAB and passed to Aspen Plus which uses them to run the plant simulations. At the completion of the simulation, Aspen Plus returns the values of the variables required to compute the objective function, as well as values of the constraints. If the constraints are violated the objective function in the PSO algorithm is given a large penalty so the algorithm's search is driven away from the infeasible region. The algorithm ends when a convergence criterion is met or a maximum number of iterations have been reached. In this work 10 particles with a maximum iteration of 100 for each particle is used. The resulting optimal values of the decision variables for the base case configurations are shown in Table 5-7.

Table 5-7. Results of optimum decision variables

	RF1	RF2	H-C
Config. 1	0.2247	0.1828	0.9050
Config. 2	0.1373	0.4414	0.8153
Config. 3	0.1556	0.6028	0.7319

5.3.2 Process modeling results

All the assessed configurations were simulated in Aspen Plus to enable quantification of their mass and energy balances, as well as size processing units. Stream conditions which correspond to Figure 5-1 for all the different configurations are detailed in the supporting information available on the journal website, while in Table 5-8 the major process modeling results for the different configurations are summarized. The table shows the major feed and product flows of the configurations, as well as their net power and energy efficiency. The plant energy efficiencies shown in the table are computed on an HHV basis, and defined as the total HHV of the output products (butanol, mixed alcohols and electricity) divided by the total HHV of the input feedstocks (wood biomass, NG, and electricity), noting the exception of course that since HHV has no meaning with regards to electric power, the actual electric energy is used instead.

Table 5-8: Major flowrates and process energy efficiency of all configurations

	Config. 1- Self sufficient plant	Config. 1a- Self sufficient + DWC plant	Config. 2 - NG import plant	Config. 3 - NG & power import plant
Biomass flow rate (kg/h)	83,384	83,384	83,384	83,384
Natural gas requirement (kg/hr)	-	-	23,730	22,161
Makeup water requirement (kg/hr)				
Boiler feed water makeup	4,093	4,049	4,190	2,105
Cooling water makeup	16,253	16,377	37,081	287,680
Product yields (kg/hr)				
Butanol	10,659	10,864	22,063	23,513
Mixed alcohols	5,154	4,930	5,541	4,212
Total product yield, mass basis	15,813	15,793	27,604	27,725
% products yield per feed (Biomass +NG), mass basis	19.0	18.9	25.8	26.3
Power (MW)				
Power generation	57.83	58.64	115.94	-
Power use	57.17	57.31	111.55	126.67
Net power produced (MW)	0.66	1.33	4.39	(126.67)
Biomass HHV (MW)	463	463	463	463
Natural gas HHV (MW)	-	-	348	325
Butanol HHV (MW)	113	116	235	250
Mixed alcohols HHV (MW)	48	46	51	39
Total input HHV + electricity import	463	463	812	915
Total output HHV + electricity export	162	163	291	289
Plant energy efficiency (%)	35.0	35.1	35.8	31.6

It can be seen from Table 5-8 that using heat from NG combustion as a high temperature heat source leads to an increase in the liquid product yields of configurations 2 and 3. This happens because the syngas flowrate to the MAS reactor is increased thus increasing the yields of butanol and mixed alcohols. It can also be seen from the table that there is a huge power import requirement of 127 MW for configuration 3 in contrast to all the other configurations which export electricity. Besides resulting in a huge power import

requirement, the decision to not generate power in configuration 3 leads to a huge makeup water requirement as excess heat from the process is not used to generate power but is instead wasted through cooling with cooling water. The large amount of makeup water required is because of increased evaporative losses in the cooling tower due to the increased water flowrate required for cooling the unused heat. The excess heat available in configuration 3 means that there is a potential for the plant to provide off-plant district heat as a way to minimize the cooling water losses. For a similar reason, the makeup water requirement for configuration 2 is twice that of configuration 1 because of the larger flowrates through the plant and thus higher cooling water requirements leading to higher evaporative water losses.

Due mainly to the higher total liquids production from configuration 2, its plant energy efficiency is higher than configuration 1. However configuration 3 which has the highest total liquids products (slightly higher than configuration 1) has the lowest plant energy efficiency because of the huge power import requirement. Note though that the plant energy efficiency of the assessed configurations are lower than the comparable thermochemical second generation biobutanol plant by Okoli and Adams [21], which is 46 % on a HHV basis, because the plants in the present work have lower once-through CO conversions (CO_2-free basis). For example the once-through CO conversion (CO_2-free basis) of configuration 1, which is a self-sufficient plant similar to that of Okoli and Adams [21] is 22 % while prior work [21] assumes 40 % conversion based on U.S. NREL MAS catalysts development targets [24].

When configuration 1 is compared to configuration 1a, in which a DWC is used in place of conventional columns in the separation section, the product yields and plant thermal efficiency are very similar though configuration 1a has twice the net power production of configuration 1. However, it is not very clear from the process results if there are any overall plant improvements obtained by utilizing a DWC in place of conventional columns. Thus any potential improvements have to be investigated through an economic analysis which factors in revenues, capital, and operating costs. This is discussed in the next section.

5.3.3   Economic analysis results

An economic assessment of all the configurations was carried out with the results summarized in Table 5-9. From the table it can be seen that amongst the base configurations, configuration 2 has the highest total capital investment (TCI) followed by configuration 3 and then configuration 1. The higher TCI of configuration 2 over configuration 1 is because the combustion of NG over syngas for high temperature heat in the tar reforming system of configuration 2 enables a higher flowrate of syngas to be available for conversion downstream. This cascades down to higher flowrates of other accompanying streams through the plant sections downstream of the gasifier leading to the requirement of larger process equipment and thus capital costs. However, as configurations 2 and 3 have similar flowrates, the lower TCI of configuration 3 is because it has no electricity generating turbines thus leading to capital cost savings.

In terms of total operating costs (TOC), configuration 3 has the highest TOC because just like configuration 1 it has higher flowrates downstream of the gasifier in comparison to

configuration 1, but unlike the other configurations there is a significant additional cost associated with electricity purchase from the grid.

When revenue from co-products is considered, configuration 2 has the highest revenue because it produces the largest amount of mixed alcohols and exports the largest amount of electricity. In contrast configuration 3 has the lowest co-products revenue because it produces the least amount of mixed alcohols and has no electricity export.

The MBSP, computed through a DCFROR analysis, unifies all the co-product revenue, capital and operating cost results into a single economic value thus allowing the economic potential of producing butanol through each considered configuration to be assessed. As can be seen from Table 5-9 configuration 2 has the lowest MBSP of 0.92 $/L meaning that it is the most economically viable plant in comparison to the others for producing biobutanol. The reason configuration 1 has a lower MBSP in comparison to configuration 1(which has the highest MBSP) is because the higher cost per energy of biomass in comparison to NG mean that it is more valuable for producing butanol than being used for high temperature head production as is done in configuration 1. Configuration 3 has the next best MBSP at 1.10 $/L. Compared to configuration 1, its result shows that the capital cost savings benefit of not investing in electricity generation infrastructure is far outweighed by the higher operating costs attributable to electricity import from the grid.

As discussed in the introduction it is difficult to compare the MBSP of second generation biobutanol because of the variety of assumptions made in the cost computation. For example in the thermochemical second generation biobutanol study carried out by Okoli

and Adams [21] an MBSP of 0.83 $/L is obtained when a catalyst once-through CO conversion of 40 % is assumed but 1.56 $/L when the catalyst literature conversion value of 8.5 % [23] is used. In the study by Tao et al. [19] on biochemical second generation biobutanol, they obtained an MBSP of 0.78 $/L when they assumed a very high butanol yield from sugars of 85 % the theoretical yield. However, when they used more realistic values of 55 - 65 % theoretical yield the MBSP drops to 1.20 - 1.02 $/L. The advantage of this work over other studies is that it does not make futuristic technological assumptions but uses data from current technology that have either been demonstrated on a pilot scale or commercially, thus the MBSP numbers obtained here are a better representation of the current economic potential of thermochemical second generation biobutanol. Note though that the MBSP values obtained in this work (0.92 - 1.13 $/L for all configurations) are still competitive with literature values for second generation biobutanol.

When configuration 1a (with DWC) is compared to configuration 1, configuration 1a has a slightly higher TCI. This is primarily because the savings obtained in the alcohol separation section (reduced capital cost and LP steam usage) are offset by the requirement for slightly larger power generating equipment (specifically the LP steam turbine). The need for a bigger LP steam turbine arises because the LP steam savings of the DWC means that extra LP is available for expansion through the steam turbine to generate electricity. Overall, the decision to use a DWC in configuration 1a leads to only a 1 cent/L MBSP saving over configuration 1. This is primarily because the separation section makes up only a small portion of the capital cost of the thermochemical biobutanol plant.

Table 5-9. Economic summary of all configurations (a more detailed breakdown is provided in the supporting information on www. macsphere.mcmaster.ca.)

Plant design	Config. 1 - Self sufficient plant	Config. 1a - Self sufficient + DWC plant	Config. 2 - NG import plant	Config. 3 - NG & power import plant
Capital Investment ($'000)				
Direct costs breakdown				
Gasification	47,364	47,364	47,364	47,364
Gas cleanup	100,622	100,853	140,527	135,281
Mixed Alcohol synthesis	18,079	18,159	41,310	35,470
Alcohol separation	9,905	9,270	13,145	12,435
Steam system & power gen.	35,692	36,115	61,400	10,306
Cooling water & other utilities	20,606	20,603	32,909	26,449
Total Direct Costs	232,268	232,364	336,654	267,307
Engineering and supervision	32,802	32,835	47,731	36,064
Construction expenses	34,852	34,887	50,714	38,318
Contractor's fee & legal expenses	23,577	23,600	34,307	25,921
Contingency	20,911	20,932	30,429	22,991
Royalties	6,888	6,892	9,997	7,812
Land	6,888	6,892	9,997	7,812
Working Capital	17,565	17,576	25,492	19,921
Total Capital Investment	*375,752*	*375,979*	*545,320*	*426,143*
Operating costs ($'000/year)				
Woody Biomass	52,571	52,571	52,571	52,571
Natural gas	-	-	51,741	48,321
Catalysts & chemicals	2,435	2,439	3,310	3,394
Waste stream treatment	848	848	1,001	995
Water makeup	80	80	162	1,137
Electricity import	-	-	-	39,139
Labour related costs	23,870	23,870	23,870	23,870
Maintenance costs	24,040	24,050	34,844	27,666
Operating overheads	7,610	7,611	8,948	8,059
Property taxes and Insurance	4,645	4,647	6,733	5,346
Total Operating Costs	*116,098*	*116,116*	*183,181*	*210,499*
Co-prod. revenues ($'000/year)				
Mixed Alcohols	38,597	36,932	41,523	31,491
Electricity export	371	744	2,448	-
Total co-prod. revenue	*38,969*	*37,677*	*43,971*	*31,491*
MBSP ($/L)	1.13	1.12	0.92	1.10

5.3.4   Cost of CO_2 equivalent emissions avoided (CCA)

The results of the CCA computations are shown in Table 5-10. Note that it is assumed that all carbon in the biomass originated from atmospheric CO_2, and thus the biogenic CO_2 uptake can be computed from the biomass ultimate analysis as shown in Table 5-1. Furthermore, an energy basis allocation factor which is computed as the fraction of butanol product in the total product mix on a HHV basis (see Table 5-8) is used to allocate GHG emissions from the well-to-gate exit emissions of the process to butanol. Configuration 1 has the cheapest CCA of 134.65 \$/tonneCO$_2$e among all the base case configurations making it the "greenest" plant. This low value can be attributed to the fact that it has zero emissions associated with NG and electricity imports (because they do not exist), thus its well-to-wheel emissions are the lowest leading to the highest CCA values. In contrast, the GHG emission penalties associated with both NG and electricity imports in configuration 3 mean that it has the highest CCA.

The reason configuration 2 has a lower CCA in comparison to configuration 3 is because configuration 2 has a lower biofuel marginal cost and higher CCA value than configuration 3. However, despite configuration 2 having a lower biofuel marginal cost than configuration 1, its CCA values are relatively much lower meaning that it ends up having a higher CCA than configuration 1. Replacing conventional distillation columns with a DWC as is done in configuration 1a leads to savings of 3 \$/tonneCO$_2$e over configuration 1 which could be significant if these technologies are implemented on a large scale.

The CCA of configurations 1 and 2 are very competitive with the range of values estimated for other biofuels in the literature. For example, the CCA for European biofuels is put at between 277 - 2,524 \$/tonneCO$_2$e (Euro converted to U.S. dollars using December 2014 exchange rate) by Ryan et al. [51] while Fulton et al. [52] estimates this cost at 180 - 874 \$/tonneCO$_2$e for ethanol from different biomass sources. Ethanol from sugarcane in Brazil with a value of around 30 \$/tonneCO$_2$e [52] is a notable exception because sugarcane crops in Brazil have low costs as a result of very high yields, and the sugarcane to ethanol conversion processes used have near zero fossil fuel requirements [51,52].

The target value of CCA for GHG emission reduction technologies generally discussed by policy makers in western countries is 50 \$/tonneCO$_2$e [52]. Though the technologies for biobutanol production studied in this work are higher than this value, it is the authors' opinion that this target can be met and even surpassed by these technologies if improvements in areas such as the biomass supply chain (to reduce biomass costs), biomass-to-butanol processing technology and MAS catalysts are obtained.

Table 5-10. Summary of CCA calculations

Plant	Config. 1 - Self sufficient plant	Config. 1a - Self sufficient + DWC plant	Config. 2 - NG import plant	Config. 3 - NG & power import plant
Biogenic CO_2 sequestered during biomass growth (from ultimate analysis)	-1,867	-1,867	-1,867	-1,867
Well-to-gate GHG emissions for biomass wood chips import	96	96	96	96
Biomass to butanol plant emissions (from simulation results)	1,355	1,356	1,819	1,764
Well-to-gate GHG emissions for NG use	-	-	140	131
Well-to-gate GHG emissions for electricity import	-	-	-	129
Well-to-gate exit emissions ($kgCO_2e$/dry tonne biomass)	-416	-415	187	253
Well-to-gate exit emissions allocated to butanol ($kgCO_2e$/GJ), product energy basis	-52.18	-51.93	13.41	18.24
Gate-to-wheel GHG emissions for biobutanol ($kgCO_2e$/GJ)	65.07	65.07	65.07	65.07
Well-to-wheel emission for butanol ($kgCO_2e$/GJ)	12.89	13.14	78.47	83.31
Avoided GHG emissions ($kgCO_2e$/GJ) [A]	80.73	80.49	15.15	10.32
MBSP ($/GJ)	37.13	36.85	30.25	36.21
Biofuel marginal cost ($/GJ) [B]	10.87	10.59	4.00	9.95
CCA ($/tonne$CO_2$e) [B/A]	134.65	131.59	263.73	964.37

5.3.5 Sensitivity analysis

A sensitivity analysis is carried out on configurations 1 and 2 as they have the lowest CCA and MBSP values respectively among the base configurations. A sensitivity analysis allows the impact of key decision variables on the CCA and MBSP to be studied.

5.3.5.1 Sensitivity analysis - impact of gasoline price changes

The effect of changing gasoline prices on the MBSP and CCA of configurations 1 and 2 are shown in Figure 5-2 and Figure 5-3 respectively. The gasoline price is varied between a ten-year (January 2005 to December 2014) maximum and minimum historical price range [41]. The minimum price of gasoline in that time was 0.43 $/L (December 2008),

while its maximum price was 1.08 \$/L (June 2008). Both Figure 5-2 and Figure 5-3 show that changes in gasoline price have an inverse effect on MBSP and CCA for the configurations assessed. This is because increasing the gasoline price increases the revenue from selling mixed alcohols and thus lowers the revenue that is needed from selling biobutanol to get a zero NPV, meaning that the MBSP and CCA are lowered. The opposite effect also holds true when gasoline prices are reduced. As can be seen from the slopes of the lines in Figure 5-2, changing the gasoline price has slightly more effect on the MBSP of configuration 1 than configuration 2. This is because the mixed alcohols co-product, whose pricing is directly correlated to gasoline price, contributes a higher percentage to the total product yield of configuration 1 than configuration 2 (see Table 5-8), thus changes in gasoline price affect configuration 1 more than configuration 2. However, the much smaller avoided GHG emissions value of configuration 2 (see Table 5-10) means that changes in gasoline price have a larger effect on its CCA in comparison to configuration 1 as is shown in Figure 5-3. Also shown in Figure 5-3 is the price of gasoline above which the CCA becomes lower than the 50 \$/tonneCO_2e benchmark. This corresponds to approximately 1 \$/L for both configurations 1 and 2.
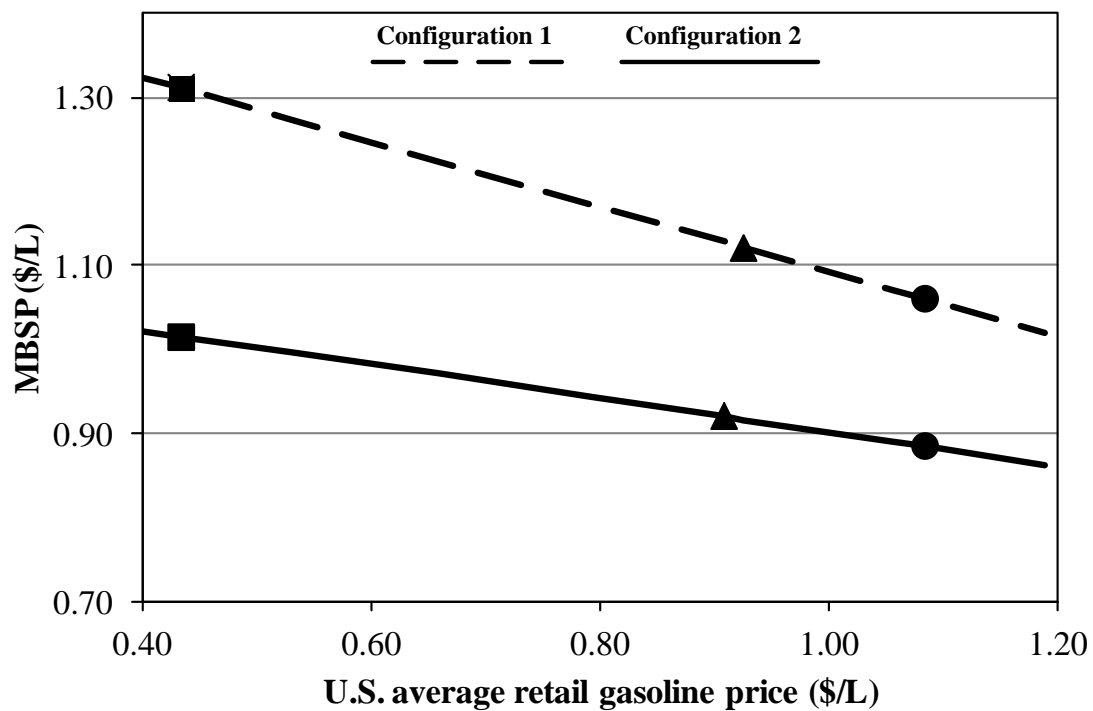
Figure 5-2. Impact of changes in gasoline price ($/L) on MBSP ($/L). Symbols: maximum gasoline price (●), minimum gasoline price (■), base case gasoline price (▲).
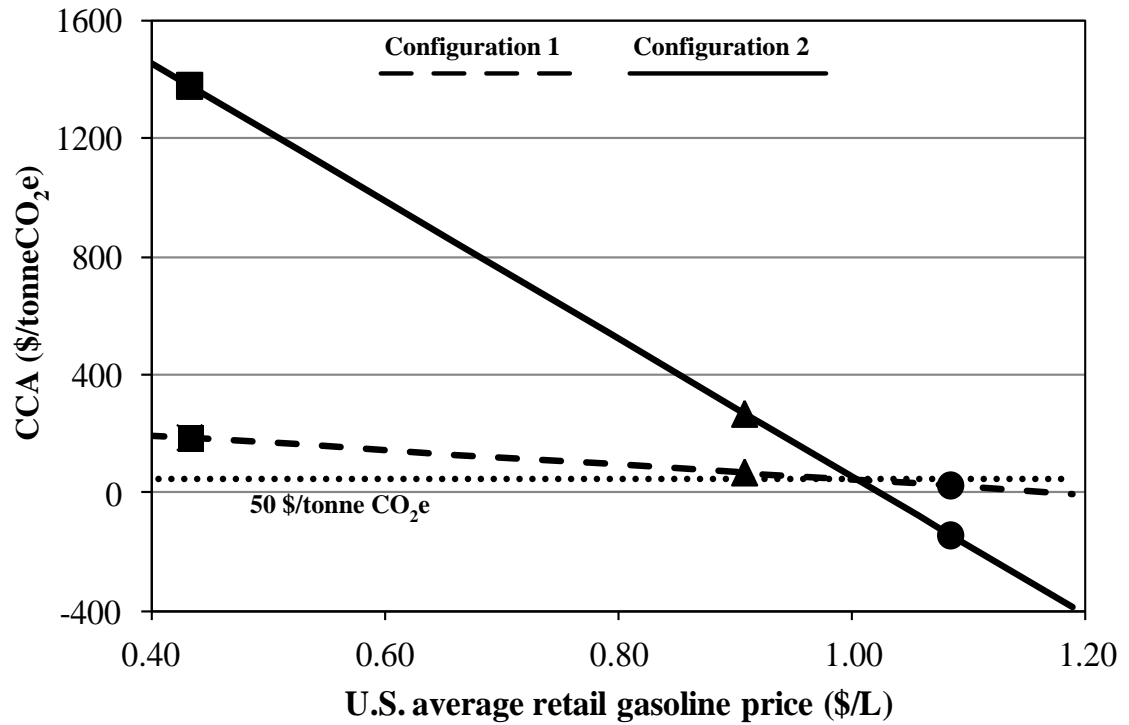
Figure 5-3. Impact of changes in gasoline price (\$/L) on CCA (\$/tonneCO$_2$e). Symbols: maximum gasoline price (•), minimum gasoline price (■), base case gasoline price (▲).

5.3.5.2   Sensitivity analysis - impact of natural gas price changes

Figure 5-4 and Figure 5-5 respectively show the effect of changing NG prices on the MBSP and CCA of configurations 1 and 2. Similar to the sensitivity analysis on gasoline price, the NG price is varied between a ten-year (January 2005 to December 2014) maximum and minimum historical price range [41]. The minimum price of NG in that time was 141.98 $/tonne (May 2012), while its maximum price was 613.97 $/tonne (July 2008). As NG is an operating cost item, the MBSP and CCA are directly correlated to it. However, note that changes in NG have no impact on configuration 1 as that plant makes no use of NG. It can be seen from Figure 5-4 that at the maximum ten-year NG historical price, the MBSP of configuration 2 is 1.31 $/L while it is 0.82 $/L at the minimum NG historical price. At the same maximum and minimum NG prices, the CCA is 942.33 $/tonneCO$_2$e and 39.33 $/tonneCO$_2$e respectively for configuration 2 as is shown in Figure 5-5. Furthermore, Figure 5-5 shows that with an NG price below 153.13 $/tonne, the CCA is lower than the 50 $/tonneCO$_2$e benchmark.
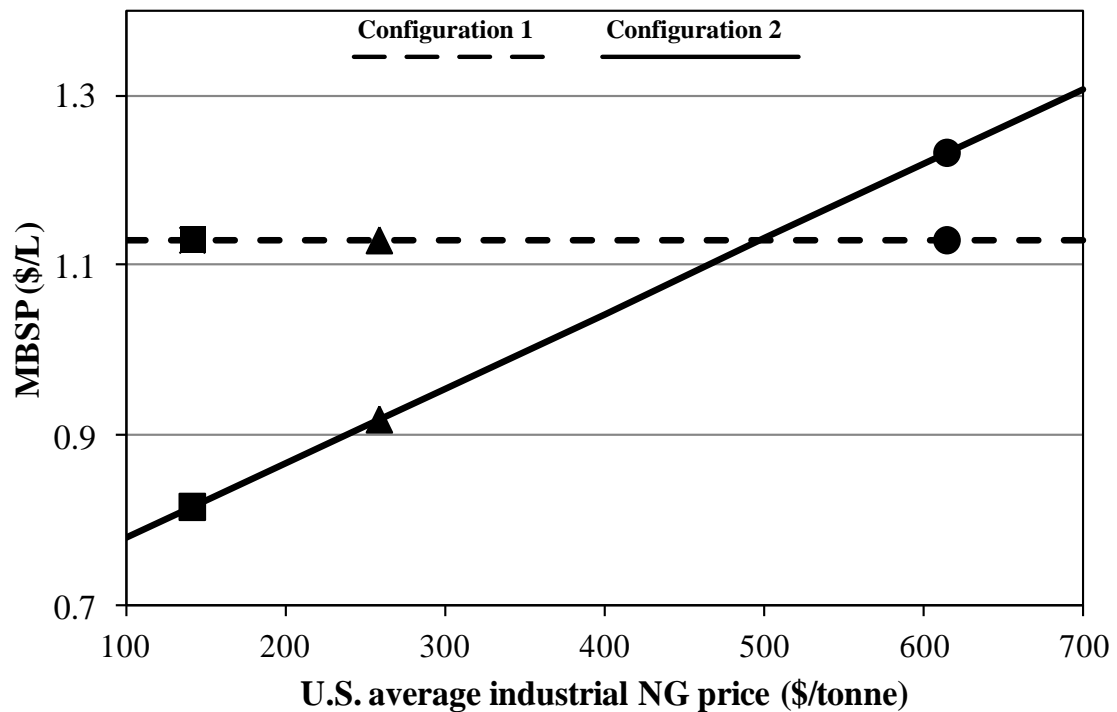
Figure 5-4. Impact of changes in NG price ($/tonne) on MBSP ($/L). Symbols: maximum NG price (•), minimum NG price (■), base case NG price (▲).
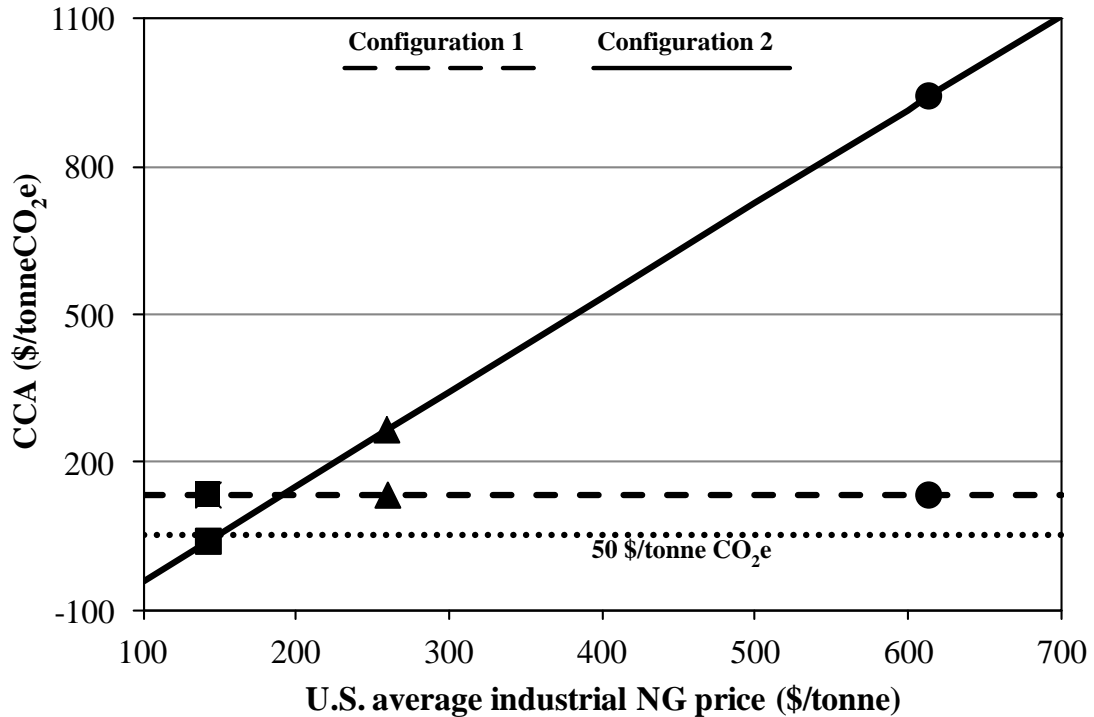
Figure 5-5. Impact of changes in NG price ($/tonne) on CCA ($/tonneCO$_2$e). Symbols: maximum NG price (●), minimum NG price (■), base case NG price (▲).

5.3.5.3   Sensitivity analysis - impact of biomass price changes

The impact of changes in biomass price on the MBSP and CCA of configurations 1 and 2 were assessed with the results presented in Figure 5-6 and Figure 5-7 respectively. As can be seen in Figure 5-6 the MBSP of configuration 1 is more sensitive to biomass price changes than that of configuration 2. This is because in configuration 1, biomass purchase makes up a greater percentage of the TOC unlike in configuration 2 in which it has a smaller percentage, primarily because of the additional significant cost of NG. However, as shown in Figure 5-7 the CCA of configuration 2 is more sensitive to biomass price changes than that of configuration 1. As previously mentioned for gasoline price changes,

this is because of the much smaller avoided GHG emissions value of configuration 2 in comparison to configuration 1 (see Table 5-10). Furthermore, Figure 5-7 shows that a minimum 41 % reduction in biomass price from the base case value of 75 $/tonne to 44 $/tonne is needed for both configurations before their CCA is below the policy threshold of 50 $/tonneCO$_2$e.
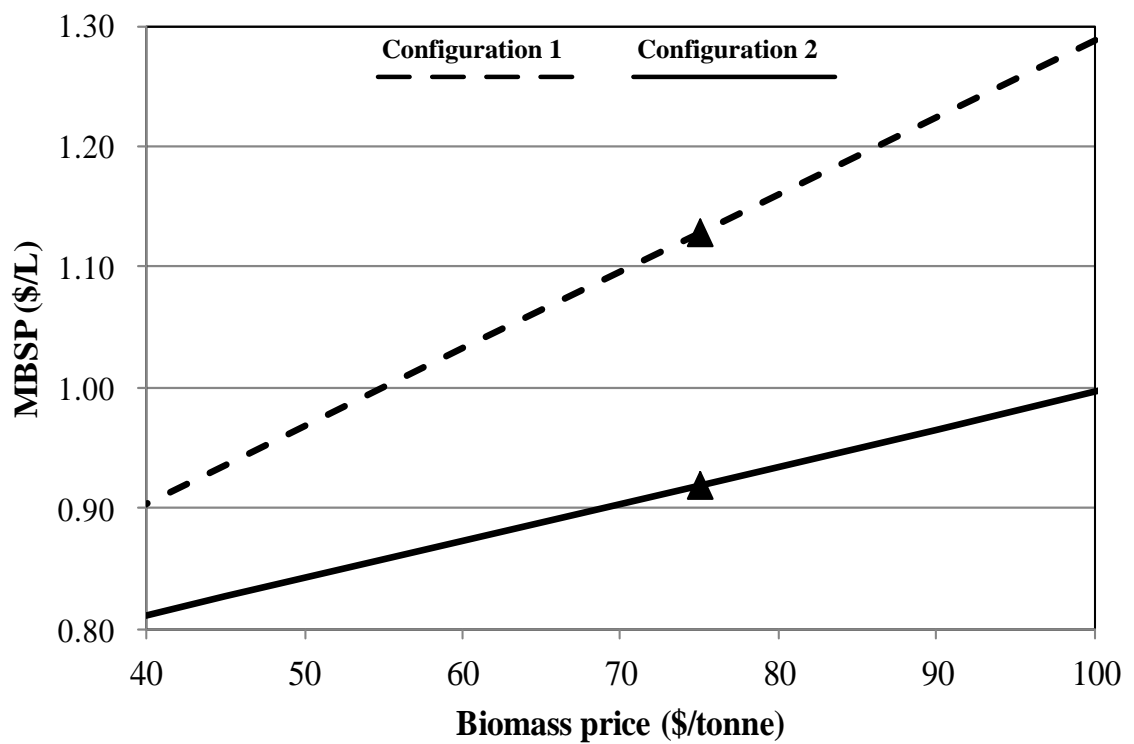
Figure 5-6. Impact of changes in biomass price ($/tonne) on MBSP ($/L). Symbol: base case biomass price (▲).
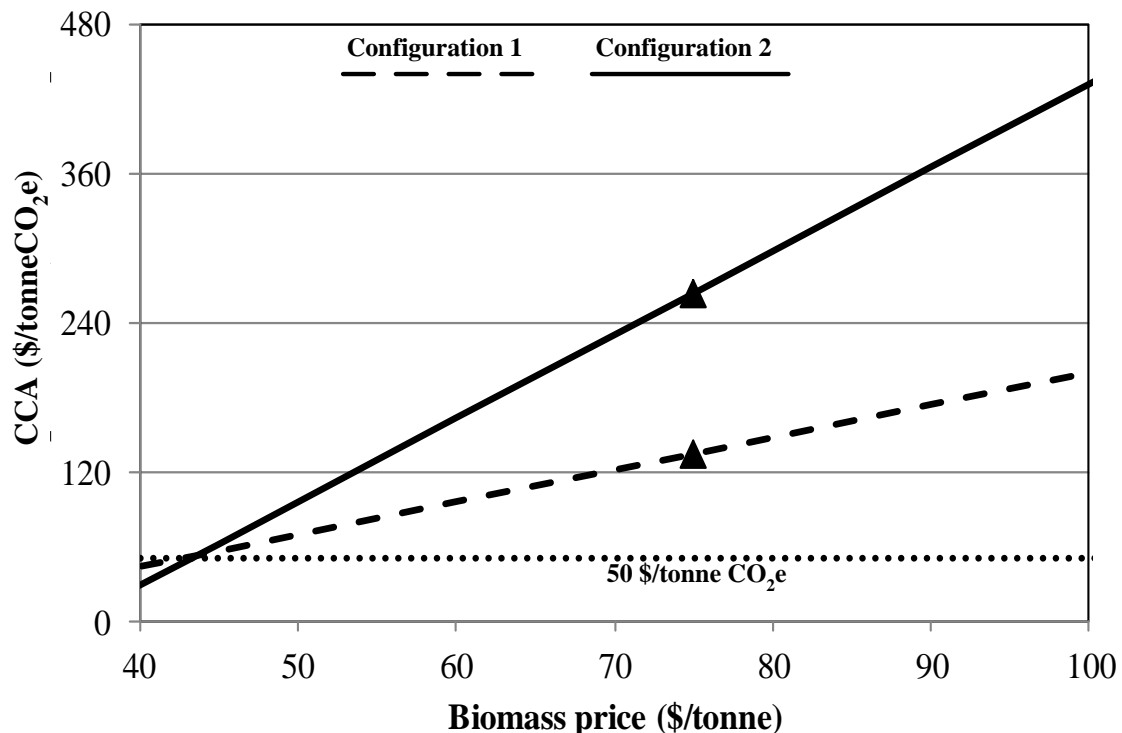
Figure 5-7. Impact of changes in biomass price ($/tonne) on CCA ($/tonneCO$_2$e). Symbol: base case biomass price ($\blacktriangle$).

5.4   Conclusion

In this work novel configurations for producing second generation biobutanol through a thermochemical route and MAS process are designed and assessed based on economic and environmental metrics. The different configurations vary based on choices regarding the use of NG combustion for high temperature heat, import of electricity to meet plant demands, and the use of DWCs for alcohols separation.

The economic results showed that the NG import configuration has the lowest MBSP at 0.92 $/L. This is because this configuration avoids the high operating costs associated with electricity import and has a high butanol yield because syngas is not diverted for

187

meeting high temperature heat requirements. However the environmental results show that the self-sufficient configuration has the lowest CCA of 134.65 $/tonneCO$_2$e among the base configurations.

The use of DWC technology over conventional columns in the alcohols separation section leads to CCA savings of 3 $/tonneCO$_2$e, which could be significant if these technologies are implemented on a large scale. Furthermore, a sensitivity analysis showed that the CCA of the NG import configuration is more sensitive than the self-sufficient configuration to changes in gasoline, NG and biomass prices.

Finally, the economic results show that the assessed thermochemical plants produce second generation biobutanol that are competitive with second generation biobutanol produced through a biochemical route.

5.5 References

[1] EIA UEIA. Annual Energy Outlook 2014 with Projections to 2040. Washington DC: 2014.

[2] Congress U. U.S. Energy Independence and Security Act of 2007. Public Law 2007:110–40.

[3] Perlack RD, Wright LL, Turhollow AF, Graham RL, Stokes BJ, Erbach DC. Biomass as feedstock for a bioenergy and bioproducts industry: the technical feasibility of a billion-ton annual supply. Oak Ridge, Tennessee: DTIC Document; 2005.

[4] Kumar M, Gayen K. Developments in biobutanol production: New insights. Appl Energy 2011;88:1999–2012. doi:10.1016/j.apenergy.2010.12.055.

[5] Ranjan A, Moholkar VS. Biobutanol: science, engineering, and economics. Int J Energy Resour 2012;36:277–323. doi:10.1002/er.

[6] Green EM. Fermentative production of butanol—the industrial perspective. Curr

Opin Biotechnol 2011;22:337–43. doi:10.1016/j.copbio.2011.02.004.

[7]   García V, Päkkilä J, Ojamo H, Muurinen E, Keiski RL. Challenges in biobutanol production: How to improve the efficiency? Renew Sustain Energy Rev 2011;15:964–80. doi:10.1016/j.rser.2010.11.008.

[8]   Dutta A, Talmadge M, Nrel JH, Worley M, Harris DD, Barton D, et al. Process Design and Economics for Conversion of Lignocellulosic Biomass to Ethanol Process Design and Economics for Conversion of Lignocellulosic Biomass to Ethanol Thermochemical Pathway by Indirect. 2011.

[9]   Kraemer K, Harwardt A, Bronneberg R, Marquardt W. Separation of butanol from acetone–butanol–ethanol fermentation by a hybrid extraction–distillation process. Comput Chem Eng 2011;35:949–63. doi:10.1016/j.compchemeng.2011.01.028.

[10]   Abdehagh N, Tezel FH, Thibault J. Separation techniques in butanol production: Challenges and developments. Biomass and Bioenergy 2014;60:222–46. doi:10.1016/j.biombioe.2013.10.003.

[11]   Ndaba B, Chiyanzu I, Marx S. n-Butanol derived from biochemical and chemical routes: A review. Biotechnol Reports 2015;8:1–9. doi:10.1016/j.btre.2015.08.001.

[12]   Lee SY, Park JH, Jang SH, Nielsen LK, Kim J, Jung KS. Fermentative butanol production by clostridia. Biotechnol Bioeng 2008;101:209–28. doi:10.1002/bit.22003.

[13]   Kazi FK, Fortman J, Anex R, Kothandaraman G, Hsu D, Aden A, et al. Techno-economic analysis of biochemical scenarios for production of cellulosic ethanol. Golden, Colorado: Citeseer; 2010.

[14]   Surisetty VR, Dalai AK, Kozinski J. Intrinsic Reaction Kinetics of Higher Alcohol Synthesis from Synthesis Gas over a Sulfided Alkali-Promoted Co−Rh−Mo Trimetallic Catalyst Supported on Multiwalled Carbon Nanotubes (MWCNTs). Energy & Fuels 2010;24:4130–7. doi:10.1021/ef1007227.

[15]   Nexant. Equipment Design and Cost Estimation for Small Modular Biomass Systems, Synthesis Gas Cleanup, and Oxygen Separation Equipment Task 9 : Mixed Alcohols From Syngas — State of Technology. San Francisco, California: 2006.

[16]   Fang K, Li D, Lin M, Xiang M, Wei W, Sun Y. A short review of heterogeneous catalytic process for mixed alcohols synthesis via syngas. Catal Today 2009;147:133–8. doi:10.1016/j.cattod.2009.01.038.

[17]   Surisetty VR, Dalai AK, Kozinski J. Alcohols as alternative fuels: An overview. Appl Catal A Gen 2011;404:1–11. doi:10.1016/j.apcata.2011.07.021.

[18]   Qureshi N, Saha BC, Cotta MA, Singh V. An economic evaluation of biological conversion of wheat straw to butanol: A biofuel. Energy Convers Manag 2013;65:456–62. doi:http://dx.doi.org/10.1016/j.enconman.2012.09.015.

[19]   Tao L, Tan ECD, McCormick R, Zhang M, Aden A, He X, et al. Techno-economic analysis and life-cycle assessment of cellulosic isobutanol and comparison with cellulosic ethanol and n-butanol. Biofuels, Bioprod Biorefining 2014;8:30–48. doi:10.1002/bbb.1431.

[20]   Kumar M, Goyal Y, Sarkar A, Gayen K. Comparative economic assessment of ABE fermentation based on cellulosic and non-cellulosic feedstocks. Appl Energy 2012;93:193–204. doi:10.1016/j.apenergy.2011.12.079.

[21]   Okoli C, Adams TA. Design and economic analysis of a thermochemical lignocellulosic biomass-to-butanol process. Ind Eng Chem Res 2014;53:11427–41.

[22]   Gapes JR. The Economics of Acetone-Butanol Fermentation: Theoretical and Market Considerations 2000;2:27–32.

[23]   Herman R. Advances in catalytic synthesis and utilization of higher alcohols. Catal Today 2000;55:233–45. doi:10.1016/S0920-5861(99)00246-1.

[24]   Phillips S, Aden A, Jechura J, Dayton D. Thermochemical Ethanol via Indirect Gasification and Mixed Alcohol Synthesis of Lignocellulosic Biomass Thermochemical Ethanol via Indirect Gasification and Mixed Alcohol Synthesis of Lignocellulosic Biomass 2007.

[25]   Beretta A, Micheli E, Tagliabue L, Tronconi E. Development of a Process for Higher Alcohol Production via Synthesis Gas 1998;5885:3896–908.

[26]   Yildirim Ö, Kiss A a., Kenig EY. Dividing wall columns in chemical process industry: A review on current activities. Sep Purif Technol 2011;80:403–17. doi:10.1016/j.seppur.2011.05.009.

[27]   Okoli CO, Adams TA. Design of dividing wall columns for butanol recovery in a thermochemical biomass to butanol process. Chem Eng Process Process Intensif 2015;95:302–16. doi:10.1016/j.cep.2015.07.002.

[28]   Zhu Y, Gerber MA, Jones SB, Stevens DJ. Analysis of the Effects of Compositional and Configurational Assumptions on Product Costs for the Thermochemical Conversion of Lignocellulosic Biomass to Mixed Alcohols - FY 2007 Progress Report. Richland, Washington: 2008.

[29]   Union   Gas.   Chemical   Composition   of   Natural   Gas   2016. https://www.uniongas.com/about-us/about-natural-gas/Chemical-Composition-of-Natural-Gas (accessed January 31, 2016).

[30] Cohen AP, Reynolds TM, Davis MM. Adsorbent for Drying Ethanol. U.S. 2010/0081851 A1, 2012.

[31] ASTM Standard D7862-15. Standard Specification for Butanol for Blending with Gasoline for Use as Automotive Spark-Ignition Engine Fuel 2015. doi:10.1520/D7862-15.

[32] Hicks TG, Wills KD. Handbook of Mechanical Engineering Calculations. New York: McGraw-Hill; 2006.

[33] Perry RH, Green DW. Perry's Chemical Engineers' Handbook. 7th ed. New York: McGraw-Hill; 1997.

[34] Consonni S, Katofsky RE, Larson ED. A gasification-based biorefinery for the pulp and paper industry. Chem Eng Res Des 2009;87:1293–317. doi:10.1016/j.cherd.2009.07.017.

[35] Dutta A, Talmadge M, Hensley J, Worley M, Dudgeon D, Barton D, et al. Techno-economics for conversion of lignocellulosic biomass to ethanol by indirect gasification and mixed alcohol synthesis. Environ Prog Sustain Energy 2012;31:182–90. doi:10.1002/ep.10625.

[36] Flnkenrath M. Cost and performance of carbon dioxide capture from power generation. Paris: 2011.

[37] BLS. Consumer Price Index - All Urban Consumers. United States Bur Labor Stat 2016. http://data.bls.gov/timeseries/CUUR0000SA0L1E?output_view=pct_12mths (accessed January 31, 2016).

[38] Seider WD, Seader JD, Lewin DR. Product & Process Design Principles: Synthesis, Analysis and Evaluation. 3rd ed. Hoboken, New Jersey: John Wiley & Sons; 2009.

[39] Peters MS, Timmerhaus KD, West RE. Plant Design and Economics for Chemical Engineers. Massachusetts: McGraw-Hill Science/Engineering/Math; 2003.

[40] CE. Economic indicators. Chem Eng 2015;122:192.

[41] EIA UEIA. Petroleum and other liquids data. U.S. Energy Inf Adm 2016. https://www.eia.gov/petroleum/data.cfm#prices (accessed January 31, 2016).

[42] BLS. Producer Price Indexes. News Release - Bur Labor Stat 2015. http://www.bls.gov/news.release/pdf/ppi.pdf (accessed January 31, 2016).

[43] IPCC. IPCC Fourth Assessment Report: Climate Change 2007. Intergovermental Panel Clim Chang 2007. https://www.ipcc.ch/publications_and_data/ar4/wg1/en/ch2s2-10-2.html (accessed April 19, 2016).

[44] Hsu DD, Inman D, Heath GA, Wolfrum EJ, Mann MK, Aden A. Life Cycle Environmental Impacts of Selected U.S. Ethanol Production and Use Pathways in 2022. Environ Sci Technol 2010;44:5289–97. doi:10.1021/es100186h.

[45] S&T CI. The Addition of Bio-Butanol to GHGenius and a Review of GHG Emissions from Diesel Engines with Urea SCR. Ottawa, Ontario: 2007.

[46] EIA. How much carbon dioxide is produced by burning gasoline and diesel fuel? U.S. Energy Inf Adm 2015. http://www.eia.gov/tools/faqs/faq.cfm?id=307&t=11 (accessed February 2, 2016).

[47] Skone TJ, Littlefield J, Marriot J, Cooney G, Jamieson M, Hakian J, et al. Life Cycle Analysis of Natural Gas Extraction and Power Generation. 2014. doi:DOE/NETL-2014/1646.

[48] Itten R, Frischknecht R, Stucki M. Life Cycle Inventories of Electricity Mixes and Grid Version 1.3. Uster: 2014.

[49] Gendreau M, Potvin J-Y. Handbook of Metaheuristics Vol. 2. New York: Springer; 2010.

[50] Kaveh A. Advances in Metaheuristic Algorithms for Optimal Design of Structures. New York: Springer; 2014.

[51] Ryan L, Convery F, Ferreira S. Stimulating the use of biofuels in the European Union: Implications for climate change policy. Energy Policy 2006;34:3184–94. doi:http://dx.doi.org/10.1016/j.enpol.2005.06.010.

[52] Fulton L, Howes T, Hardy J. Biofuels for transport: An international perspective. Paris: 2004.

CHAPTER 6   Conclusions and future work

6.1   Conclusions

The overarching objective of this thesis was to contribute to the understanding of the thermochemical route for second and third generation biobutanol production, through the development of novel thermochemical plants for producing second and third generation biobutanol, and assessing their economic and environmental potential.

The research work begins by developing, and economically evaluating a first-of-its-kind process for second generation biobutanol production through a thermochemical route. This is the focus of chapter 2. The plant was designed to be "self-sufficient", meaning that it is 100% powered by biomass, including all utility needs. The heart of this plant is the mixed alcohol synthesis (MAS) reaction process in which syngas is converted to butanol and other alcohols over a low pressure modified methanol synthesis catalyst [1]. Using an assumed MAS catalyst CO conversion of 40%, based on U.S. National Renewable Energy Laboratory (NREL) research targets for MAS catalysts, the plant is able to produce biobutanol at a MBSP of 0.83 $/L. This value makes second generation biobutanol from this thermochemical plant design competitive with gasoline for crude oil prices greater than 85 $/bbl. However, at the current catalyst CO conversion of 8.5% [1] the MBSP is 1.22 $/L which would require crude oil prices of 126 $/bbl to be competitive with gasoline. The results obtained in this chapter highlighted the potential benefits improved MAS catalysts would have on the economics of thermochemical second generation biobutanol production, and provides a motivation for research into MAS catalyst improvements.

The thermochemical plant design developed in chapter 2 for producing second generation biobutanol is extended, with modifications to the gasification and cleanup sections, to the production of third generation biobutanol from macroalgae. The motivation for using macroalgae as a feedstock for the thermochemical plant is based on its fast growth rates, yielding up to 4-6 harvest cycles per year, and its ability to be grown aquatically thus eliminating issues with respect to land use faced by first and second generation biofuel feedstocks. The MBSP results obtained for thermochemical third generation biobutanol in chapter 3 ranged from 1.97 \$/L to 3.33 \$/L, which is high in comparison to second generation biobutanol from the thermochemical route. Furthermore, the CCA ranged from 620 - 2,720 \$/tonneCO$_2$e which is much higher than the break-even value of 50 \$/tonneCO$_2$e recommended by policy makers in western countries for investment in greenhouse gas emission reduction technologies [2]. Overall, the results from chapters 2 and 3 demonstrate that the thermochemical route is more competitive for producing second generation biobutanol than third generation biobutanol.

As process intensification has been shown in numerous studies to reduce capital and operating costs of unit operations, one objective of this thesis was to improve the economic potential of biobutanol thermochemical plants by integrating process intensification technology into their design. The utilization of process intensification technology in the form of dividing wall columns (DWC) in place of conventional distillation columns for separating raw alcohols from the MAS reactor into finished products was identified as a technology to investigate. This is because the alcohols distillation process of the thermochemical plant designed in chapter 2 consumed 10% of

the plant's energy related costs, thus any savings here would potentially improve the overall process. Chapter 4 takes a step towards investigating this potential for DWCs by focusing on the development of a methodology for designing three-product and four-product DWCs capable of separating multicomponent zeotropic mixtures. This methodology was then applied to design three-product and four-product DWCs for separating a multicomponent butanol rich stream. The results showed that all the DWCs provide significant cost savings in comparison to a standard design of three conventional distillation columns. In particular, the four-product DWC provided the most savings with up to 31% saved in operating costs and 28% saved in total annualized costs.

The research carried out in chapter 5 improved on the work done in chapter 2 on designing thermochemical plants for second generation biobutanol, by replacing chapter 2's assumption of a simplistic MAS reactor conversion model using a futuristic catalyst based on U.S NREL research targets, with a detailed kinetic model using a high-pressure methanol synthesis catalyst that has been demonstrated at the pilot scale [3]. This change depicts a more realistic representation of the MAS reactions of the thermochemical plant, and allowed the impact of different design decisions such as the impact of unreacted syngas recycle choices on butanol production to be evaluated. Furthermore the NG import, and NG & power import configurations first developed in chapter 3 were also assessed for the improved MAS reactor model. In addition, chapter 5 makes use of the DWC design methodology developed in chapter 4 to study the plant-wide benefits of integrating a DWC into a self-sufficient thermochemical plant for second generation biobutanol production. The results of chapter 5 showed that the NG import configuration

has the lowest MBSP at 0.92 $/L making it the best economically, while the self-sufficient configuration has the lowest CCA at 134.65 $/tonneCO$_2$e. Furthermore, integrating DWC technology into the self-sufficient configuration leads to additional savings of 3 $/tonneCO$_2$e which could be significant if the thermochemical plant technology is implemented on a large scale for second generation biobutanol production. The potential for the NG import and self-sufficient thermochemical plant designs were further highlighted through sensitivity analysis which considered the impact of changes in biomass, NG and gasoline prices on the MBSP and CCA of these plants. It is important to note that no formal system level optimization has been carried out on this process, and thus there is significant scope for improving the MBSP and CCA of these plants through optimization.

Another point to note here that all unit operations and technology discussed in this work have been demonstrated at a commercial level, with exceptions to only the gasifier, tar reforming catalysts, MAS reactor and catalysts which have been demonstrated only at a pilot-scale [4]. A comprehensive discussion of the status of these technologies in 2007 and R&D improvement targets to 2012 are reported by the U.S. NREL in appendix B of their thermochemical ethanol report [4]. That report summarized that more gasification studies need to be done to determine how feedstock composition affects the syngas composition, quality and gasifier efficiency, while more studies and research need to be done on the tar reforming catalysts to improve their long-term reforming activity. Furthermore, more research is needed on developing mixed alcohol synthesis catalysts with higher activity at lower operating pressures, as well as improved CO conversion and

alcohols selectivity. Finally, improved temperature control is required for current MAS reactor designs so as to improve the process yields and thus economics.

In summary, the work carried out in this thesis has improved the understanding of the thermochemical route for producing both second and third generation biobutanol. In particular, the economic and environmental results obtained for the second generation biobutanol plant in chapters 2 and 5 show that the technology can be profitable using existing catalysts and technologies without the need to wait for further technological innovations, and that the integration of process intensification technology in the form of DWCs into the design of thermochemical plants can lead to even more improvements.

6.2   Future work

As with any research work, there is always scope for improvements as well as identified new research areas to be investigated. Some future areas of research that have been brought to light through this thesis are discussed below:

[1]   The optimization work carried out to determine the optimal recycle configuration of the thermochemical plants in chapter 5 can be improved by changing the objective function to consider directly minimizing the MBSP or the CCA. This will entail integrating the capital cost estimation, as well as discounted cash flow rate of return analysis, and CCA computation into the objective function evaluation of the PSO algorithm. Though this will increase the complexity and solution time of the optimization setup, it will potentially lead to better results as the feasible solution search space for the MBSP and CCA is enlarged in comparison to the optimization setup used in chapter 5. To

help with reducing the solution time of the optimization, consideration should be put into moving the PSO algorithm from MATLAB to Python, so as to have a direct link to Aspen Plus and thus allow the opportunity for parallel computing.

[2]   Consider other process intensification technologies for process improvements. Two process intensification technologies that can be investigated are (i) Membrane reactors for the MAS reactor. Using membrane reactors is a way to remove CO_2 from the MAS reactor thus allowing more unreacted syngas to be recycled directly to the MAS reactor. This could potentially improve the butanol yield of the thermochemical plant. (ii) Primary tar reforming. In primary tar reforming the gasification and tar reforming step are combined. Doing this can potentially reduce the capital cost and MBSP of the thermochemical biobutanol plant as the significant equipment cost of the secondary tar reformer is eliminated.

[3]   Extend this work to consider CO_2 capture: this will require replacing the low pressure indirect gasifier system with a high pressure direct gasification system. The advantage of this would be the ability to produce high pressure CO_2 which can be captured after the gasification step, thus potentially leading to a lower CCA. The downside of doing this is the higher costs associated with using an air separation unit to provide O_2 for the gasifier, and any additional costs associated with CO_2 capture, which when put together can lead to a higher MBSP. However the trade-off between a higher MBSP and a lower CCA could be interesting to investigate.

[4] More detailed life cycle assessments (LCA) studies should be carried out on the thermochemical biobutanol process so as to consider other environmental impacts relating to water use, ozone depletion etc. Plant location and the associated prices and emissions of the area of location should be included. This is because though the CCA for the assessed thermochemical biobutanol plants are greater than the policy threshold of 50 $/tonneCO$_2$e, a detailed LCA which considers other environmental impacts might show that biobutanol produced from a thermochemical plant provides significant improvements over gasoline in other environment impact areas and should thus be invested in. Furthermore detailed LCA studies can be useful tools to highlight areas in the biomass feedstock supply chain for improvements. For example, one area not considered in this work is the environmental impact associated with waste water treatment. It is assumed that as the thermochemical process is non-biological, and the cost of off-site waste water treatment is less than 1% of the operating costs in all the designs considered, its GHG emissions will be insignificant in comparison to the rest of the thermochemical process. However, more detailed LCA in future work will be needed to validate this.

[5] Improved biorefinery concepts. Though the thermochemical biobutanol plants designed and assessed in this thesis are examples of the biorefinery concept, these designs can be extended to consider improved biorefinery concepts in which overall process improvements are obtained through synergy derived from process integration. For example, a thermochemical biobutanol plant can be integrated with a biochemical biobutanol plant such that the lignin based waste from the biochemical plant is a feedstock to the thermochemical plant. Furthermore, these thermochemical plants can be

integrated into pulp and paper mills such that they use lignin-rich "black liquor" from the pulp and paper mills as feedstock, and in turn supply power and steam to the pulp and paper mill. Larson et al. [5,6] have demonstrated the potential of this integration for a thermochemical bioethanol process.

[6] Finally, the results of this thesis have shown than it is worthwhile to carry out research into (i) improving the upstream biomass supply chain in order to increase biomass availability, and lower biomass costs (ii) improving the CO conversion and butanol selectivity of MAS catalysts. This is because the sensitivity analyses carried out in chapters 2, 3 and 5 of this thesis have demonstrated that improvements in the cost of biomass and CO conversion of MAS catalysts can lead to significant improvements in the economic and environmental potential of thermochemical biobutanol plants, and thus increase the probability for commercial implementation of this technology.

6.3   References

[1]   Herman R. Advances in catalytic synthesis and utilization of higher alcohols. Catal Today 2000;55:233–45. doi:10.1016/S0920-5861(99)00246-1.

[2]   Fulton L, Howes T, Hardy J. Biofuels for transport: An international perspective. Paris: 2004.

[3]   Beretta A, Micheli E, Tagliabue L, Tronconi E. Development of a Process for Higher Alcohol Production via Synthesis Gas 1998;5885:3896–908.

[4]   Phillips, S.; Aden, A.; Jechura, J.; Dayton, D.; Eggeman, T. *Thermochemical Ethanol via Indirect Gasification and Mixed Alcohols Synthesis of Lignocellulosic Biomass*; Technical Report for National Renewable Energy Laboratory: Golden, CO, 2007.

[5]   Larson ED. A Cost-Benefit Assessment of Gasification-Based Biorefining in the Kraft Pulp and Paper Industry Volume 1 Main Report 2006;1.

[6]   Larson ED, Xun W. A Cost-Benefit Assessment of Gasification-Based Biorefining in the Kraft Pulp and Paper Industry Volume 2 Detailed Biorefinery Design and Performance Simulation 2006;2.

Appendix - Parameter estimation study to improve mixed alcohols synthesis kinetic model predictions of alcohols production

A.1 Description of kinetic model

The kinetic model developed by Beretta et al. [1] is based on a high temperature modified methanol synthesis catalyst. The particular catalyst is a K-promoted Zn/Cr/O catalyst, with a Zn-Cr ratio of 0.75. The kinetic experiments were performed in the temperature range of 613 to 713 K, absolute pressure of 100 to 180 bar, a CO/H_2 ratio from 0.5 to 2, and an inlet % CO_2 of 0 to 5 %. The generated experimental data was then used for a kinetic study to determine rate expressions and estimate kinetic parameters.

The reacting system was reduced to a selected number of components and pseudo-components as follows, CO, H_2, CO_2, H_2O, methanol, ethanol, propanol, isobutanol, C_{4+} higher alcohols, methane and C_{2+} hydrocarbons. For further simplicity in this work, the C_{4+} higher alcohols are approximated as pentanol and the C_{2+} hydrocarbons as ethane. The mixed alcohols reaction scheme is thus given as:

$$CO + 2H_2 \leftrightarrow CH_3OH \tag{A1}$$

$$CO + H_2O \leftrightarrow CO_2 + H_2 \tag{A2}$$

$$2CH_3OH \rightarrow C_2H_5OH + H_2O \tag{A3}$$

$$CH_3OH + C_2H_5OH \rightarrow C_3H_7OH + H_2O \tag{A4}$$

$$CH_3OH + C_3H_7OH \rightarrow iC_4H_9OH + H_2O \qquad (A5)$$

$$2CH_3OH + C_3H_7OH \rightarrow C_5H_{11}OH + 2H_2O \qquad (A6)$$

$$2CH_3OH \rightarrow (CH_3)_2O + H_2O \qquad (A7)$$

$$CO + 3H_2 \rightarrow CH_4 + H_2O \qquad (A8)$$

$$2CO + 5H_2 \rightarrow C_2H_6 + 2H_2O \qquad (A9)$$
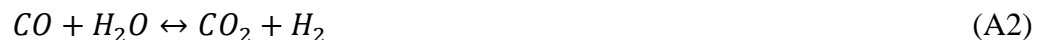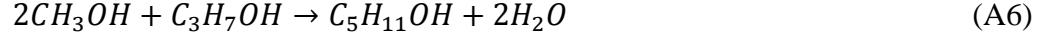
The unit of the rate expression is mol/(kg of catalyst.h), while T is in K and P is in bar.

The corresponding rate expressions for the reaction scheme are given as:

Methanol synthesis:

$$r_{MeOH} = k_{MeOH}P_{CO}P_{H2}^2 - \frac{k_{MeOH}}{K_{MeOH}}P_{MeOH} \qquad (A10)$$

where:

$$K_{MeOH} = \frac{1}{K_{y,MeOH}} \exp\left(-\frac{\Delta G^\circ_{MeOH}}{RT}\right), (bar)^{-2} \qquad (A11)$$

$$\Delta G^\circ_{MeOH} = -24306 + 58.57T, \text{(cal/mol)} \qquad (A12)$$

$$K_{y,MeOH} = 1 - P(6.713 \times 10^{-5})exp\left(1.7308 \times \frac{10^3}{T}\right), (bar)^2 \qquad (A13)$$

The reference values of P = 180 bar, and T = 673 K were used to compute $K_{y,MeOH}$ in

equation (A13), resulting in $K_{y,MeOH}$ = 0.841841 $(bar)^2$.

Water gas shift reaction:

$$r_{SHIFT} = k_{SHIFT}P_{CO}P_{H_2O} - \frac{k_{SHIFT}}{K_{SHIFT}}P_{CO_2}P_{H_2} \qquad (A14)$$

where:

$$K_{SHIFT} = \exp\left(-\Delta G^{\circ}_{SHIFT}/RT\right) \tag{A15}$$

$$\Delta G^{\circ}_{SHIFT} = -8514 + 7.71T, \text{ (cal/mol)} \tag{A16}$$

Ethanol synthesis:

$$r_{EtOH} = k_{EtOH}P_{MeOH}/P_{H2} \tag{A17}$$

Propanol synthesis:

$$r_{PrOH} = k_{PrOH}\frac{P_{EtOH}/P_{H2}}{(1+K_{H2O}P_{H2O})} \tag{A18}$$

Isobutanol synthesis:

$$r_{i-ButOH} = k_{i-ButOH}\frac{P_{PrOH}/P_{H2}}{(1+K_{H2O}P_{H2O}+K_{HA}P_{HA})^2} \tag{A19}$$

Pentanol synthesis:

$$r_{PentOH} = k_{PentOH}P_{PrOH} \tag{A20}$$

DME formation:

$$r_{DME} = k_{DME}P_{MeOH} \tag{A21}$$

Methane formation:

$$r_{CH4} = k_{CH4}P_{H2} \tag{A22}$$

Ethane formation:

$$r_{Ethane} = k_{C2H6}P_{H2} \tag{A23}$$

The kinetic constants are of the form

$$k_i = k_i^{\circ} \exp\left[-\frac{1000 E_{att,i}}{R}\left(\frac{1}{T}-\frac{1}{T^{\circ}}\right)\right]$$ (A24)

where:

k_i = kinetic constant of product i

k_i° = pre-exponential factor of product i

$E_{att,i}$ = Activation energy of product i

R = gas constant = 1.987 (cal/mol.K)

T° = reference temperature = 673 K

The values of the kinetic parameters are given in Table A-1.

Table A-1. Values of original kinetic parameters from Beretta et al. [1]

Kinetic parameter	Value	Units
k_{MeOH}	2.244×10^{-10}	$\dfrac{kmol}{kgcat.sec.(bar)^3}$
k_{SHIFT}	1.169×10^{-6}	$\dfrac{kmol}{kgcat.sec.(bar)^2}$
k_{EtOH}	1.163×10^{-5}	$\dfrac{kmol}{kgcat.sec}$
k_{PrOH}	3.117×10^{-3}	$\dfrac{kmol}{kgcat.sec}$
$k_{\text{i-ButOH}}$	2.883×10^{-3}	$\dfrac{kmol}{kgcat.sec}$
k_{PentOH}	7.872×10^{-6}	$\dfrac{kmol}{kgcat.sec.bar}$
k_{CH4}	3.744×10^{-9}	$\dfrac{kmol}{kgcat.sec.bar}$
k_{Ethane}	3.419×10^{-9}	$\dfrac{kmol}{kgcat.sec.bar}$
k_{DME}	5.961×10^{-8}	$\dfrac{kmol}{kgcat.sec.bar}$
K_{H2O}	1.556	$(bar)^{-1}$
K_{HA}	1.303	$(bar)^{-1}$
$E_{att,MeOH}/R$	1.626×10^1	$(-)$
$E_{att,SHIFT}/R$	3.491	$(-)$
$E_{att,EtOH}/R$	1.412×10^1	$(-)$
$E_{att,PrOH}/R$	2.974	$(-)$
$E_{att,i-ButOH}/R$	7.198	$(-)$
$E_{att,PentOH}/R$	2.114×10^{-3}	$(-)$
$E_{att,CH4}/R$	9.068	$(-)$
$E_{att,HYD}/R$	1.422×10^1	$(-)$
$E_{att,DME}/R$	6.620	$(-)$
$-(\Delta H_{ads,H2O}/R)$	2.513×10^1	$(-)$
$-(\Delta H_{ads,HA}/R)$	2.109×10^{-1}	$(-)$

A.2 Model regression and parameter estimation

The kinetic model is implemented in Aspen Plus V8.0 using a plug flow reactor (RPlug) and feed conditions and an experimental setup representative of the information reported in Beretta et al. [1], with the RPlug reactor operated at isothermal and isobaric conditions similar to the kinetic testing unit in Beretta et al. [1]. Table A-2 shows the standard conditions and range of conditions used for the model validation.

Table A-2. Experimental conditions explored

Parameters explored	Standard conditions	Test range
Temperature, K	673	$633 - 713$
Pressure, bar	180	$100 - 180$
GHSV, L (STP)/kg of catalyst/h	20,000	$12,000 - 70,000$

The kinetic model and parameters discussed in section 1 were inputted into Aspen Plus using the power law and Langmuir-Hinshelwood-Hougen-Watson (LHHW) models. The help file of Aspen Plus provides information on how to set up these models.

The kinetic model setup in Aspen Plus as well as kinetic parameters shown in Table A-1 were used to simulate the varying test conditions shown in Table A-2, and the computed alcohol yield results were then compared against experimental data. It was noted that the original parameters (solid lines in Figures A-1 $-$ A-5) of the kinetic model did not appropriately predict the production of C_{2+} alcohols, thus for this work a model regression was carried out to better estimate the parameters of the kinetic model so that alcohols predictions are improved. This was done by using the parameters of the original kinetic model as initial guesses in the model regression.

Model regression for estimating new pre-exponential parameters of the $C_1 - C_5$ alcohols was performed in Aspen Plus V8.0 using the Data Fit - Regression tool. In Aspen Plus, under Model Analysis Tools | Data Fit, point data sets were made using experimental data results of alcohols (methanol to pentanol) product yields with respect to changes in GHSV, pressure and temperature [1]. Also included are measurement standard deviations of the experimental data as provided by the original work [1]. The data sets inputted in Aspen Plus are shown in Tables A-3, while Table A-4 shows the results of the regressed parameters.

As can be seen from Figures A-1 - A-5, the new model parameters provide an overall better fit to the experimental data than the original model parameters. The only exception being the prediction of methanol yield with respect to temperature, pressure and GHSV in Figures A-5(a - c) for which the original model parameters do better.

The goodness of fit for the product yields predicted by both the original model parameters and new model parameters are quantitatively shown using the relative root mean square error (rRMSE) metric in Table A-5. The rRMSE normalizes the absolute error in a model prediction versus experimental results dataset and thus allows different datasets to be compared. Its computation for the predictions of both the original and new model parameters is shown in equation (A25). The rRMSE is computed for each product in each input dataset and also for all the products in each input dataset. As can be seen from Table A-5, the new model parameters provide the better fit to experimental data.

$$rRMSE = \sqrt{\frac{\sum_{i=1}^{n}\left(\frac{y_{pred,i}-y_{exp,i}}{y_{exp,i}}\right)^2}{n}} \qquad\qquad (A25)$$

$y_{pred,i}$ = predicted product yield for data point i.

$y_{exp,i}$ = experimental product yield for data point i.

n = number of data points in the dataset.

Table A-3. Experimental data of change in mole fraction alcohols with respect to Temperature, Pressure and GHSV [1]

	Mole fraction				
	Methanol	Ethanol	Propanol	Butanol	Pentanol
Measurement std-dev.	0.3742	0.00707	0.00707	0.031623	0.031623
Temperature (K)					
633	0.08157	0.00028	0.0003	0.00043	0.00151
653	0.06314	0.00029	0.00043	0.00119	0.00269
673	0.04392	0.00032	0.00049	0.0024	0.00444
693	0.02784	0.00029	0.0005	0.00351	0.00624
713	0.01843	0.00027	0.00048	0.005	0.00931
Pressure (bar)					
100	0.01455	0.00007	0.00012	0.0011	0.00175
150	0.02927	0.0002	0.00032	0.00204	0.0035
180	0.04404	0.00032	0.00049	0.0023	0.00451
GHSV (m3/kg_cat.h)					
12	0.03911	0.00041	0.00063	0.00384	0.00677
20	0.04377	0.00034	0.00053	0.00234	0.00413
30	0.04444	0.00022	0.00034	0.00155	0.00276
40	0.04559	0.00018	0.00028	0.00105	0.00214
70	0.04058	0.00016	0.0002	0.00049	0.00128

Table A-4: Original [1] and new parameters of pre-exponential factors after model regression

Pre-exponential parameter	Original parameters	New parameters	Units
k°_{MeOH}	2.24×10^{-10}	8.04×10^{-11}	$\dfrac{kmol}{kgcat.sec.(bar)^3}$
k°_{EtOH}	1.16×10^{-5}	1.45×10^{-5}	$\dfrac{kmol}{kgcat.sec}$
k°_{PrOH}	3.12×10^{-3}	4.32×10^{-3}	$\dfrac{kmol}{kgcat.sec}$
$k^{\circ}_{i-ButOH}$	2.88×10^{-3}	1.61×10^{-3}	$\dfrac{kmol}{kgcat.sec}$
k°_{PentOH}	7.87×10^{-6}	1.54×10^{-5}	$\dfrac{kmol}{kgcat.sec.bar}$
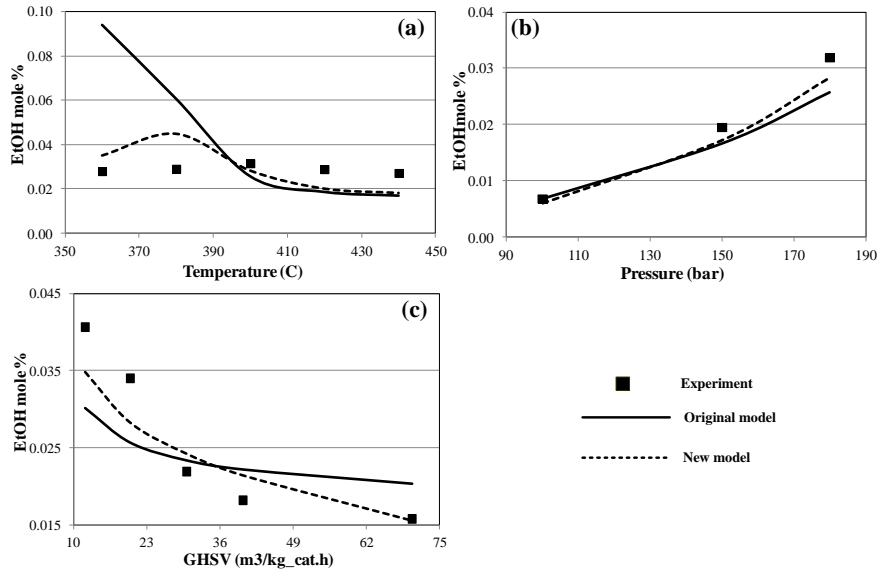
Figure A-1: Experimental and calculated (original-model and new model) trends of ethanol concentration with varying operating conditions from standard conditions (a) Temperature (b) Pressure (c) GHSV.
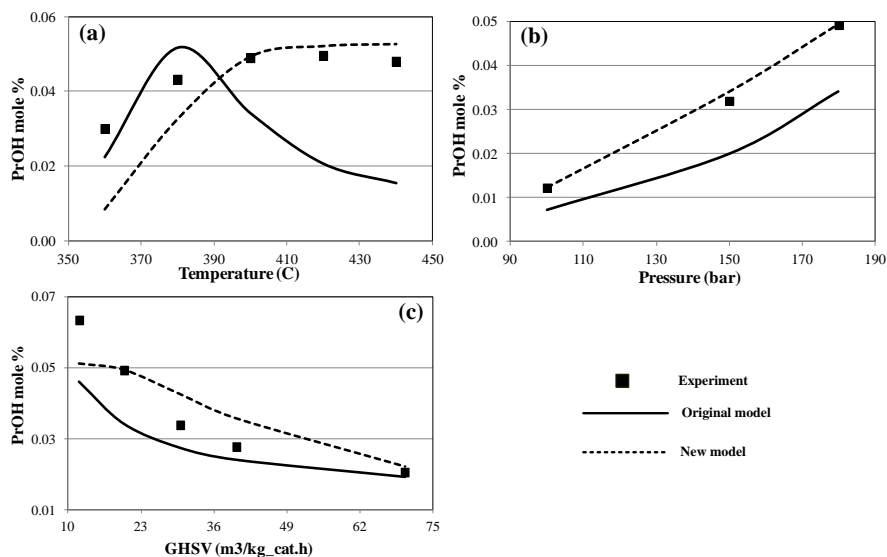
Figure A-2: Experimental and calculated (original-model and new model) trends of propanol concentration with varying operating conditions from standard conditions (a) Temperature (b) Pressure (c) GHSV.
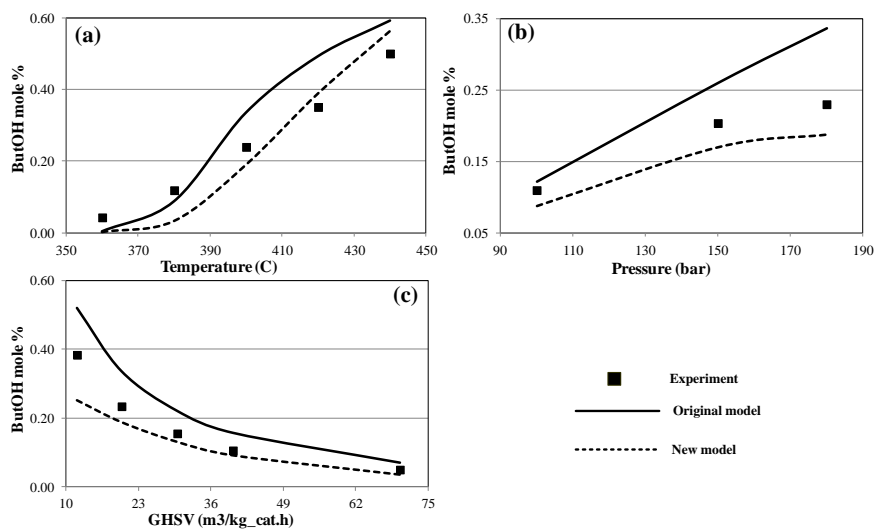
Figure A-3: Experimental and calculated (original-model and new model) trends of butanol concentration with varying operating conditions from standard conditions (a) Temperature (b) Pressure (c) GHSV.
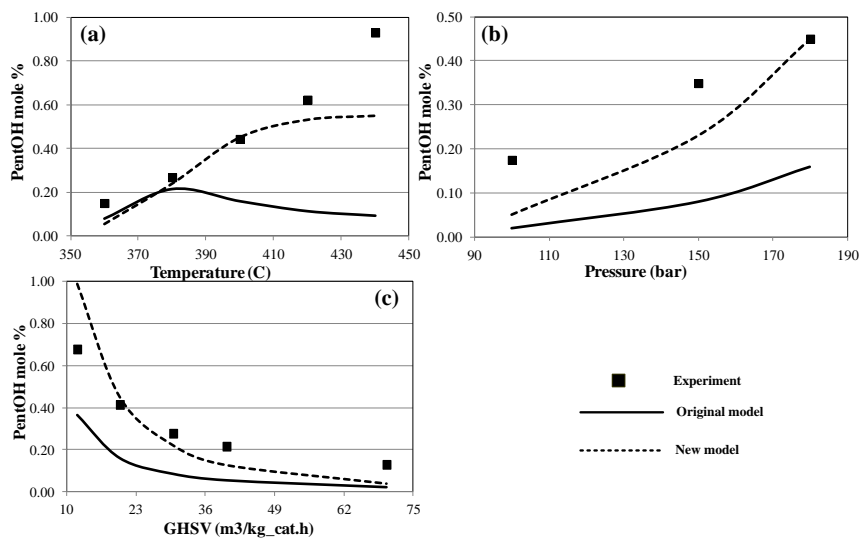
Figure A-4: Experimental and calculated (original-model and new model) trends of pentanol concentration with varying operating conditions from standard conditions (a) Temperature (b) Pressure (c) GHSV.
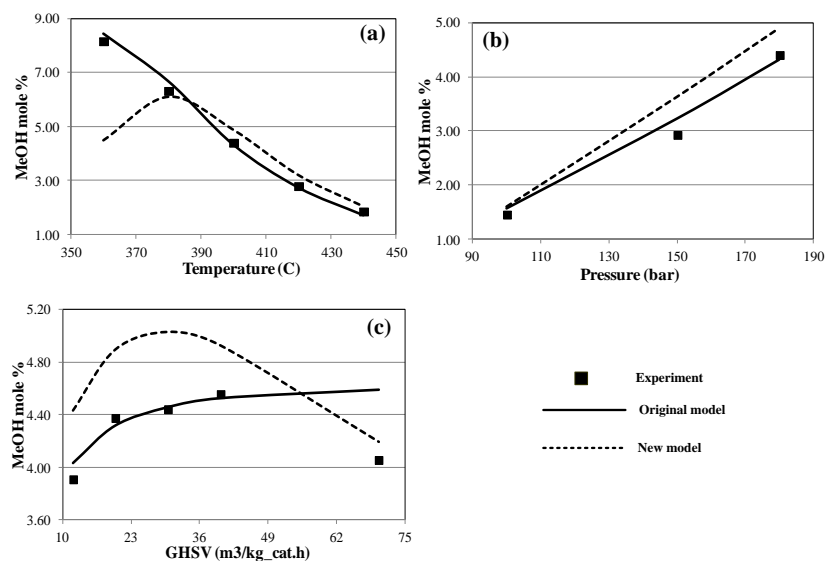
Figure A-5: Experimental and calculated (original-model and new model) trends of methanol concentration with varying operating conditions from standard conditions (a) Temperature (b) Pressure (c) GHSV.

Table A-5: Percentage rRMSE of original and new model parameter predictions

Original model parameters						
	Methanol	Ethanol	Propanol	Butanol	Pentanol	Overall
Temperature	4.89	118.52	44.57	50.59	65.77	67.74
Pressure	7.46	14.50	37.12	31.39	77.65	41.61
GHSV	6.07	22.89	22.73	42.87	68.48	39.00
New model parameters						
	Methanol	Ethanol	Propanol	Butanol	Pentanol	Overall
Temperature	22.30	34.25	34.40	55.72	35.25	37.95
Pressure	16.20	12.00	3.58	18.77	45.48	23.83
GHSV	10.62	13.53	20.13	23.93	43.26	25.08

A.3   References

[1]   A. Beretta, E. Micheli, L. Tagliabue, and E. Tronconi, "Development of a Process for Higher Alcohol Production via Synthesis Gas," vol. 5885, no. 97, pp. 3896–3908, 1998.